POLITECNICO DI TORINO

Collegio di Ingegneria Chimica e dei Materiali

Master of Science Course in Materials Engineering for Industry 4.0

Master of Science Thesis

Study of dimensional variability and the effect of extrusion parameters in extruded multi-chambered Aluminum Profiles



Supervisors Candidate

Prof. Ragnar HOLTHE

Prof. Cédric COURBON

Prof. Daniele UGUES

Prof. Milena SALVO

SM Faysal AHMED

September 2025

Erasmus Mundus Joint Master in Manufacturing 4.0 by intElligent and susTAinable technologies



MASTER's Degree Thesis

Study of dimensional variability and the effect of Extrusion parameters in extruded multi-chambered Aluminum Profiles

Supervisors

Prof. Ragnar HOLTHE

Prof. Cédric COURBON

Prof. Milena SALVO

Prof. Daniele UGUES

Candidate

SM Faysal AHMED

September 2025













Abstract

The growing demand for lightweight and high-performance materials in the automotive industry has intensified the need for precision in aluminum extrusion, particularly for multi-chambered structural profiles. Though the alloys are known to have high strength-to-weight ratios and better recyclability, dimensional accuracy is a major challenge. This thesis investigates extruded profile wall thickness variation, straightness, and twist, evaluating compliance with DIN EN 755-9:2016-10 standards and exploring how process parameters and the alloy composition influence extrusion behavior.

A large dataset from Benteler Automotive Raufoss was investigated, combining industrial measurement with machine learning algorithms. Maximum stem force was examined in terms of billet temperature, ram speed, and dead cycle time and determined that billet thermal conditions and cycle control affect extrusion force characteristics. Statistical analysis also confirmed that profiles generally met tolerance levels, with small positional deviations to rear sections caused by thermal gradients and flow fluctuations. Machine learning models, including Random Forest and Gradient Boosting, also considered the relative importance of process parameters, with SHAP analysis indicating that billet temperature and dead cycle time were significant contributors to force variability.

The findings indicate that thermal management maximization and idle time minimization can reduce stem forces quite significantly, increase tool lifetime, and enhance dimension stability. While chemical composition, particularly Mg and Zn content, plays a secondary role, its interaction with process conditions influences overall extrusion efficiency. By integrating experimental analysis with predictive machine learning, an enduring process optimization model is obtained that offers actionable approaches to energy saving, reduction in scrap rates, and reduction in variability for industrial manufacturing.

This work makes a scientific contribution to aluminum extrusion mechanics as well as an industrial best practices contribution, centered on data-driven process control as the path to enhanced quality, sustainability, and competitiveness in automotive production.

Acknowledgments

The current thesis has been conducted as part of the Erasmus Mundus Joint Master's Degree program Manufacturing 4.0 by intElligent and susTAinable technologies- Meta4.0. I would like to acknowledge my supervisor, Ragnar Holthe, for his professional guidance, excellent advice, and continuous support throughout this work. His experience and support have been vital to both the process and the quality of this thesis.

I am truly grateful to Benteler Automotive Raufoss for providing me with the opportunity to collaborate with their team and be exposed to real industrial problems. In particular, I would like to thank Krzysztof Zaborowski and Praveen Chathuranga for sparing their time to provide their knowledge, experience, and hands-on skills, which were vital to propel this project forward to completion.

I am also grateful to Meta 4.0 program coordinators, especially Cédric Courbon, as well as to Niels Peter Ostbø, our local NTNTU coordinator, for their continued offer of advice and support over the course of the thesis. Their dedication in allowing smooth academic and administrative progress is greatly valued.

Finally, I would like to acknowledge all my colleagues and professors for the support and teamwork, and most of all, my parents, whose constant support, encouragement, and trust in me have been the pillars of my educational endeavors.

Table of Contents

Abstract		I
Acknowle	dgments	II
Table of C	ontents	III
List of Fig	ures	VI
List of Tal	oles	VIII
Nomencla	ture	IX
Chapter 1	Introduction and Background	1
1.1. Intro	duction	1
1.2. Back	ground	2
1.2.1.	Aluminum Extrusion in Automotive Applications	2
1.2.2.	Dimensional Accuracy: Straightness, Twist, and Wall Thickness	3
1.2.3.	Peak Stem Force and Its Relation to Process Parameters	3
1.2.4.	Influence of Alloy Composition (6XXX and 7XXX Series)	4
1.2.5.	Industrial and Research Motivation	4
1.3. Obje	ctives	5
1.4. Scop	e and Limitations	5
1.5. Struc	ture of the Thesis	6
Chapter 2	Literature Review	7
2.1. Over	view of Aluminum Extrusion Processes	7
2.2. Dime	ensional Tolerances and Geometric Deviations in Aluminum Extrusion	9
2.2.1.	Standard Specification: DIN EN 755-9:2016-10	10
2.2.2.	Forms of Dimensional Deviations	11
2.2.3.	Causes of Geometric Inaccuracy	12
2.2.4.	Quality Inspection and Compliance with Standards	12
2.3. Indu	strial Measurement Techniques	13
2.3.1.	Function of Dimensional Inspection in Extrusion	13
2.3.2.	Industrial Measurement Techniques Overview	13
2.3.3.	Accuracy, Calibration, and Suitability	13
2.3.4.	Measurement Approach in This Study	14

2.4. Peak	Stem Force and Its Relation to Process Parameters	14
2.4.1.	Definition and Significance of Peak Stem Force	15
2.4.2.	Process Parameter Influence	15
2.4.3.	Relevance to Current Study	17
2.4.4.	Models and Industrial References	17
2.5. Effect	t of Chemical Composition on Extrusion Behavior	18
2.5.1.	Overview of 6000 and 7000 Series Alloys	18
2.5.2.	Impact on Peak Stem Force and Extrusion Properties	18
2.5.3.	Implication for Dimensional Accuracy	19
2.6. Sumr	nary of Literature Gaps and Justification for the Study	19
Chapter 3	Methodology	21
3.1. Resea	arch Design and Methodology	21
3.2. Data	Collection	21
3.2.1.	Wall Thickness Measurements	22
3.2.2.	Straightness and Twist Measurements	22
3.2.3.	Process Parameters and Chemical Composition	23
3.3. Data	Preprocessing and Cleaning	24
3.3.1.	Validations and Cleaning of Wall Thickness Data	24
3.3.2.	Preprocessing of Process Parameters	25
3.3.3.	Twist and Straightness Data Processing	25
3.3.4.	Chemical Composition Data	25
3.4. Data	Analysis	26
3.4.1.	Wall Thickness Evaluation	26
3.4.2.	Twist and Straightness Deviation Analysis	26
3.4.3.	Impact of Process Parameters on Maximum Stem Force	27
3.4.4.	Chemical Composition Effects	27
3.4.5.	Data Visualization and Statistical Tools	27
3.4.6.	Summary	28
3.5. Softw	vare and Tools	28
Chapter 4	Results and Discussion	30
4.1. Main	Observations and overview of Data	30
42 Wall	Thickness Analysis	30

4.3. Dimensional Deviations: Straightness and Twist	37
4.4. Correlation Analysis of Process Parameters and Peak Stem Force	41
4.5. 3D Scatter Plot Analysis: Influence of Alloying Elements and Process Paramete	rs on Peak
Stem Force	44
4.6. Feature importance analysis	48
4.7. SHAP-Based Model Interpretation	50
Chapter 5 Discussion	57
5.1. Wall Thickness Variation	57
5.2. Dimensional Accuracy – Straightness and Twist	58
5.3. Process Parameter and Chemical Composition Effects on Peak Stem Force	58
5.4. Machine Learning Insights	60
5.5. Industrial Practical Consequences for Extrusion Plants	61
5.6. Limitations & Sources of Error	62
5.7. Recommendations and Future Directions	63
Chapter 6 Conclusion	64
Appendix A	66
Bibliography	84

List of Figures

Figure 1.1 : Aluminum Alloy for Aerospace and Automotive Industry: Current Status and Fu	ıture
Prospects	1
Figure 1.2 : Evolution of aluminum content in automobile sector	2
Figure 2.1 : A schematic diagram of direct and indirect extrusion	7
Figure 2.2 : Flow diagram of the industrial extrusion process	8
Figure 2.3 : Aluminum Extrusion Flowchart	9
Figure 2.4 : Dimension defined by EN 755-9:2008	10
Figure 2.6 : Measurement of deviation from straightness	11
Figure 2.7 : Twist Measurement	11
Figure 2.8 : Variation of load with ram travel for both direct and indirect extrusion process	15
Figure 2.9 : Peak load vs billet temperature and extrusion ratio	15
Figure 2.10 : Loads versus stroke under different billet temperatures	`16
Figure 2.11 : Loads versus stroke under different die temperatures	16
Figure 2.12 : Billet temperature variation at different stem speeds	17
Figure 2.13 : Plot of extrusion force vs. stem speed	17
Figure 3.1 : Feeler gauges (0.01 to 1.00 mm)	22
Figure 3.2 : Measurement setup of straightness and twist	23
Figure 3.3 : Multi-chambered Aluminum profiles	23
Figure 4.1 : Histogram for RAB5954, Pos 14	31
Figure 4.2 : Profile RAB5954	31
Figure 4.3 : Histogram for RAB5954, Pos 15	31
Figure 4.4: Histogram for RAB5954, Pos 17	31
Figure 4.5: Histogram for RAB5954, Pos 12	32
Figure 4.6: Histogram for RAB5954, Pos 13	32
Figure 4.7: Histogram for RAB5954, Pos 9.	32
Figure 4.8: Histogram for RAB5954, Pos 10	32
Figure 4.9: Histogram for RAB5954, Pos 3.	33
Figure 4.10: Histogram for RAB5954, Pos 5	33
Figure 4.11: Histogram for RAB6146, Pos 30	34
Figure 4.12: Profile RAB6146	34
Figure 4.13: Histogram for RAB6146, Pos 25	34
Figure 4.14: Histogram for RAB6146, Pos 32	34
Figure 4.15: Histogram for RAB6146, Pos 33	34
Figure 4.16: Histogram for RAB6146, Pos 21	34
Figure 4.17: Histogram for RAB6146, Pos 39	35
Figure 4.18: Histogram for RAB6146, Pos 26	35

Figure 4.19: Histogram for RAB6146, Pos 15	35
Figure 4.20: Profile RAB6146, Pos 18	35
Figure 4.21: Histogram for RAB6146, Pos 16	35
Figure 4.22: Profile RAB6146, Pos 17	35
Figure 4.23: Histogram for RAB6782, Pos 14	36
Figure 4.24: Profile RAB6782	36
Figure 4.25: Histogram for RAB6782, Pos 11	36
Figure 4.26: Profile RAB6782, Pos 5	36
Figure 4.27: Histogram for RAB6782, Pos 3	37
Figure 4.28: Profile RAB6782, Pos 8	37
Figure 4.29 : Straightness deviation Measurement	39
Figure 4.30 : Twist deviation Measurement	39
Figure 4.31 : Max Deviations per Billet Position Straightness and Twist	40
Figure 4.32 : Measurement comparison between CMM and Feeler Gauge	41
Figure 4.33 : Heatmap for correlation analysis	42
Figure 4.34 : 3D scatter plot- billet temperature, DCT, (Mg) vs peak stem force	44
Figure 4.35 : 3D scatter plots - billet temperature, DCT, zinc (Zn) vs peak stem force	45
Figure 4.36 : Machine learning Model wise feature importance analysis	48
Figure 4.37 : SHAP summary plot of the regression model.	50
Figure 4.38 : SHAP value for DCT values, color-coded by Average Billet Temperature	52
Figure 4.39 : SHAP value for Average Billet Temperature, color-coded by Ram Speed Average	53
Figure 4.40 : SHAP values for Mg content, color-coded by Zn content	54
Figure 4.41 : SHAP values for Zn content, color-coded by Mg content	55

List of Tables

Table 1.1 : Composition and properties of aluminum alloy series	04
${\bf Table~4.1: Straightness~and~Twist~Values~of~Profiles~for~Different~Billet~Positions}$	38
Table 4.2 : The min, max, mean and % of tolerance of straightness and twist	38

Nomenclature

Abbreviations & acronyms

CMM Coordinate measuring machines

DCT Dead Cycle Time

LSL Lower Specification Limit

Mg Magnesium

ML Machine learning

Min Minimum

Max Maximum

OEM Original Equipment Manufacturer

Pos Position

RMSE Root Mean Square Error

SHAP SHapley Additive exPlanations

Zn Zinc

Chapter 1 Introduction and Background

1.1. Introduction

Aluminum extrusion is among the major production processes in the automobile industry, particularly in the move towards lightweight and efficient vehicles. Demand for lightweight, high-strength structural elements has risen significantly in recent years with more stringent emissions controls and the global drive towards green transportation. Multi-chamber aluminum profiles are particularly well-suited to the automotive industry due to their stiffness-to-weight ratio, excellent corrosion resistance, and recyclability. However, the achievement of dimensional stability and the minimization of deviation in extruded profiles remain the main challenge in high-precision industrial uses such as vehicle body structures. An Insight View of the Evolution of Advanced Aluminum Alloy for Aerospace and Automotive Industry is shown in Figure 1.1.

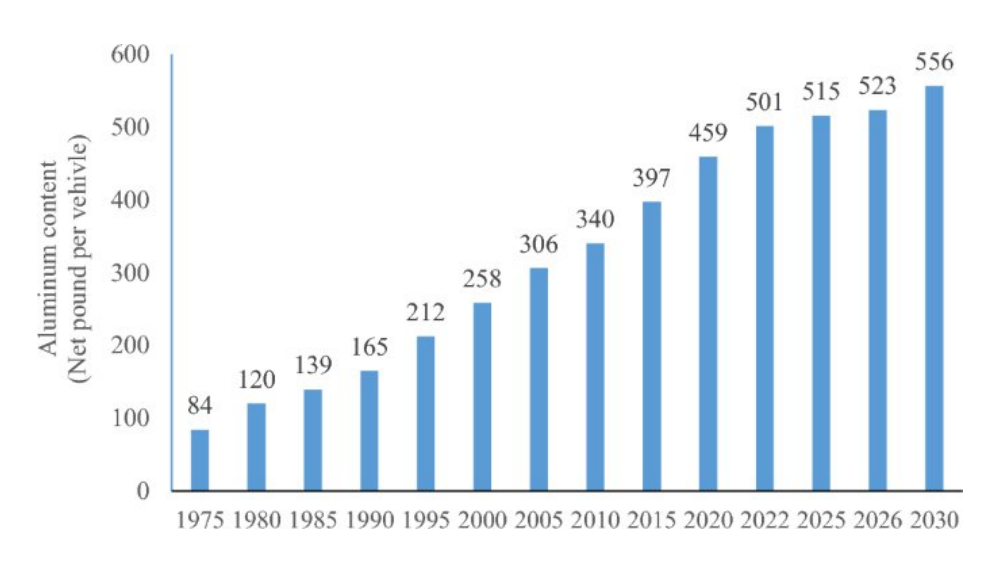


Figure 1.1 : Aluminum Alloy for Aerospace and Automotive Industry: Current Status and Future Prospects[1]

This thesis investigates the dimensional variability of multi-chambered aluminum extruded profiles, focusing specifically on straightness, twist, and wall thickness variations, in line with the tolerance requirements of the DIN EN 755-9:2016-10 standard. In addition, the study explores how chemical composition and process parameters including billet temperature, peak stem force, ram speed and dead cycle time influence the dimensional stability and extrusion behavior of aluminum alloys.

The work is conducted in collaboration with Benteler Automotive Raufoss, a leading Norwegian manufacturer of structural aluminum components to global automotive OEMs. By using industrial real-world data, this work bridges the gap between theoretical modeling and actual manufacturing problems, contributing practical insight into better control quality, reduce waste, and increase the sustainability of aluminum extrusion activities.

1.2. Background

1.2.1. Aluminum Extrusion in Automotive Applications

Aluminum extrusion is employed to force a heat-treated aluminum billet through a shape die to produce profiles with specific cross-sectional geometries. In the automotive sector, this technique permits mass production of light yet rigid structural components such as bumper beams, crash boxes, battery enclosures, and side impact bars [2]. Extruded aluminum applications have increased in popularity in recent years due to its recyclability, formability, and superior performance under crash conditions [3]. The evolution of aluminum content in automobile sector over the last 50 years is shown in Figure 1.2.

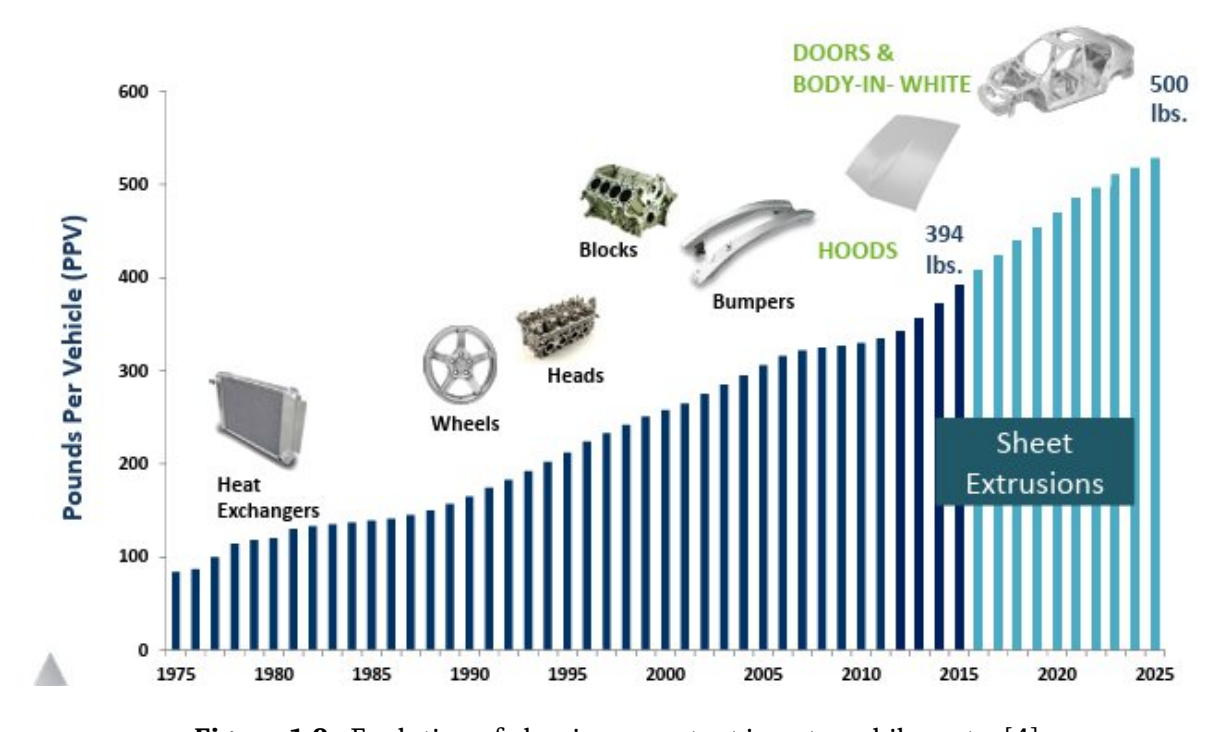


Figure 1.2: Evolution of aluminum content in automobile sector[4]

Benteler Automotive has emerged as a world leader in this area, manufacturing high-precision aluminum profiles to meet the needs of hybrid and electrified vehicle platforms. Their extrusions encompass complex die designs and sophisticated process controls, particularly for multichambered profiles, which are more susceptible to distortion and dimensional variation.

1.2.2. Dimensional Accuracy: Straightness, Twist, and Wall Thickness

Dimensional tolerances are of crucial quality specifications during the manufacture of aluminum profiles. Straightness and twist are particularly relevant to gaining appropriate fit and structural integrity of assembled automobile components. Specification for allowed deviations in straightness and twist of extruded profiles, considering cross-sectional area and profile class, are outlined in the DIN EN 755-9:2016-10 standard [5].

These tolerances may be exceeded because of several factors such as inhomogeneous die temperature, uneven heating of the billet, non-uniform metal flow, die wear, and improper cooling. The thickness variation of the wall, especially in complex multi-chambered structures, is another critical dimension that affects both mechanical properties and follow-up joining processes such as welding and riveting [6].

Physical measurements for twist, straightness, and wall thickness were taken with feeler gauges, micrometers, and coordinate measuring machines (CMM) on test samples directly from Benteler production lines. These are then compared against the DIN standard to quantify conformance and to define the most important sources of deviation.

1.2.3. Peak Stem Force and Its Relation to Process Parameters

Extrusion force is one of the important parameters in aluminum extrusion, affecting die wear and product quality. Among the various stages in the extrusion cycle, Peak Stem Force — the maximum force that the extrusion press generates in shaping the billet—is particularly important. This force represents mechanical resistance to the billet passing through the die and is directly affected by a number of interdependent process variables [7].

In this thesis, the analysis concentrated specifically on the peak stem force measured during the extrusion of multi-chambered aluminum profiles using industrial data provided by Benteler Automotive. The purpose was to determine how key process parameters such as billet temperature, ram speed, and dead cycle time correlate with variations in peak stem force.

Therefore, a statistical analysis was conducted to evaluate these interactions. The results of this study are significant because they provide an insight into how process parameters can be optimized in more precision to decrease peak forces and facilitate improved energy efficiency, tool life, and overall extrusion stability.

This focus on optimal stem force is most relevant to high-performance alloys, well known to react differently under various thermal and mechanical states. By an analysis of patterns of force fluctuation, the thesis contributes to future planning to maximize energy efficiency, dimensional stability, and equipment life—all subjects closely tied to sustainable manufacturing objectives.

1.2.4. Influence of Alloy Composition (6XXX and 7XXX Series)

The extrudability as well as the final mechanical properties of aluminum alloys are significantly affected by their composition based on the chemical composition. 6XXX series (e.g., Al-Mg-Si) alloys are widely used in structural automotive applications due to good corrosion resistance and moderate strength, while 7000 series (e.g., Al-Zn-Mg-Cu) alloys are stronger but more difficult to extrude [8]. Table 1.1 shows the composition and properties of the Aluminum alloy series.

Alloy	1xxx	3xxx	5xxx	6xxx	7xxx	2xxx
Designation	(Al)	(Al-Mn)	(Al-Mg-Cr)	(Al-Mg-Si)	(Al-Zn-Mg)	(Al-Cu)
Typical alloy	1050	3004	5083-H116	6063-T6	7075-T6	2024-T4
Ultimate tensile	110	215	317	241	572	469
Strength (UTS)						
(MPa)						
Elongation (%)	12	10	12	18	3	5
Yield strength	105	172	228	214	503	324
(MPa)				11550		

Table 1.1: Composition and properties of aluminum alloy series[9]

Chemical composition information provided by Benteler is analyzed in this thesis to determine its impact on extrusion behavior, with specific consideration of required force and dimensional accuracy. This allows for the determination of optimal alloy formulations that maximize both mechanical performance and manufacturability.

1.2.5. Industrial and Research Motivation

The increasing demand for light energy-efficient vehicles has made aluminum an essential material in modern car manufacturing. Multi-chambered extruded aluminum profiles are particularly valuable for structural components due to their enhanced strength-to-weight ratio. Maintaining dimensional stability and extrusion pressure in high-speed production is, however, a long-standing industrial challenge [10].

This thesis is inspired by real-life problems encountered in Benteler Automotive, which is a leading supplier of automobile components. In practice, fluctuations in peak stem force and inconsistencies in wall thickness and profile straightness can lead to increased energy consumption, tool wear, and part rejection. Addressing these problems requires a deeper understanding of how process parameters and chemical composition influence extrusion outcomes.

From a broader perspective, the work contributes to sustainable manufacturing, a core pillar of the Manufacturing 4.0 paradigm and the Meta4.0 Erasmus Mundus program. Through the use of real process data and quality requirements (e.g., DIN EN 755-9:2016-10), the thesis closes the gap between industrial applicability and scientific soundness. The goal is not only to solve immediate production challenges but also to support long-term improvements in efficiency, quality, and environmental impact.

1.3. Objectives

The primary objective of this thesis is to investigate the dimensional variation and extrusion characteristics of multi-chambered aluminum profiles in the automotive industry, with respect to peak stem force and wall thickness uniformity. The research has been conducted based upon real production data from Benteler Automotive.

The specific research objectives are:

- 1. To quantify straightness, twist, and wall thickness deviations of extruded profiles and ascertain their compliance with the DIN EN 755-9:2016-10 standard.
- 2. To examine the effect of billet temperature, ram speed, and dead cycle duration on peak stem force during extrusion.
- 3. To explore the influence of chemical composition on stem force characteristics.
- 4. In order to apply real industrial data to determine the variables that affect the dimensional variability and energy consumption in producing aluminum profiles.

1.4. Scope and Limitations

This thesis investigates the dimensional variability and extrusion force behavior of multichambered aluminum profiles produced at Benteler Automotive. The research specifically focuses on geometric deviations—such as straightness, twist, and wall thickness and their conformity to the DIN EN 755-9:2016-10 standard. In addition, research explores ultimate stem force required during extrusion in relation to the most critical process factors that include billet temperature, ram speed, and dead cycle time. The study also examines the effect of chemical composition of aluminum alloys on extrusion performance.

The following are the limitations of this work:

- -The planned investigation into cooling rate effects and their influence on dimensional stability could not be carried out due to time constraints and lack of real-time data. This topic is proposed as future work.
- -The study is limited to the extrusion processes, machinery, and operational conditions at Benteler, and results may not directly generalize to other production environments or equipment configurations.
- -The thesis does not cover mechanical property testing, e.g., tensile or hardness measurements because of scope limitations.

1.5. Structure of the Thesis

This thesis is divided into six main chapters, each one of which deals with a separate aspect of the research:

Chapter 1 – Introduction and Background: Presents the industrial and research background of the work, explains the motivation, states the research problem, and determines the objectives, scope, and limitations.

Chapter 2 – Literature Review: Summarizes some of the most significant research and standards related to aluminum extrusion processes, dimension tolerances, extrusion force simulation, and the effect of composition of alloy and process parameters.

Chapter 3 – Methodology: Describes the measurement methods for measuring straightness, twist, and wall thickness, data acquisition in Benteler, and data analysis methodology employed in Excel and Python.

Chapter 4 and 5 – Results and Discussion: Presents the findings regarding dimensional accuracy and peak stem force behavior. The results are supported by visualizations and compared against standards DIN EN 755-9:2016-10 and in-house industrial requirements.

Chapter 6 – Conclusions: Summarizes the key results of the work, takes account of limitations, recommends future lines of research.

Chapter 2 Literature Review

This chapter provides a comprehensive literature review related to the aluminum extrusion process, specifically as it relates to automotive structural components. The review addresses the theory of extrusion, how aluminum profiles are placed in the manufacturing of vehicles, the nature of multi-chambered designs, and the challenge of dimension control. It also gives an overview of how process parameters influence the peak stem force, and how performance is influenced by alloy chemistry. The aim is to define the context for the present study, highlight essential gaps in knowledge, and provide industrial justification for the study.

While the majority of research is based on theoretical or lab-based results, relatively few use actual industrial production real-time data to quantify geometric accuracy in addition to process force behavior. That gap is addressed by this thesis, which considers process and profile quality data at Benteler Automotive with an aim at maximum stem force and dimensional deviation. The following paragraphs provide scientific and industrial motivation for the present work.

2.1. Overview of Aluminum Extrusion Processes

Aluminum extrusion is a widely utilized metal forming process whereby intricate cross-sectional shapes can be created through the forcing of hot aluminum billets into a pre-shaped die. The two primary modes of extrusion are direct extrusion—where billet and ram move in the same direction and indirect extrusion, where the die moves towards a fixed billet. Direct extrusion is more prevalent in manufacturing processes due to its versatility and equipment simplicity despite higher frictional losses [11]. A schematic diagram of direct and indirect extrusion is shown in Figure 2.1, and a simple flow diagram of the industrial extrusion process in Figure 2.2.

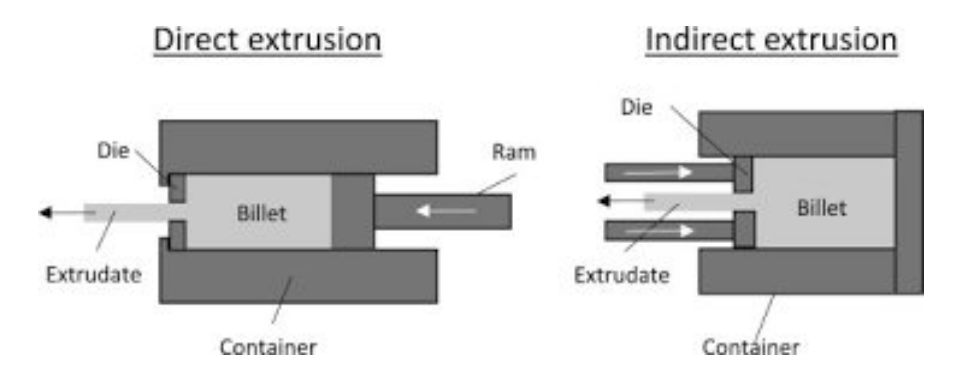


Figure 2.1: A schematic diagram of direct and indirect extrusion [12]

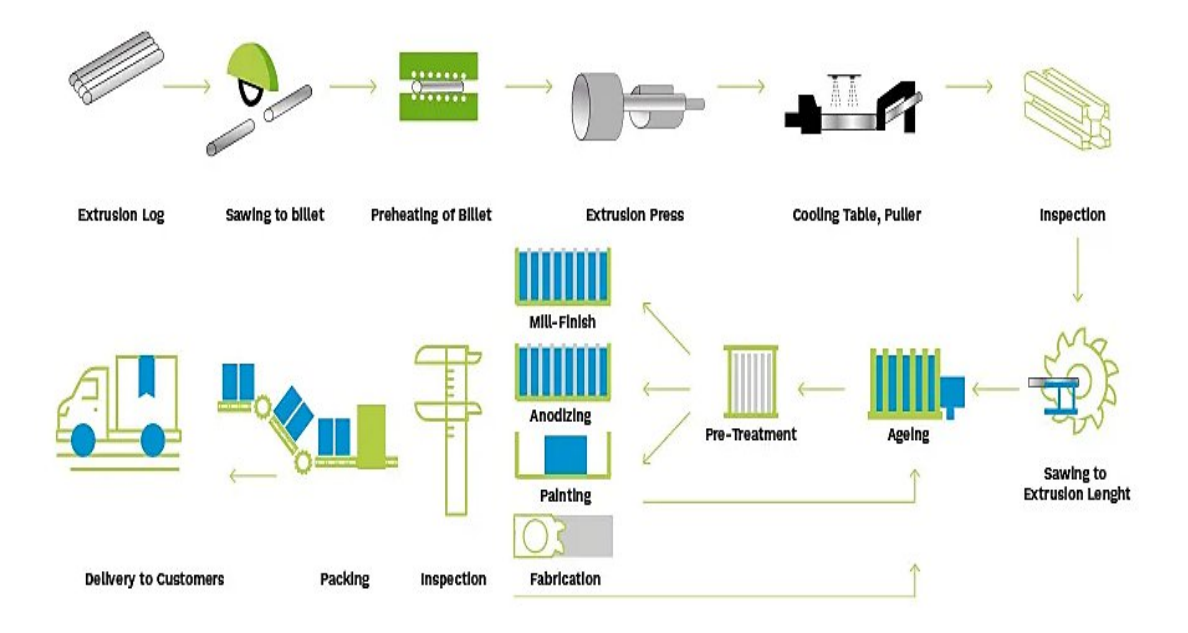


Figure 2.2: Flow diagram of the industrial extrusion process [13]

The conventional extrusion process has several steps:

Billet preheating, where billets are preheated uniformly (typically to 450–500 °C);

Extrusion, by which the billet is pushed through the die with a hydraulic ram;

Cooling, using forced air or water to reduce thermal distortion; and

Cutting and secondary working, e.g., straightening of profiles and artificial aging for the achievement of required properties [14][15].

Extrusion of aluminum is an integral part of automobile manufacture, particularly of light but strong components. Vehicle light-weighting pressure due to emission regulations and fuel efficiency requirements has accentuated the importance of extruded profiles in crash management structures, subframes, bumper beams, and battery enclosures of electric vehicles [16], [17]. Extrusion has numerous benefits over casting or machining, including high material utilization, lower tooling cost, better surface finish, and alignment with recycling goals [18]. Figure 2.3 shows the Flowchart of Aluminum Extrusion.

However, the process does require sensitive control of parameters such as billet temperature, die condition, and press speed to achieve dimensional stability and mechanical properties. Such control is more critical in the case of multi-chambered profiles, which exhibit more complex flow behavior and larger sensitivity to thermal gradients and die misalignment.

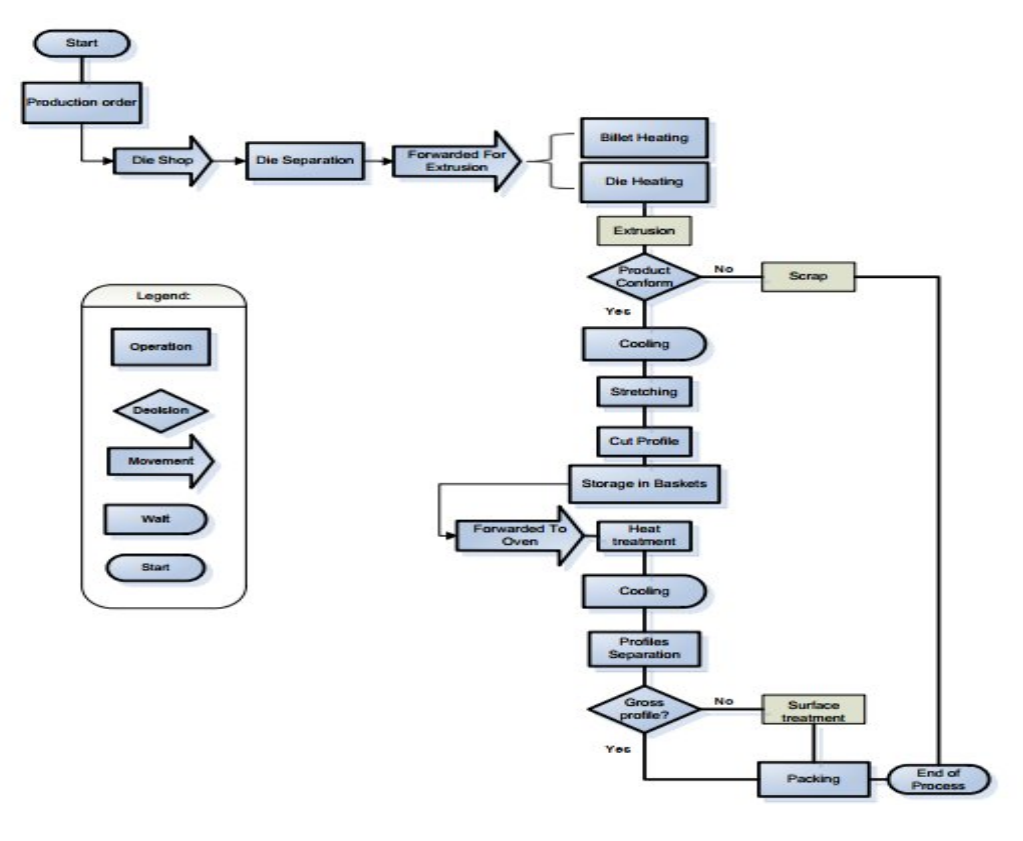


Figure 2.3: Aluminum Extrusion Flowchart [19]

Since the multi-physics nature of extrusion has thermal, mechanical, and material effects, an ongoing evolution of process knowledge based on actual industry experience is necessary. This thesis is one contribution toward this goal by considering production data in terms of variability in stem force behavior and dimension accuracy, on profiles manufactured at Benteler.

2.2. Dimensional Tolerances and Geometric Deviations in Aluminum Extrusion

Dimensional accuracy is one of the most important quality parameters in aluminum extrusion, especially for automotive structural products where tolerances must satisfy very demanding international specifications. Geometric changes of profile—the twist, bowing, wall thickness variation, and straightness variation—would have significant effect on the mechanical fit, assembly alignment, and crash performance of structural components. This section addresses the most significant dimensional tolerance specifications and geometric deviation sources, with emphasis on their use on industrial extrusion lines.

2.2.1. Standard Specification: DIN EN 755-9:2016-10

The standard DIN EN 755-9:2016-10 specifies dimensional tolerances for aluminum and aluminum alloy extruded profiles for general and structural applications. The standard defines limits for:

Straightness deviation (typically determined as deviation along the profile length), Twist (torsion), typically in degrees per meter, Wall thickness tolerance, relative to nominal size and alloy type, Flatness, squareness, angular tolerance for more complex shapes.

Tolerances vary with cross-sectional dimension, wall thickness, and series of alloy used. As per DIN EN 755-9:2016-10 standard straightness specifies a limit of 1.5 mm per metre of profile length and for twist, the standard sets a tolerance of 0.6 mm per 300 mm length. For instance, thin-walled profiles with high-strength alloys like 6XXX & 7XXX series can have a stricter process control due to greater sensitivity to distortion at cooling and quenching phases (DIN EN 755-9:2016-10) [5] Figure 2.4 shows the cross-sectional dimensions and the dimensional definition is provided below as per standard.

A: wall thickness except those enclosing the hollow spaces in the below profiles.

B: wall thickness enclosing the hollow spaces in hollow profiles except those between two spaces hollow spaces.

C: wall thickness between two hollow spaces in hollow profiles.

E: the length of the shorter leg of profiles with open ends.

H: all dimensions except wall thickness. [5]

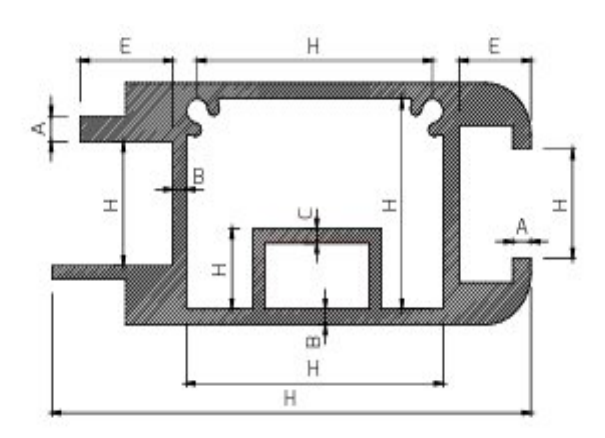


Figure 2.4: Dimension defined by EN 755-9:2008 [5]

Compliance with these standards is critical for the manufacturers providing safety-critical automotive parts. Minor differences may cause fitment, rework of assembly, or loss of structural performance, particularly in multi-chambered profiles used in crash structures and battery enclosures [20].

2.2.2. Forms of Dimensional Deviations

The most common dimensional deviations in aluminum extrusion lines are:

Straightness deviation: Usually caused by nonuniform cooling, thermal gradients along the profile, or die asymmetry. Measured by placing the profile on a flat surface and measuring the maximum offset.

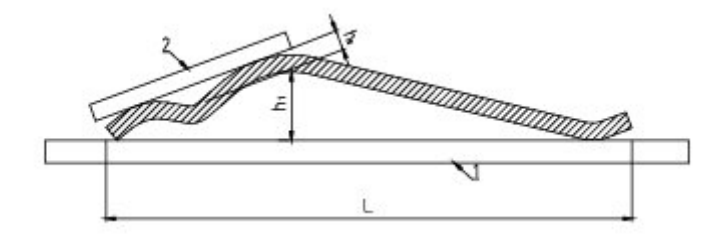


Figure 2.6: Measurement of deviation from straightness [5]

Twist or torsion: A rotation along the length of the profile, usually produced by non-symmetrical extrusion pressure or die misalignment. It is particularly problematic in multi-void or hollow profiles where walls may collapse or deform unevenly.

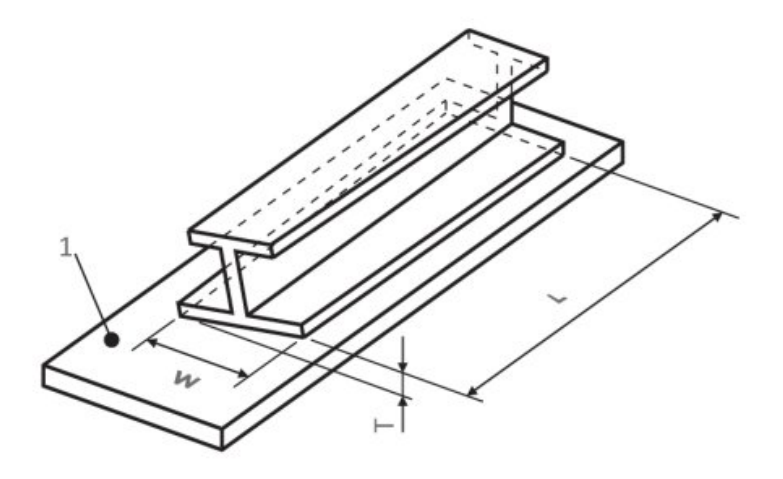


Figure 2.7: Twist Measurement [5]

Wall thickness variation: Occurs due to die design inaccuracy, non-uniform metal flow, or die bearing wear. Wall thickness stability is crucial in crash-critical regions where mechanical performance must be consistent. [21]

Bow and bend: Mechanical handling-induced longitudinal distortions due to inhomogeneity of cooling method or improper quenching. These tend to happen more predominantly in high-aspect ratio profiles or thin webs.

2.2.3. Causes of Geometric Inaccuracy

Dimensional variations can be due to a variety of thermal, mechanical, and material conditions including:

Billet and die temperature differences: Thermal imbalance during extrusion causes uneven metal flow and warping after extrusion.

Die wear or design fault: Tooling problems can cause metal to flow faster through one section of the die than another.

Insufficient cooling or quenching: Non-uniform cooling rates produce internal stresses, causing bending, warping, or twisting.

Handling and cut-off errors: Mechanical stress during handling, sawing, or transportation following extrusion can lead to geometric defects.

Alloy-specific behavior: Alloys of the 6XXX series and 7XXX series exhibit varying flow and thermal strain sensitivity and hence influence final profile geometry.

A study by Shamsudin (2017) pointed out that dead cycle time management (between billet loading and extrusion start) and keeping stable billet preheating had measurable effects on automotive extrusion line dimensional accuracy[22].

2.2.4. Quality Inspection and Compliance with Standards

Industrial extrusion plants, e.g., Benteler Automotive ,employ a combination of optical gauges, digital calipers, laser measurement technology, and optical scanners to verify dimensional tolerances. Profile measurements are referenced against in-house standards and international standards like DIN EN 755-9, under which sampling is typically conducted on a shift or batch basis.

Advanced quality control systems now use real-time sensors and AI-based image processing to detect and fix profile deviations in the early stages of the production line. However, it is still a limitation to be totally automated with the inspection of complex multi-chambered segments, particularly when internal void geometry must also be verified. [23].

Geometric twist, wall thickness, and straightness deviations are examined in this thesis based on industrial data. The outcomes aim to associate the variations with upstream process parameters and suggest enhancement for real-time control and prediction models.

2.3. Industrial Measurement Techniques

Accurate and reliable measurement of extruded aluminum profile geometry is essential in today's manufacturing operations, particularly in the automotive industry where parts must meet demanding dimensional tolerances as well as structural integrity specifications. Because extrusion runs produce long, complex profiles at high rates, real-time or near-real-time inspection methods become increasingly important for maintaining quality and minimizing scrap. Factors such as wall thickness, twist, straightness, and angular misalignment require constant monitoring and documentation according to specifications such as DIN EN 755-9:2016.

2.3.1. Function of Dimensional Inspection in Extrusion

Aluminum extrusions utilized in crash-critical vehicle applications (i.e., bumper beams, crash boxes, side impact structures) must meet stringent dimensional tolerance needs for proper assembly into vehicle assemblies as well as repeated crash energy absorption. Even minor wall thickness or twist profile deviations can impact mechanical performance or cause rejection at quality checks. Therefore, dimensional inspection is not only a quality control test but also an optimization process tool providing feedback into parameter adjustment for extrusion[24] [25].

2.3.2. Industrial Measurement Techniques Overview

Several measurement systems are used by industry to quantify extruded profiles. These range from manual to advanced optical and laser-based units. Traditional manual tools include calipers, micrometers, and feeler gauges, which are widely used because they are affordable and convenient to operate. Optical measurement systems, such as ATOS or Cognex vision systems, offer high-resolution, noncontact analysis suitable for taking detailed geometry or variation such as twist and flatness. Laser triangulation sensors and coordinate measuring machines (CMM) provide precise 3D surface measurement but tend to be available for laboratory or offline application only due to cost and complication[26] [27].All the methods have compromises. Although the automated equipment has better repeatability and quicker response times, manual equipment continues to be predominant in most extrusion facilities for some characteristics or where access to advanced equipment is limited.

2.3.3. Accuracy, Calibration, and Suitability

The selection of a measurement instrument is driven by accuracy required, feature complexity, and machine limitations. Twist and straightness, for example, require measurements across large intervals and hence manual feeler gauges or laser displacement measurement are appropriate. Wall thickness may be measured precisely using micrometers or ultrasonic gages. Tool calibration and user training are essential to minimizing systematic errors. Repeatability of

measurement also relies on environmental conditions like temperature, handling of the profile, and the reflectivity of the surface in optical systems [11] [28].

2.3.4. Measurement Approach in This Study

Dimensional testing of multi-chambered aluminum profiles was carried out at Benteler Automotive Raufoss using practical and reproducible industrial methods in this thesis. Specially, straightness and twist deviations at front and rear ends of extruded profiles were measured using feeler gauges. The simple technique made it possible to inspect for geometric deviations, as defined in DIN EN 755-9:2016-10, efficiently without special tools.

For straightness measurement, profiles were placed against a reference flat and the gaps between profile edge and flat were checked with feeler gauges at multiple points. Twist was checked by placing the profile on two references and taking elevation difference across corners with feeler gauges at regular intervals. It was a method of comparative analysis of geometrical conformity and variation between samples.

Although more accurate surface data could be obtained from laser or optical systems, the utilization of the feeler gauge method was derived from its applicability within the plant setting, simplicity of operation, and compliance with existing quality control practices. This measurement method introduced consistency and reliability of the data for subsequent analysis of dimensional variations and their relationship with process parameters.

Dimensional measurement is an important aspect of aluminum extrusion quality management. There are various methods of measuring profile geometry with the pros of each. Feeler gauges were selected for this study as a handy and effective tool for measuring twist and straightness based on practicality and suitability considerations for industries. The results of measurement form the basis of the subsequent process parameter influence on the dimensional stability of products analysis.

2.4. Peak Stem Force and Its Relation to Process Parameters

Extrusion in the aluminum profiles manufacturing process is regulated by a combination of material flow, thermal energy, mechanical pressure, and die profile. One of the key indicators of the efficiency and stability of the extrusion process is peak stem force-the maximum force exerted by the press ram on the billet during steady-state deformation. This force represents not only the resistance provided by the tooling and billet material but also embodies process parameters like billet and die temperatures, ram speed, and dead cycle time. The significance of peak stem force comprehension is that it must control both tool life, energy economy, and dimensional tolerances.

2.4.1. Definition and Significance of Peak Stem Force

Peak stem force is the highest value of ram force measured during the steady-state extrusion phase, typically upon occurrence immediately after billet breakthrough. It provides information related to material flow resistance, die friction, and efficiency of lubrication. Increased peak forces may lead to tool wear, size fluctuation, and process stoppages. Low and consistent peak forces indicate a well-behaved process with low thermal-mechanical loading on equipment[29].

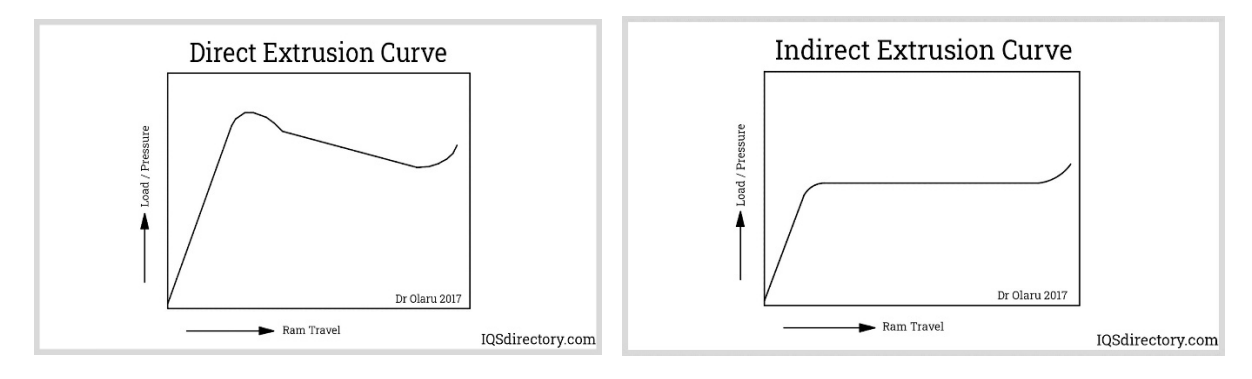


Figure 2.8: Variation of load with ram travel for both direct and indirect extrusion process[30]

In multi-chamber extrusions of aluminum such as crash management systems or side members, peak stem force becomes relevant by virtue of complex flow paths and asymmetrical die geometries. These introduce local pressure pulsations, which may enlarge geometric deviations or die deflection unless force is optimized.

2.4.2. Process Parameter Influence

Billet Temperature: Billet temperature directly influences the material's flow stress. Higher billet temperatures reduce flow stress and then reduce the required peak stem force.[31]. Too high temperatures, however, can deteriorate mechanical properties and surface finish. In manufacturing, it is realized that optimum billet temperature optimization is most important in achieving the right balance between energy efficiency and profile quality.

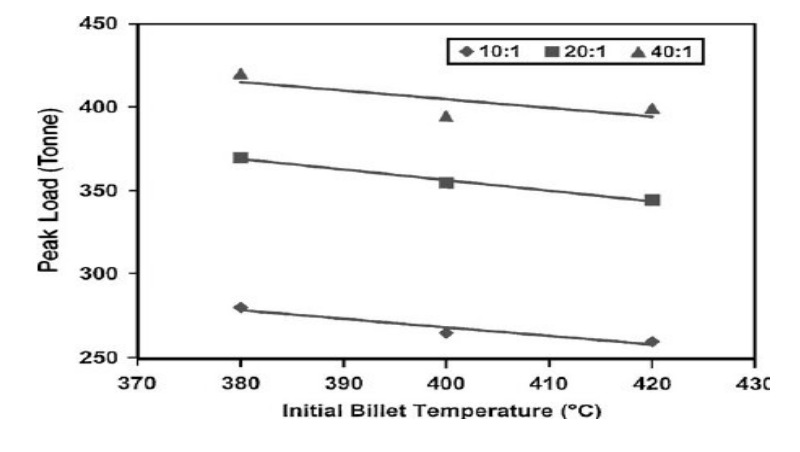


Figure 2.9: Peak load vs billet temperature and extrusion ratio. [32]

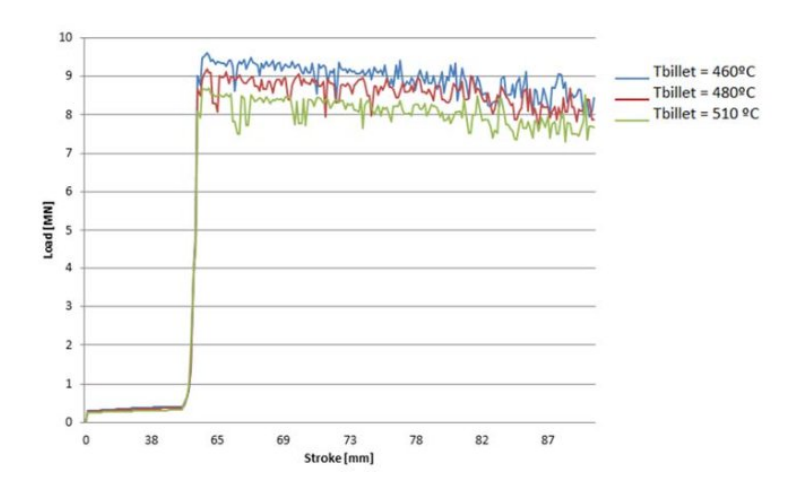


Figure 2.10: Loads versus stroke under different billet temperatures. [31]

Die Temperature: Die temperature is employed to provide flow uniformity and to reduce thermal gradients. A cold die increases friction and resists the flow of material, causing more peak force. Die preheating equalization results in lower flow roughness, decreased extrusion force, and longer die life[33].

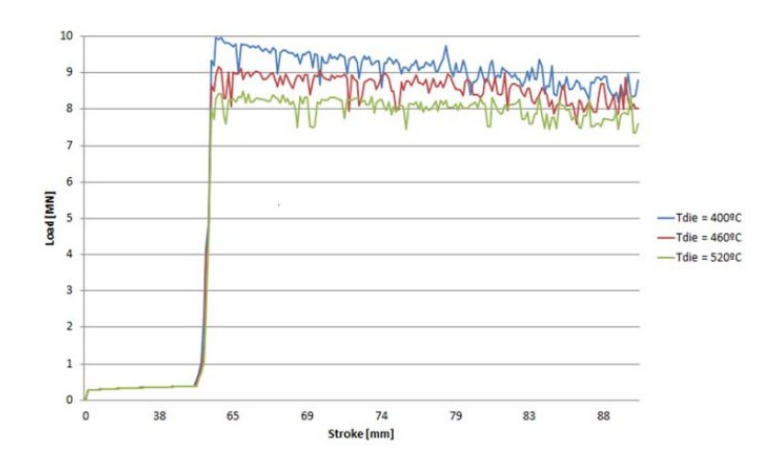


Figure 2.11: Loads versus stroke under different die temperatures. [31]

Dead Cycle Time: Dead cycle time is the time between the end of a cycle and the start of the next one. Higher dead cycles can provide die and tooling cooling, and this can prolong the force required at the beginning of the next cycle. On the other hand, smaller cycles can provide thermal stability, and this can create fewer fluctuations in peak force [14].

Extrusion Speed and Friction Conditions: Although not the explicit topic of this thesis, extrusion speed and lubrication do play a big influence on the stem force. A faster speed can add additional heat due to deformation and lower force in the short term but maybe create surface defects. Adequate lubrication minimizes frictional losses at the die/billet interface and tends to generate smoother extrusion force profiles [34],[35].

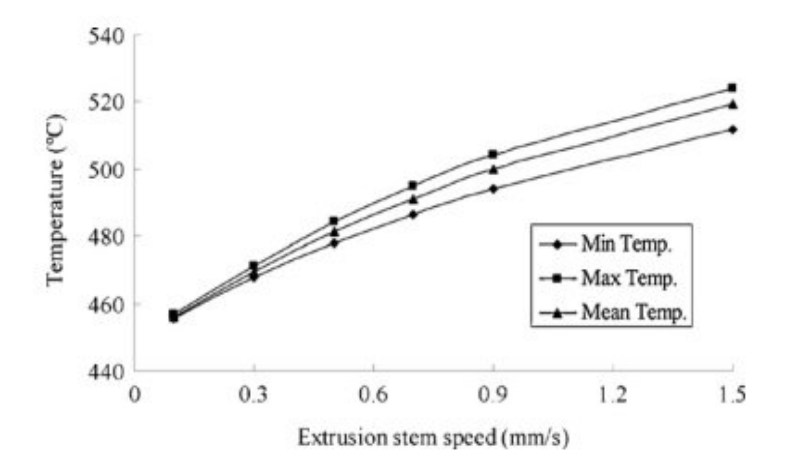


Figure 2.12: Billet temperature variation at different stem speeds [36]

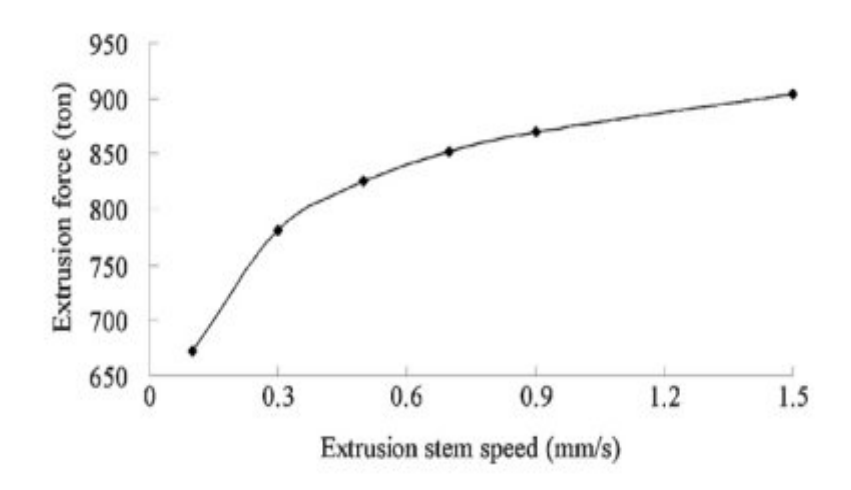


Figure 2.13: Plot of extrusion force vs. stem speed [36]

2.4.3. Relevance to Current Study

In this thesis, stem force data was recorded from real-time process monitoring equipment. The maximum stem force values were analyzed against various billet temperatures, ram speed, and dead cycle times. The study in this way identifies main cause-effect drivers of force variation and provides clues into the improvement of dimensional stability with force optimization in multichambered profiles.

2.4.4. Models and Industrial References

The literature comprises several empirical and analytical, and numerical models for predicting peak extrusion force. Sheppard's equation of 1999 relates material flow stress, die geometry, and container dimensions. Subsequent work by Duran et al. in 2004[37] introduced a model sensitive to temperature gradients, relying on finite-element techniques. More recently, Wei et al. in 2021 [38] suggested a data-driven approach with artificial neural networks (ANNs) for breakdown

extrusion force prediction in large-scale processes. These models show that while process parameters correlate, peak stem force can be reliably optimized by integrating material response, thermal management, and data-driven prediction approaches.

These findings provide the theoretical foundation for the analysis of the peak stem force data presented in Chapter 4, where specific relations with real process parameters are explored.

2.5. Effect of Chemical Composition on Extrusion Behavior

The chemical composition of aluminum alloys provides the foundation upon which extrusion performance should be defined, in particular, flow stress, temperature sensitivity, and peak stem force needs. In commercial use—such as in Benteler Automotive—extruded components are primarily made from the 6XXX and 7XXX series aluminum alloys due to their strength-to-weight ratio, corrosion resistance, and formability. Nevertheless, their different alloying elements offer a different extrusion behavior with direct application to process stability as well as dimensional control.

2.5.1. Overview of 6000 and 7000 Series Alloys

The 6XXX series alloys (typically Al-Mg-Si based) have widespread usage in structural and automotive components due to their good extrudability and modest heat-treated strength. The principal strengthening phases— Mg_2Si —enable good extrudability-strength trade-off. In comparison, 7XXX series alloys (Al-Zn-Mg-Cu based) have significantly greater strength but at the cost of greater flow resistance, especially during hot working, and are therefore more exacting in terms of peak extrusion loads and thermal control [39].

2.5.2. Impact on Peak Stem Force and Extrusion Properties

On the processing front, 7XXX series alloys exhibit greater peak stem forces due to their greater flow stress and reduced hot workability. The additional elements especially Zn and Cu raise the recrystallization temperature and reduce the flowability of the material at normal extrusion temperatures. The alloys therefore require high billet temperatures and die heating stringently controlled in order to obtain acceptable extrusion speeds and avoid tool overload. [40].

Conversely, 6XXX series alloys tend to need lower peak stem force and more stable flow conditions and thus are suitable for thin-walled or complex profiles. Additionally, they are sensitive to balance between Mg and Si, such that minor deviation in composition leads to inhomogeneous flow and dimensional variations like twist or wall thickness inconsistency[9].

2.5.3. Implication for Dimensional Accuracy

Dimensional accuracy depends on alloy chemistry. Non-uniform chemical composition or low homogenization alloys can form localized hard zones, which are deformation-resistant and can lead to asymmetrical flow when extruded. This will create straightness deviation, twist, or non-uniform wall thickness, particularly in multi-chambered profiles. These effects are emphasized in dies with non-symmetrical flow channels or asymmetrical chamber distribution.[41]

2.6. Summary of Literature Gaps and Justification for the Study

Literature covered in this chapter provides a general view of the aluminum extrusion process and particularly how dimensional tolerances, extrusion force modeling, and the influence of alloy composition are implicated. Various pioneering studies have outlined extrusion mechanics[11], the role of process parameters[15],[33],[36] and standards for dimensional accuracy specification (DIN EN 755-9:2016-10)[5]. Along with that, the focus has been highlighted on the significance of billet temperature, dead cycle time, and alloying elements on extrusion behavior.

Despite such progress, some fundamental gaps remain:

Limited Industrial Case Studies: The majority of literature remains theoretical or performed under controlled laboratory conditions. An apparent lack exists of literature based on real-world industrial data especially high-volume automotive extrusion plants to examine peak stem force behavior and dimensional variability.

Lack of Data Analysis: Due to confidentiality restrictions, raw industry extrusion data are rarely available. Results based on actual data are presented in few studies, making it difficult to cross-validate results across different manufacturing setups. This thesis overcomes this limitation by using production data without losing statistical validity and confidentiality.

Underrepresentation of Multi-Chamber Profiles: Symmetric or single-chamber profiles are the subject of most modeling and tolerance research. Multi-chambered aluminum profiles employed in the automotive crash management systems possess certain flow issues that influence stem force as well as the dimensional accuracy. Multi-chambered aluminum profiles are underrepresented in research.

Dissociated Geometry and Force Analysis: Past studies often dissociate dimensional deviations and extrusion force. No integrated analysis has been employed that connects geometric deviations (e.g., twist, straightness), process parameters and peak stem force behavior in a production environment.

With such limitations, the current investigation makes notable contributions by:

Examining the correlation between peak stem force and key process parameters using real production data.

Focusing on multi-chambered profiles, which are critical in automotive structural components.

Establishing direct correspondence between the deviations in size (i.e., straightness and twist) and extrusion behavior, offering insight into optimizing the process.

Probing within data analysis as a way to extract useful trends while maintaining industrial confidentiality intact. The foregoing aspects make the study a useful practical and academically new contribution to aluminum extrusion research, particularly for automobile manufacturing.

Chapter 3 Methodology

3.1. Research Design and Methodology

This thesis applies a quantitative, case-study research methodology to investigate dimensional variation and extrusion force behavior i.e., peak stem force of multi-chambered aluminum profiles manufactured in Benteler Automotive. The research was conducted in close cooperation with production and quality control personnel at the company based on real process data obtained under actual industrial operating conditions.

The study aims to analyze the relationships between process parameters (billet temperature, dead cycle time, ram speed) and peak stem force and differences in dimensions (twist, straightness, wall thickness) arising in the resulting profiles. The selected research method is exploratory-descriptive augmented with statistical correlation and trend analysis tools using Excel and Python. This method enables patterns and potential dependency among the variables to be identified without the use of complex simulation models or destructive testing.

This method represents a bottom-up industrial research in which fieldwork begins at the process line and data are gathered, cleaned, and then analyzed to make inferences of relationship. The research is therefore context-driven, focusing on optimizing dimensional stability and extrusion force performance within production limits in Benteler. While the findings provide helpful insights, their extension to extrusion systems or materials outside those examined may be limited without further validation.

3.2. Data Collection

This section explains the data collection approach taken to obtain the process and dimensional parameters related to aluminum profile extrusion. Data were collected from shop floor measurement systems and manual quality checks. The acquired datasets include measurements of wall thickness, straightness, chemical compositions and twist, as well as process parameters such as peak stem force, billet temperature, ram speed and dead cycle time.

3.2.1. Wall Thickness Measurements

The principal strength of this work is the availability of large quantities of real production data. To obtain wall thickness measurements directly, automated measurement tools on the shop floor were used. Wall thickness was taken at selected profile points by means of automated noncontact gauges. The gauges were internally calibrated by using quality procedures, and readings were entered directly into the production database. The profiles studied are:

RAB5954: 37,005 samples in 214 batches (2018–2024)

RAB6146: 69,037 samples in 351 batches (2018–2024)

RAB6782: 8,847 samples in 70 batches (2021–2024)

The readings were made at designated die positions (e.g., Pos 03, Pos 14, Pos 28, etc.) for the front (Position 1) and back (Position 2) parts of the extruded billets. Sampling was conducted with varying die conditions to facilitate an efficient assessment of dimensional stability.

Specifications for each profile—wall thickness values as well as the respective Upper Specification Limit (USL) and Lower Specification Limit (LSL) were sourced from engineering drawings and used as reference values. Data accuracy and consistency were ensured by consistent sampling patterns and the use of calibrated measuring equipment.

3.2.2. Straightness and Twist Measurements

Straightness and twist dimensional fluctuations were obtained manually from the shop floor using a range of feeler gauges from 0.01 mm to 1.00 mm. The 27 extruded profiles considered those made from the front, middle, and rear billet position.



Figure 3.1 : Feeler gauges (0.01 to 1.00 mm)

In order to further enhance reliability, straightness and twist were also measured with a Coordinate Measuring Machine (CMM) to allow cross-validation between manual and automated techniques. Having both manual and automatic techniques provided a higher level of confidence in measurements and allowed verification of accuracy and limitations of manual techniques within the industrial setting.

Straightness: Measured as the greatest gap between profile and reference straight edge by application of feeler gauges.

Twist: Measured as a function of rotational displacement across the profile cross-section at different points. For straightness, DIN EN 755-9:2016-10 standard specifies a limit of 1.5 mm per metre of profile length. For twist, the standard sets a tolerance of 0.6 mm per 300 mm length, which remained the applicable limit for each measured segment. Figure 3.2 shows the measurement setup of twist and straightness using a feeler gauge and figure 3.3 shows various type of multi-chambered Aluminum profiles.

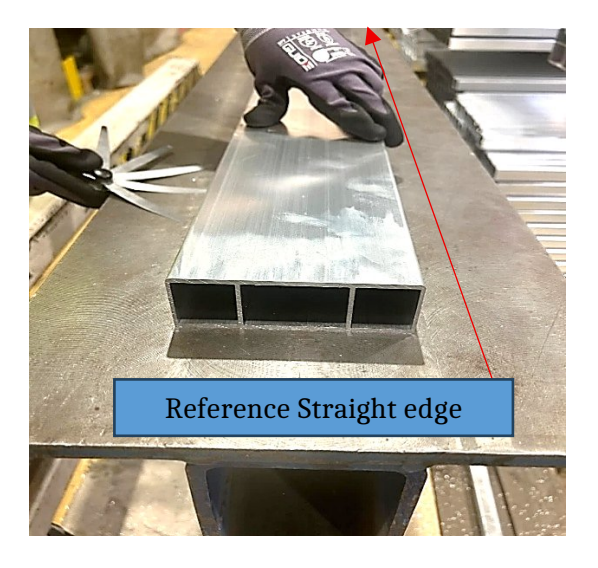


Figure 3.2 : Measurement setup of straightness and twist

Figure 3.3: Multi-chambered Aluminum profiles

3.2.3. Process Parameters and Chemical Composition

In addition to measurements of dimensions, process data were also quantified to analyze how extrusion conditions interact with maximum stem force. These data sets are:

Peak Stem Force: Measured from online process monitoring systems.

Billet Temperature: Recorded for each extrusion cycle.

Dead Cycle Time: Time between two successive billets, measured through press control system.

In addition to process conditions, chemical composition data of billets used for selected profiles was gathered from Benteler's internal records. These included elemental composition (e.g., Mg,

Si, Zn, Fe, Cu, Mn) relevant to the aluminum series. Chemical data were used to investigate potential interactions between alloying elements and peak stem force variation.

This chapter presented the measurement of wall thickness, twist, straightness, and process data to be employed for dimensional variation and extrusion performance. The integration of both manual and automatic data, as well as historical datasets, provides a full basis for the subsequent analysis in Chapter 4.

3.3. Data Preprocessing and Cleaning

Raw data collected from Benteler's shop floor was subjected to a systematic preprocessing phase to make it accurate, consistent, and usable for statistical analysis prior to it. The sets of data contained automated as well as manual measurements such as wall thickness, maximum stem force, temperature of billet, twist, straightness, and chemical composition. Due to the nature of the industrial environment, some amount of variability and noise were expected that needed proper filtering and structuring.

3.3.1. Validations and Cleaning of Wall Thickness Data

There was substantial wall thickness data comprised of more than 114,000 measurements of three aluminum profiles (RAB5954, RAB6146, and RAB6782). The datasets were first filtered out for errors and inconsistencies in measurements:

Missing Values: Missing thickness values or missing position labels in entries were excluded from analysis to maintain dataset integrity.

Outlier Detection and Removal: Statistical thresholds (typically beyond ±3 standard deviations of the mean) were employed to detect outliers, and validated through visual inspection using boxplots and histograms. Suspected logging or equipment mistakes were removed.

Consistency Checks: Position numbers (front = 1 and rear = 2) and measurement points (e.g., Pos 03, Pos 14, Pos 28) were inspected against drawing specifications.

Batch Filtering: Batches with only measurements at front and rear positions were retained to ensure statistical comparison has symmetry.

3.3.2. Preprocessing of Process Parameters

Online monitoring system data and control log data for billet temperature, dead cycle time, and peak stem force were collected. To ensure confidentiality requirements:

Synchronization: The measurements were synchronized by batch number and combined with corresponding data to ensure temporal correspondence among parameters.

Unit Standardization: Units were standardized to the SI system, with temperature in degrees Celsius (°C), thickness in millimeters (mm), and time in seconds (s).

Although values were used in statistical analysis, actual wall thickness values were kept in plots such as histograms and process capability indices (Cpk), as confidentiality constraints were not placed on these dimensions.

3.3.3. Twist and Straightness Data Processing

Twist and straightness manual readings were recorded with feeler gauges (0.01–1.00 mm range) and in sample instances, verified with a Coordinate Measuring Machine (CMM). Values were preprocessed as follows:

Position Classification: The recorded measurements were classified into front, middle, and rear billet positions to evaluate the trend of deformation along the extrusion length.

Error Elimination: All data with inconsistent measurement methods (i.e., feeler gauge measurements combined with CMM measurements without associated samples) were eliminated.

3.3.4. Chemical Composition Data

Chemical composition data for each billet was obtained from the Benteler quality control system. These measurements were cross-checked with respective batches and profiles:

Standardization: Chemical elements were given as weight percentages and grouped according to alloying type (e.g., Si, Fe, Cu, Mn, Mg, Zn).

Label Matching: Billet IDs and extrusion batches were used to match composition data to the appropriate force and wall thickness measurements.

The structured preprocessing ensures high data integrity and statistical significance so that robust analysis is enabled in subsequent chapters. Both industrial traceability and scientific reproducibility were prioritized during the process.

3.4. Data Analysis

Analysis of data in the present thesis entailed various steps in order to investigate dimensional stability and force behavior of extruded aluminum profiles. The analysis was focused on several broad topics: variation of wall thickness, twist and straightness deviation, and influence of process parameters on peak stem force. The chemical composition of the billet was also investigated for its potential impact on stem force.

3.4.1. Wall Thickness Evaluation

The basis of the dimensional analysis was an analysis of variation of wall thickness across three aluminum profiles—RAB5954, RAB6146, and RAB6782. Profiles were measured at several predefined positions (e.g., Pos 03, Pos 15, Pos 28), with thickness taken at both the front (Position 1) and rear (Position 2) of the billet. Measurement data drawn directly from shop floor comprised in excess of 110,000 samples across several years of production (2018–2024).

For each profile and position, the key descriptive statistics were derived, i.e., the mean, standard deviation, and percentiles. These were giving an initial look at the spread of data and helping in detecting anomalous variations. The measurements were also compared with the engineering specifications—Upper Specification Limit (USL), Lower Specification Limit (LSL), and Nominal values. Cases when measured values deviated beyond the specification limits were highlighted for closer investigation.

Process capability indices (Cpk) were then computed to ascertain whether the process was stable in producing within specified limits. Any Cpk > 1.33 was considered to be reflective of a capable process. For example, RAB5954 Pos 12 (Front) had its Cpk computed to be 1.82, confirming excellent process stability. Surprisingly, rear-end reading had a tendency to reflect a bit more variation, which suggests slight deformation due to material flow towards the end of the tail of extrusion.

3.4.2. Twist and Straightness Deviation Analysis

For the geometric conformity of profile analysis, twist and straightness were measured manually using a 0.01 mm to 1.00 mm feeler gauge. The measurement was carried out on 27 profiles in various die conditions and at front, middle, and rear billet positions. For straightness, the standard specifies a limit of 1.5 mm per metre of profile length; this was proportionally adjusted to 1.35 mm for the 900 mm samples measured in this work. For twist, the standard sets a tolerance of 0.6 mm per 300 mm length, which remained the applicable limit for each measured segment. For some of the samples, a Coordinate Measuring Machine (CMM) was also utilized for the verification of manual measurement accuracy.

This dual-measurement technique provided comparative validation, determining that the manual procedure using feeler gauges is a reliable alternative in production conditions. Twist was measured as deviation from planarity, while straightness deviation was the measure of longitudinal curvature along the profile length. Inspection indicated that rear-end regions were more prone to both twist and straightness deviation, most likely due to non-uniform exit flow or die wear towards cycle end.

3.4.3. Impact of Process Parameters on Maximum Stem Force

One of the central part of this thesis was to investigate the impact of the process parameters of extrusion on maximum stem force, rather than cumulative extrusion force. Process information like billet temperature, ram speed, and dead cycle time was sampled from the shop floor.

Scatter plots and regression equations were created using Python to graph and examine the relationship. The analysis found that higher billet temperature and lower dead cycle time were found to be correlated with lower peak stem force, likely due to greater material ductility and heat distribution within the die. Higher dead cycle times or reduced die temperatures, however, caused sudden surges in peak force, which reflected poorer forming conditions.

3.4.4. Chemical Composition Effects

In addition to the process conditions, chemical composition data of billets—provided by Benteler were also examined for their impact on peak stem force. Particular focus was placed on variations in elements such as Magnesium (Mg) and Zinc (Zn), which affect the flow stress of the material and, consequently, extrusion force that would be required.

Correlation analysis revealed small but repeatable trends wherein increased Mg content led to slightly greater peak forces. While these effects were not dominant, they suggest that slight chemical differences can be a source of force scatter and potentially an influence in die design or billet selection in applications where quality is an important consideration.

3.4.5. Data Visualization and Statistical Tools

For the analysis support, Python packages like Pandas, Matplotlib, Seaborn, and SciPy were utilized. Histograms for all profiles were plotted for the description of thickness distribution at varied positions of dies with vertical reference lines being USL, LSL, and Nominal values. Overlaid histograms were used to compare front and rear readings so that a visual process symmetry or process imbalance inference could be drawn. Scatter plots were created for tracking trends among process parameters and peak stem force, while correlation matrices were used in an attempt to numerically capture inter-variable relationships. These graphical tools played a fundamental role in rendering raw data into intelligible implications, guaranteeing stability within the analysis.

3.4.6. Summary

This article provided a thorough profiling of dimensions and force of extrusion behavior on the basis of structured data analytics methodology. Wall thickness analysis showed global process stability, and straightness and twist analysis testified to the validity of manual measurement techniques. Impacts of the most critical process parameters —billet temperature, dead cycle time and chemistry of the billet on peak stem force were statistically analyzed and plotted, explaining factors influencing dimensional accuracy and efficiency of the process.

These analyses form the empirical foundation for the ensuing discussion in Chapter 4, where results are interpreted and brought into relation with production performance and industrial importance.

3.5. Software and Tools

A combination of industrial-scale measurement systems and high-level computational tools was employed in this research to ensure precise data collection, accurate processing, and dependable statistical analysis. Benteler's automated inline gauge system provided wall thickness measurements by capturing readings at defined die positions and recording corresponding billet number, die number, and billet position (Front or Rear). Straightness and twist manual readings were obtained with a 0.01 mm to 1.00 mm feeler gauge set. Manual measurements were confirmed by utilizing a Coordinate Measuring Machine (CMM) with high-resolution dimensional inspection, enabling direct comparison of the manual and automatic techniques.

Peak stem force and related process parameters i.e., billet temperature, ram speed, and dead cycle time were directly obtained from Benteler's proprietary data logging system. These data sets were synchronized with records of dimensional measurements so that correlation analysis of the process conditions against product quality could be performed.

Data preprocessing, statistical calculations, and visualization were conducted in Python 3.x, using Pandas and NumPy libraries to support the handling and calculation of structured data. Matplotlib and Seaborn libraries were used for generating histograms, scatter plots, and trend lines, enabling the visual determination of patterns and outliers. Microsoft Excel was used for preliminary investigation of the data, quick descriptive summaries, and checking of computational outcomes.

The integration of precise measurement hardware with versatile computational software ensured that all analysis was performed on high-fidelity data sets, thereby enhancing the repeatability and reliability of results. The methodology provided a solid foundation for the evaluation of dimensional variability and the identification of the influence of process variables on peak stem force in industrial extrusion processing.

This chapter presented the research design, data sources, and methods of analysis applied to investigate the inter-relationships between process parameters, chemical composition, peak stem force, and dimensional variation in multi-chambered aluminum profiles. By combining actual factory production data with good statistical analysis and visualization techniques, the method is designed to ensure that the results derived are industrially relevant as well as compliant with confidentiality requirements. The following chapter demonstrates the results resulting from this methodology framework.

Chapter 4 Results and Discussion

4.1. Main Observations and overview of Data

Major observations on the study of multi-chambered aluminum profiles extrusion process data are presented in this chapter. The study encompasses dimensional measurement (straightness, wall thickness, twist), maximum stem force, and their relationship with chemical composition and process parameters.

Data for several production batches were utilized to determine pattern and deviation effects on profile quality and process stability. Initial findings suggest variation with front and rear billet positions and correlations of maximum stem force with parameters like billet temperatures, ram speed and chemical composition.

In-depth descriptions of these parameters are presented in the subsequent sections to assist with optimization efforts for the process.

4.2. Wall Thickness Analysis

Wall thickness in aluminum profiles is a significant structural stability and functional performance determining dimension. During the research, three profiles, namely RAB5954, RAB6146, and RAB6782, were studied using large datasets collected from Benteler Automotive assembly line.

I. Profile 1: RAB5954

Outside Body Wall Dimensions -

Main Findings:

- Front Measurements at Position 14 are evenly distributed around the nominal value; no remarkable deviations were detected.
- Rear measurements at Pos 15 and Pos 17 indicate a wider scatter.

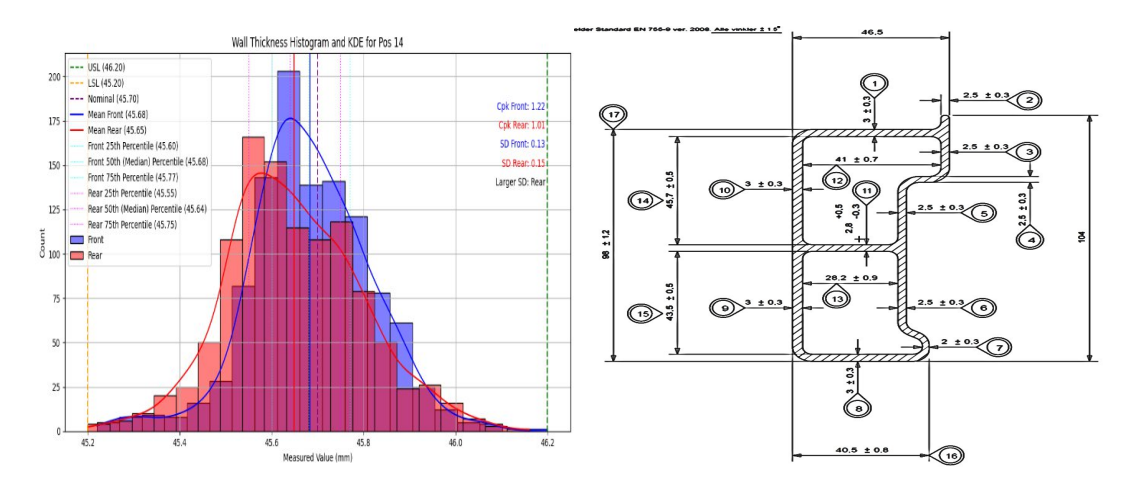


Figure 4.1 : Histogram for RAB5954, Pos 14, showing a uniform distribution near the nominal value.

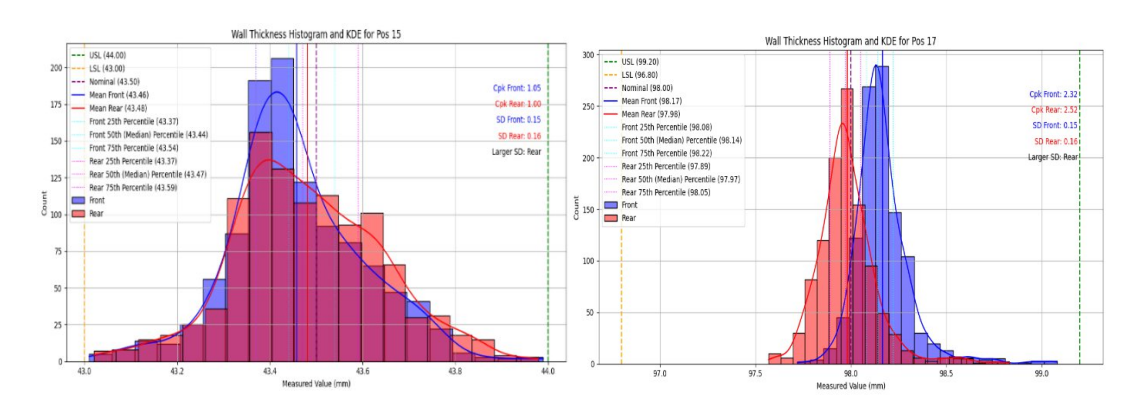


Figure 4.3: Histogram for RAB5954, Pos 15 Figure 4.4: Histogram for RAB5954, Pos 17

• Cpk Analysis-

- Cpk for Front: Ranges from 0.54 (Pos 9) to 2.36 (Pos 13).
- Cpk for Rear: Ranges from 0.61 (Pos 07) to 2.52 (Pos 17).
- Process Capability: Many positions have Cpk values below 1.33, indicating marginal process capability at several positions.

Percentile Analysis Summary-

- Front measurements generally show tight distributions around the nominal values, with the 50th percentile (median) typically close to the target value, indicating good process consistency.
- Rear measurements exhibit more variability, with wider percentile ranges observed.

Mandrel Chamber Dimensions-

Main Findings:

- The front dimensions are all approximate to the nominal values with only slight variations.
- Rear readings are still within tolerance but show a bit more spread.

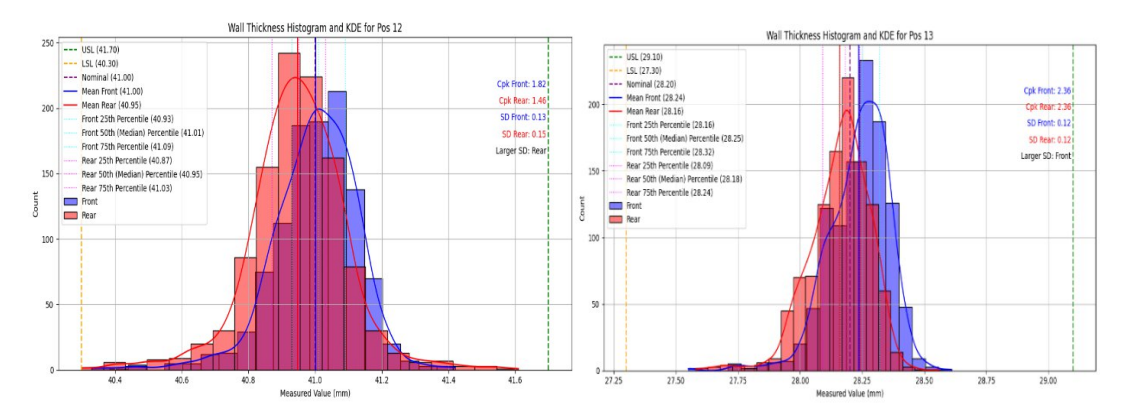


Figure 4.5: Histogram for RAB5954, Pos 12

Figure 4.6: Histogram for RAB5954, Pos 13

■ <u>Internal Wall Thickness</u>-

Main Findings:

- Front measurements are stable and close to nominal values and minor deviations are observed in Pos 09 and Pos 10.
- Rear readings are Broader spread and more deviations at Pos 3 and Pos 5 whereas some points exceed LSL.

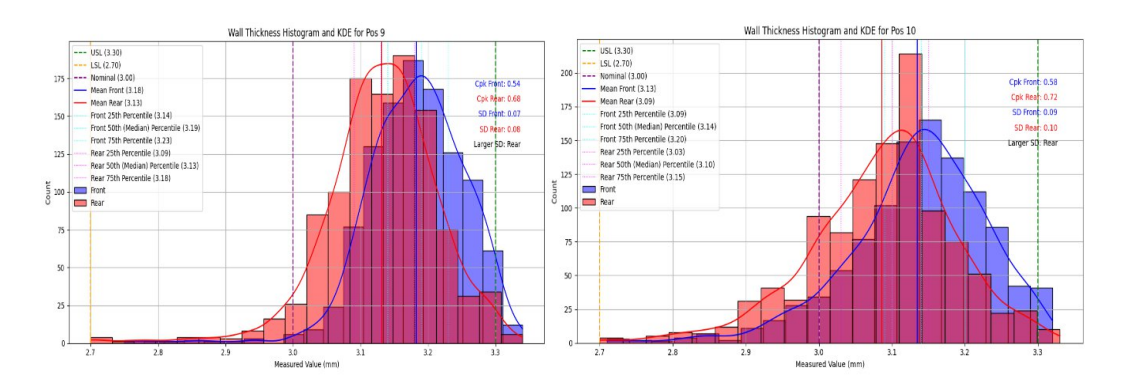


Figure 4.7: Histogram for RAB5954, Pos 9.

Figure 4.8: Histogram for RAB5954, Pos 10.

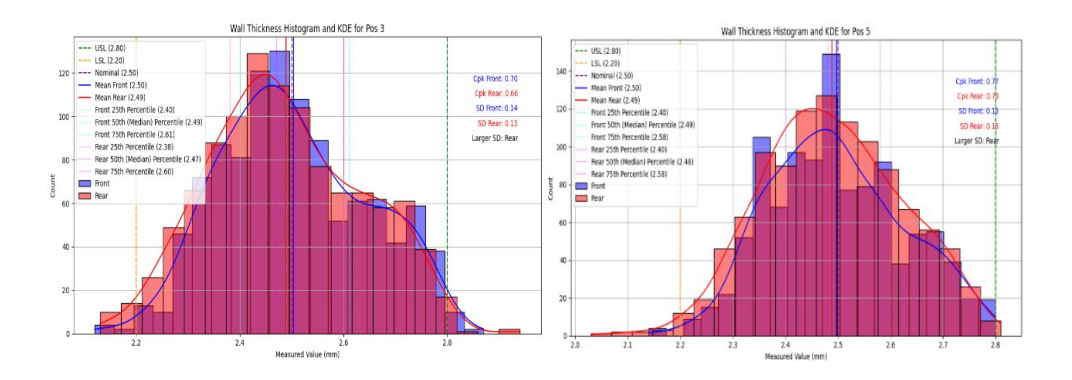


Figure 4.9: Histogram for RAB5954, Pos 3.

Figure 4.10: Histogram for RAB5954, Pos 5

II. Profile 2: RAB6146

Outside Body Wall Dimensions-

Main Findings:

- Both Front and Rear measurements are tightly distributed within USL and LSL, which means the extrusion processes are stable. Rear deviations are minimal compared to the Front.
- Pos 37 shows minor Front and Rear measurement fluctuations close to USL and Pos 28 shows more deviation in front.

• Cpk Analysis:

- Front: Cpk values range from 0.45 (Pos 16) to 1.44 (Pos 30).
- Rear: Cpk values range from 0.45 (Pos 16) to 1.57 (Pos 30).
- Stable positions include Pos 30, with both Front and Rear measurements demonstrating high process capability.

Percentile Analysis:

- Positions with low Cpk values, such as Pos 37 and Pos 16, have broader percentile spreads, especially for Front measurements.
- Stable positions like Pos 30 show compact percentiles with minimal deviations.

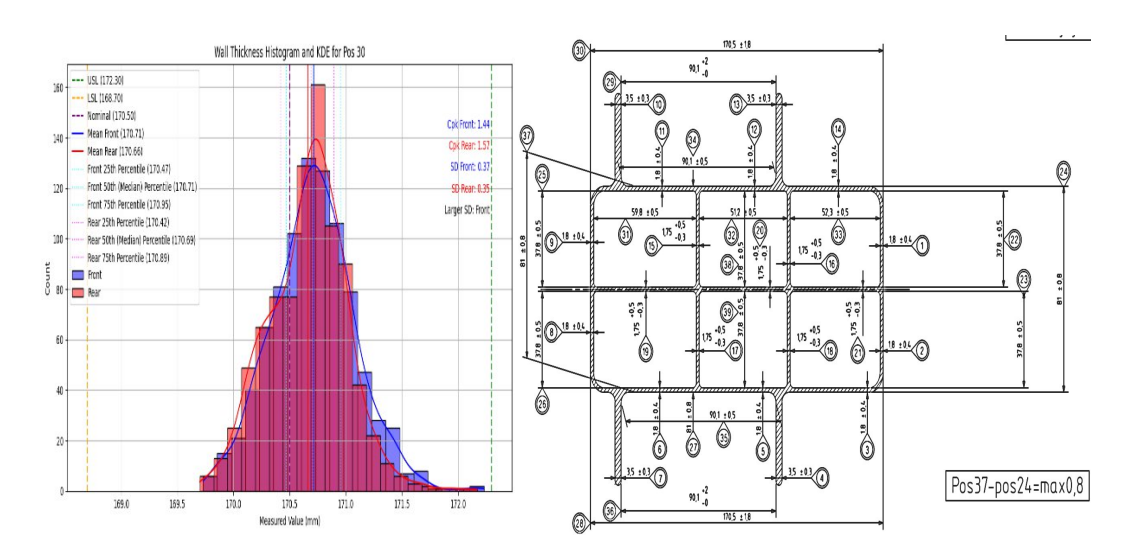


Figure 4.11: Histogram for RAB6146, Pos 30

Figure 4.12: Profile RAB6146

Mandrel Chamber Dimensions-

Main Findings:

• Rear measurements have tighter distributions than Front, which indicates stable material flow.

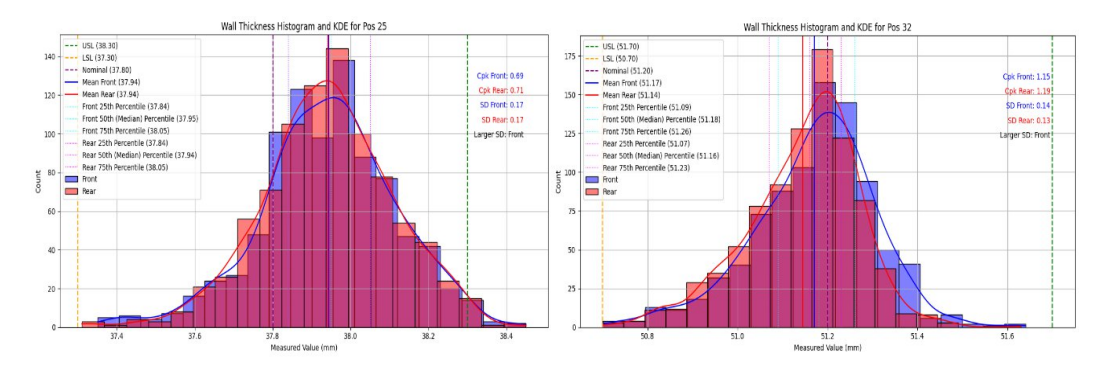


Figure 4.13: Histogram for RAB6146, Pos 25. Figure 4.14: Histogram for RAB6146, Pos 32

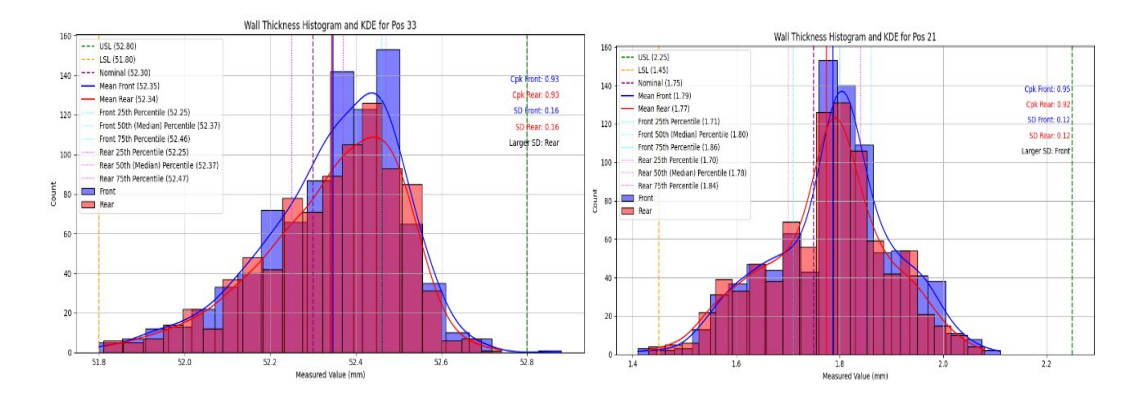


Figure 4.15: Histogram for RAB6146, Pos 33. Figure 4.16: Histogram for RAB6146, Pos 21

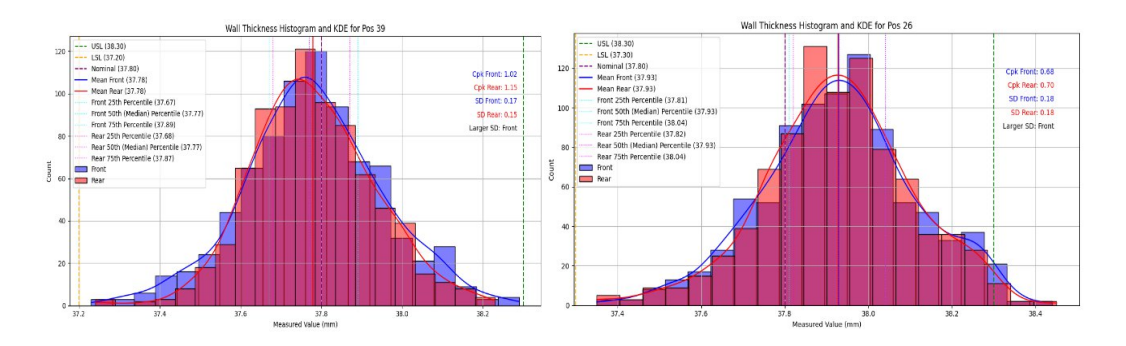


Figure 4.17: Histogram for RAB6146, Pos 39. Figure 4.18: Histogram for RAB6146, Pos 26.

Internal Wall Thickness-

Main Findings:

Rear deviations at Pos 15, and Pos 18 are beyond LSL, and front deviations at Pos 16, and Pos 17 are near to USL.

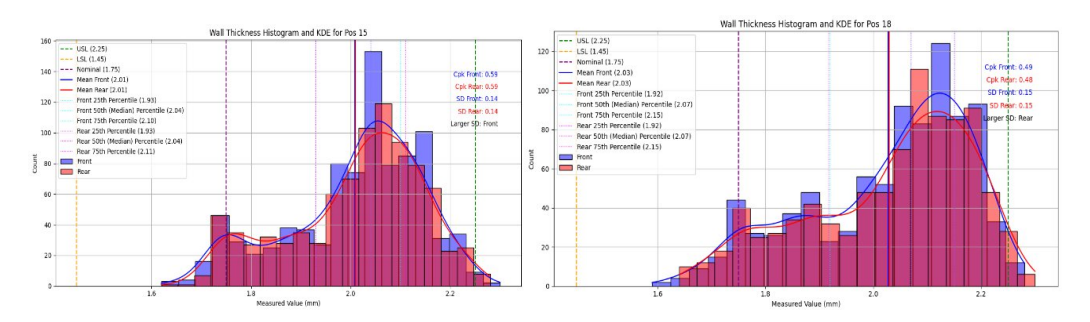


Figure 4.19: Histogram for RAB6146, Pos 15

Figure 4.20: Profile RAB6146, Pos 18

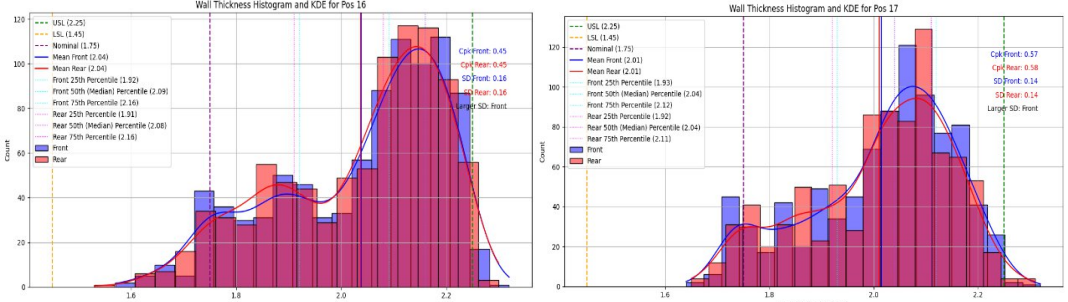


Figure 4.21: Histogram for RAB6146, Pos 16

Figure 4.22: Profile RAB6146, Pos 17

III. **Profile 3: RAB6782**

Outside Body Wall Dimensions-

Main Findings:

- Front distributions are tighter and closer to nominal values.
- Rear measurements at Pos 14 show much higher deviations, indicating cooling variations.

Cpk Analysis-

- Cpk for Front: Ranges from 0.35 (Pos 06) to 2.28 (Pos 11), indicating that the Front measurements are mostly close to the nominal value, but some positions (like Pos 06) need improvement.
- Cpk for Rear: Ranges from 0.47 (Pos 06) to 2.12 (Pos 11). Similar to the Front, the Rear measurements also show significant variability, with several positions not meeting the Cpk > 1.33 threshold.
- Process Capability: The process particularly at Pos 06 and Pos 08 is not capable with Cpk values mostly below 1.33.

• Percentile Analysis-

 The Front percentile distribution shows that most values are around the nominal, while Rear has a slightly higher spread, indicating some rear sections are deviating from the nominal.

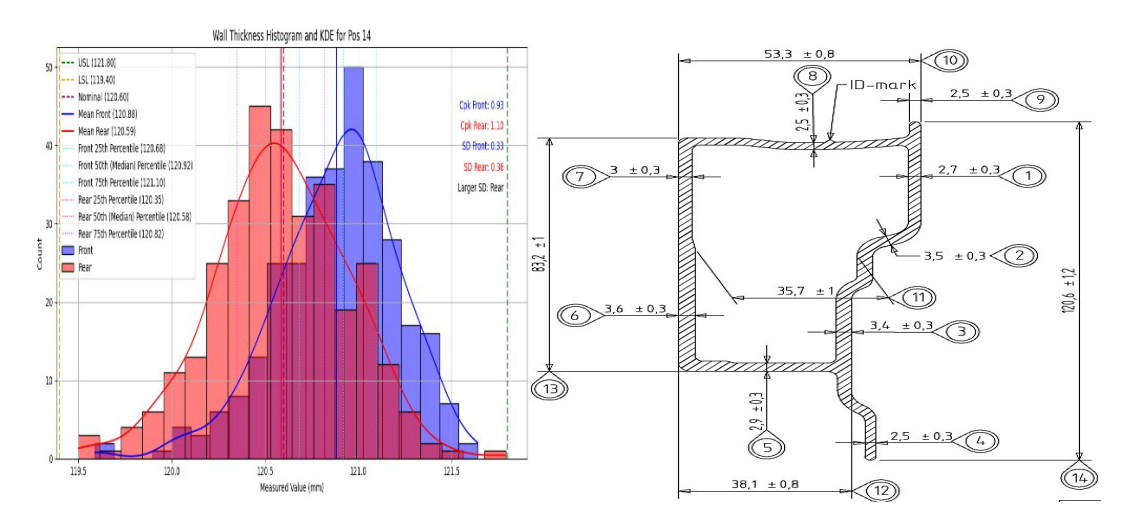


Figure 4.23: Histogram for RAB6782, Pos 14

Figure 4.24: Profile RAB6782

Mandrel Chamber Dimensions-

Main Findings:

• Front sizes are all nominal, but the Rear dimension at Pos 11 differs slightly from nominal.

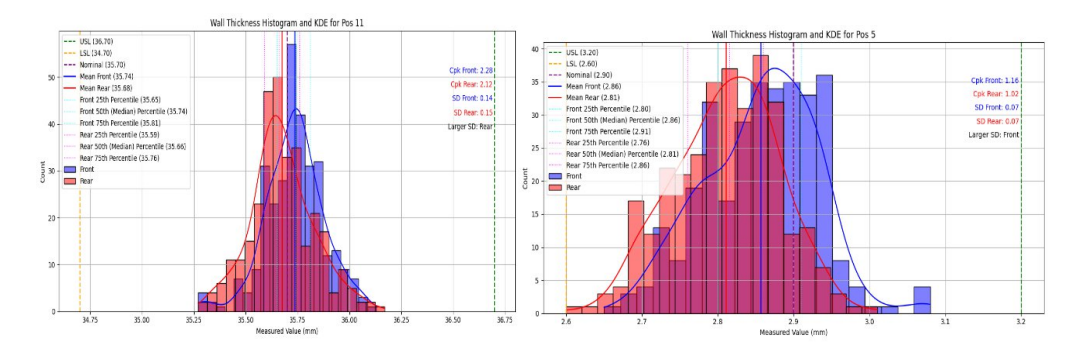


Figure 4.25: Histogram for RAB6782, Pos 11

Figure 4.26: Profile RAB6782, Pos 5

Internal Wall Thickness-

Main Findings:

• Front at Pos 03 exceeds the USL, but the Rears measurements are stable across most positions.

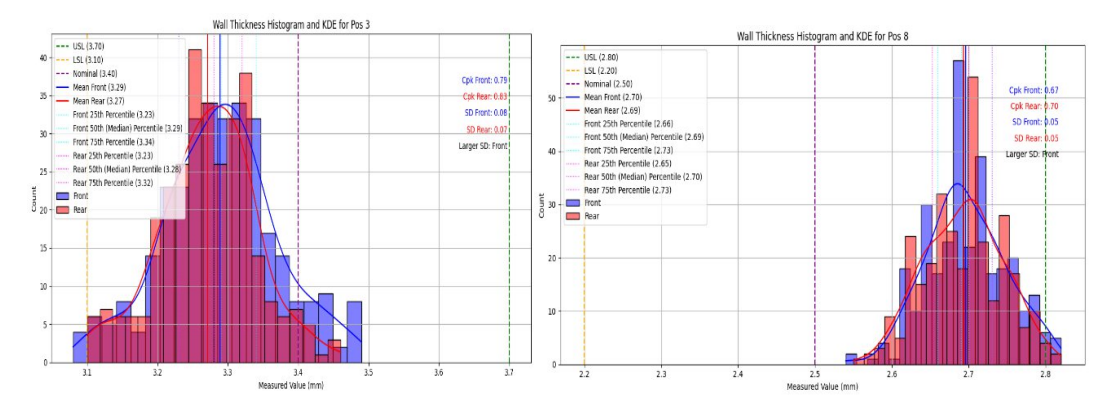


Figure 4.27: Histogram for RAB6782, Pos 3

Figure 4.28: Profile RAB6782, Pos 8

4.3. Dimensional Deviations: Straightness and Twist

Dimensional precision in extruded aluminum profiles is a vital quality requirement for automobile applications, where precision fit and structural integrity are of paramount importance. The two significant geometric parameters straightness and twist were quantified based on the tolerance requirement of the DIN EN 755-9:2016-10 standard within this study. For straightness, the standard specifies a limit of 1.5 mm per metre of profile length; this was proportionally adjusted to 1.35 mm for the 900 mm samples measured in this work. For twist, the standard sets a tolerance of 0.6 mm per 300 mm length, which remained the applicable limit for each measured segment.

Measurements were taken at three positions of the billet length of front, middle, and rear to establish positional effects on dimensional stability. Straightness deviations were measured using feeler gauges (having a resolution of 0.01 mm) and also by a coordinate measuring machine (CMM) for having accuracy and reproducibility. Twist was measured per 300 mm segment by assessing angular displacement between reference faces. Table 4.1 represents straightness and twist values of profiles produced from different billet positions. The minimum, maximum, mean and % of tolerance of straightness and twist are also shown in Table 4.2.

Profile	Straightness	Straightness	Straightness	Twist Front	Twist Middle	Twist Rear
No	Front Billet	Middle Billet	Rear Billet	Billet Profile	Billet Profile	Billet Profile
	Profile	Profile	Profile			
1	0.1	0.08	0.12	0.05	0.03	0.08
2	0.12	0.14	0.18	0.07	0.05	0.1
3	0.15	0.12	0.25	0.06	0.08	0.13
4	0.12	0.2	0.25	0.09	0.07	0.15
5	0.14	0.16	0.22	0.08	0.09	0.12
6	0.15	0.18	0.25	0.09	0.1	0.14
7	0.12	0.15	0.2	0.07	0.06	0.1
8	0.1	0.1	0.25	0.08	0.09	0.11
9	0.12	0.15	0.35	0.06	0.05	0.13

Table 4.1 : Straightness and Twist Values of Profiles for Different Billet Positions

Pos.	Straightness	Straightness	Straightness	Straightness	Twist	Twist	Twist	Twist
	Min	Max	Mean	% of	Min	Max	Mean	%of
				Tolerance				Tolerance
Front	0.1	0.15	0.124	9.218	0.05	0.09	0.072	12.037
Middle	0.08	0.2	0.142	10.53	0.03	0.1	0.068	11.481
Rear	0.12	0.35	0.229	17.037	0.08	0.15	0.117	19.629

Table 4.2 : The min, max, mean and % of tolerance of straightness and twist

The results revealed a clear positional trend (Figure 4.29 and 4.30). Straightness deviations in the front position ranged from 0.10 to 0.15 mm, averaging 0.12 mm (approximately 9% of the tolerance limit). The middle position showed a slightly wider range (0.08–0.20 mm, mean 0.14 mm), corresponding to 10.5% of the limit. The rear position exhibited the highest deviations,

ranging from 0.12 to 0.35 mm, with a mean of 0.23 mm approaching 17% of the permissible tolerance. Twist measurements were the same trend: front position was 0.05-0.09 mm (mean 0.07 mm, 12% of tolerance), middle 0.03-0.10 mm (mean 0.07 mm, 11% of tolerance), and rear 0.08-0.15 mm (mean 0.12 mm, 19.6% of tolerance).

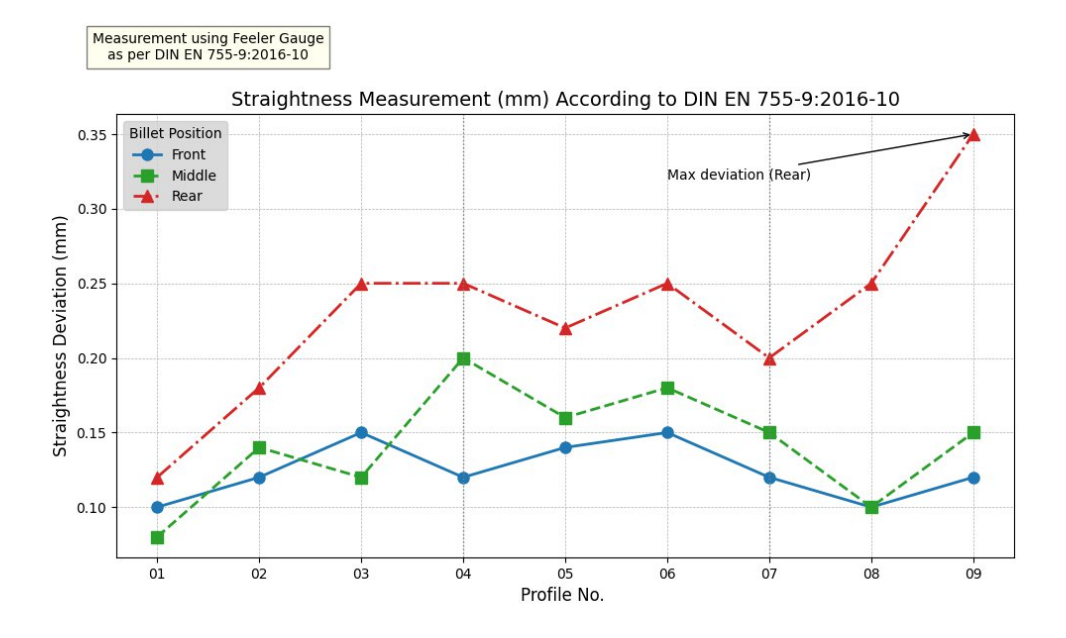


Figure 4.29: Straightness deviation Measurement

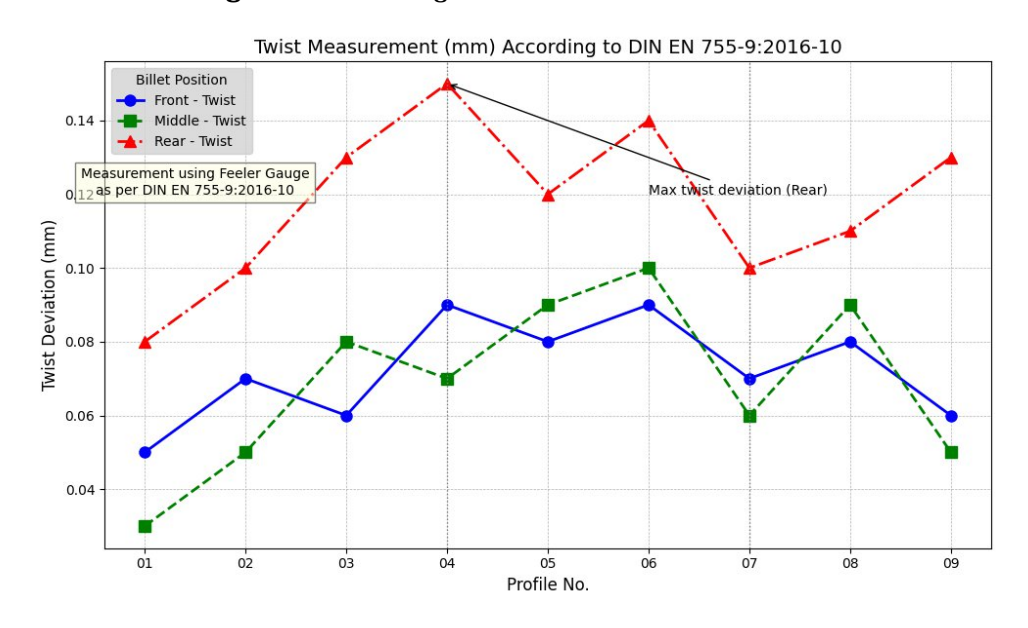


Figure 4.30 : Twist deviation Measurement

While all measured deviations were well within the DIN EN 755-9 limits, the consistent increase in both straightness and twist deviations towards the rear billet position is noteworthy. This is consistent with well-established extrusion behavior, since thermal gradients, non-uniform metal flow, and die wear toward the end of the extrusion cycle can reduce dimensional stability. These

phenomena, while below specification limits, may require process control measures to present even quality along the length of the billet.

To visually represent these findings, figures are prepared. Figure 4.31 is a grouped bar chart illustrating maximum deviations in straightness between the three billet positions with a horizontal reference line showing the tolerance limit of 1.35 mm. It also shows twist deviations per 300 mm section in a similar format, with the 0.6 mm tolerance clearly marked. The visual data reinforce the tabulated results and highlight the positional deviation patterns observed.

In summary, the profiles met all geometric requirements set by the relevant standard, but the systematic variation along the billet length suggests potential optimization opportunities in temperature control, billet handling, or die condition management. These findings complement the wall thickness and process parameter analyses, providing a holistic view of the dimensional quality in multi-chambered aluminum extrusion.

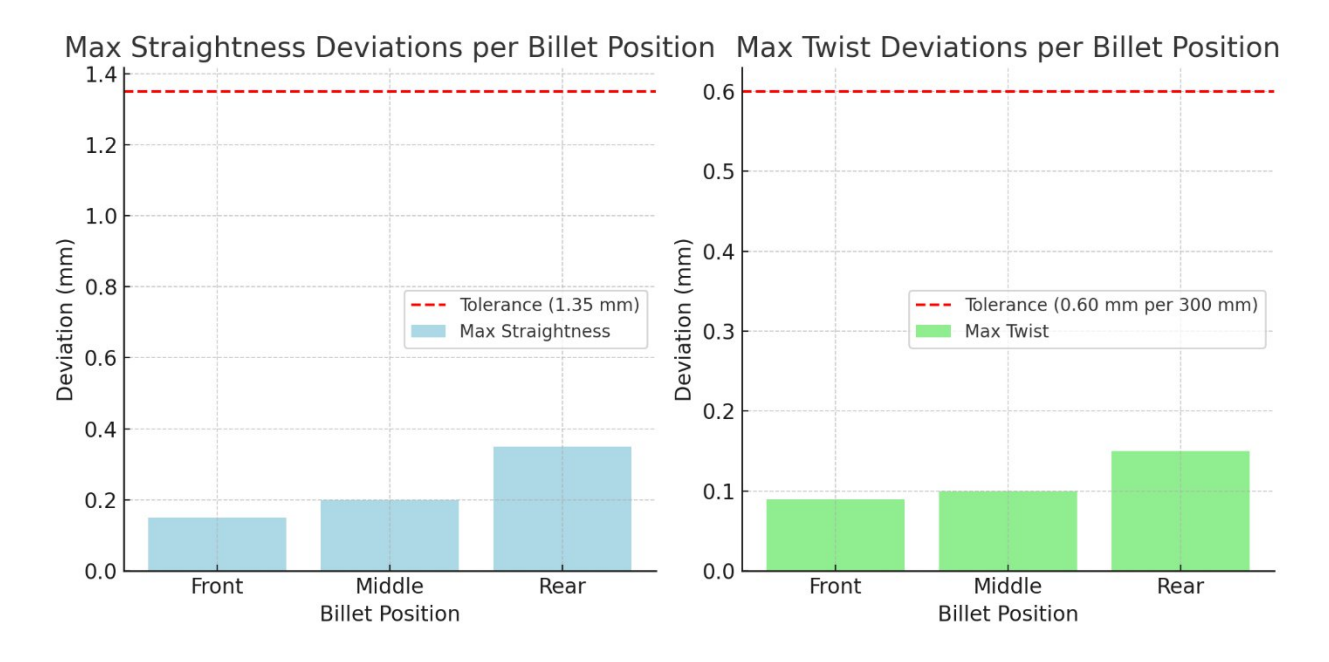


Figure 4.31: Max Deviations per Billet Position Straightness and Twist

For ensuring the reliability of manual measurements, a sample of rear billet profiles were also measured with a Coordinate Measuring Machine (CMM). CMM gave high-resolution values, generating continuous deviation curves along profile length. The trend of variation (Figure 4.32) being compared with feeler gauge values was, overall, consistent, setting the adequacy of the manual method to assess straightness and twist. However, the CMM captured more accurate local deviation and was more accurate at quantifying small-scale geometric variation.

The feeler gauge method, while simple and widely applied in industry, has certain drawbacks. Its accuracy would be compromised by the roughness of the straightedge reference surface, the presence of burrs or dust, and unevenness between the profile surface and the straightedge. Also, consistency of measurements and alignment of the operators play crucial roles in minimizing error. To prevent these, the profiles and straightedge were cleaned extensively before each measurement, and there was a uniform measurement plan that was implemented.

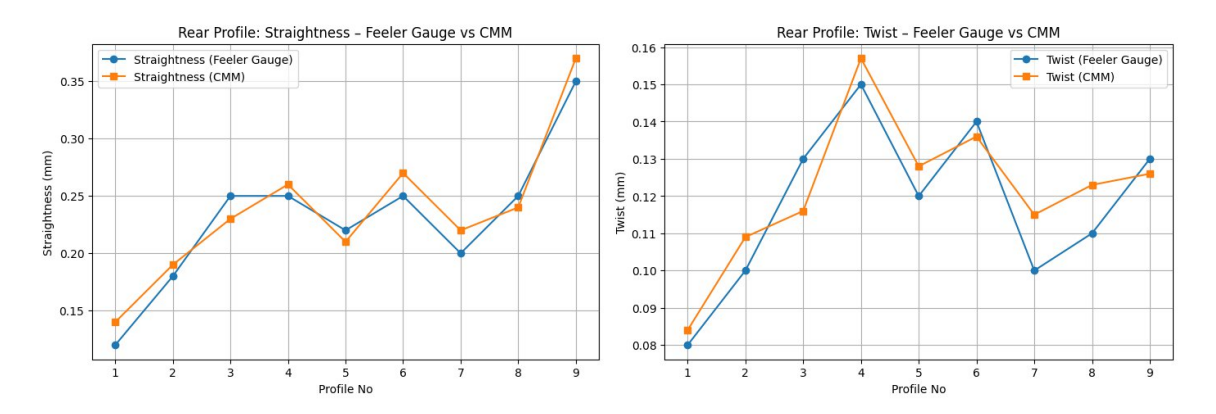


Figure 4.32: Measurement comparison between CMM and Feeler Gauge

Overall, the evidence indicates that the feeler gauge is a robust and reliable tool for routine checking of straightness and twist in production environments. For precise verification and scientific testing applications, the CMM nevertheless offers a finer level of reference. Continuing research might involve larger sample sets derived from CMM measurements, while retaining the feeler gauge as a more convenient method to rapid shop-floor testing.

4.4. Correlation Analysis of Process Parameters and Peak Stem Force

The heatmap (Figure 4.33) findings provide a detailed correlation analysis of process parameters of relevance, chemical composition, and Peak Stem Force on 7XXX series alloys extrusion on aluminum. This enables one to determine significant relationships that are imperative in optimizing the extrusion process. The outcome points out the influence of process factors such as Dead Cycle Time (DCT), billet temperature, and chemical composition on the peak stem force, which directly impacts extrusion efficiency and quality of the product.

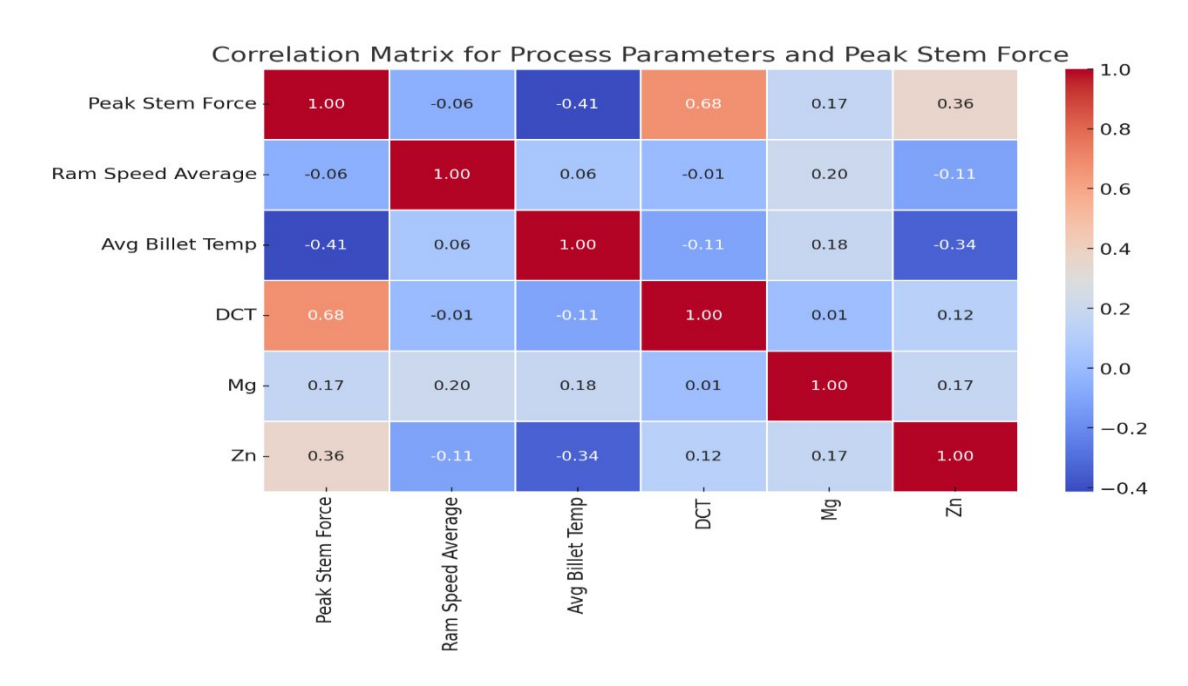


Figure 4.33: Heatmap for correlation analysis

Key Insights from the Correlation Heatmap:

(i) Peak Stem Force and Dead Cycle Time (DCT):Correlation: 0.68 (Strong Positive)

Peak Stem Force and Dead Cycle Time having high positive correlation implies that peak stem force also grows with an increase in Dead Cycle Time. Dead Cycle Time is the duration of time in the extrusion cycle when the ram doesn't move, and when this time, material gets hardened or resists flow, leading to growing forces when the ram starts moving again.

It is imperative to reduce Dead Cycle Time to maximize the extrusion process. Reducing DCT would help in reducing the build-up of force, and the material flow would be more efficient and smoother. The extrusion process has to be optimized so that idle time would be minimized in order not to have unnecessary force build-up, which could lead to inefficiency or excessive tool wear.

(ii) Peak Stem Force and Average Billet Temperature: Correlation: -0.41 (Moderate Negative)

The negative relationship between Peak Stem Force and Average Billet Temperature indicates that if the billet temperature is greater, the peak stem force needed would be lower. Increased billet temperatures lower the resistance of material to deformation and thus the work is easier to perform and requires less force. The temperature of the billet shall be optimized to prevent peak stem force. At elevated temperatures, the billet is soft, and therefore less energy is needed in its extrusion. Overheating, however, should be prevented as it changes the material properties. It is therefore extremely critical in the control of the billet temperature where maximum optimization of performance in extrusion is at stake.

(iii) Peak Stem Force and Magnesium (Mg) Content: Correlation: 0.17 (Weak Positive)

The weak positive relationship between Peak Stem Force and Magnesium (Mg) content leads to a moderate increase of magnesium in the alloy, consequently producing a moderate increase in strength with a resulting small increase in peak stem force. Magnesium tends to improve the strength and corrosion resistance of aluminum alloys. While the magnesium's effect on peak stem force is minimal, the factor must be considered when designing high-strength alloys. If the alloy's composition is altered to have higher levels of magnesium, the extrusion press would need slight adjustments to accommodate the increased force.

(iv) Peak Stem Force and Zinc (Zn) Content: Correlation: 0.36 (Moderate Positive)

There is a moderate level of positive correlation between Peak Stem Force and Zinc (Zn) content. Zinc serves to enhance the hardness and strength of aluminum alloys, which increases material resistance to deformation, hence the need for more force during extrusion.

The application of alloys with more zinc content ought to be related to slightly higher peak stem forces. This places a value premium on levels of extrusion press force capability and could necessitate equipment settings adjustment such as changes in ram speed or press force to account for the increased resistance.

(v) Peak Stem Force and Ram Speed: Correlation: 0.06 (Very Weak Positive)

The correlation between Peak Stem Force and Ram Speed is quite weak, thereby indicating that changes in ram speed have little effect on the peak stem force. Even though ram speed is crucial for a calculation of efficiency of the extrusion cycle, ram speed does not have any significant impact upon the force required in order to push material through a die.

The effect of ram speed on peak stem force is not statistically significant, but the key variables must be further optimized to optimize the value of other process variables in alloy composition and billet temperature to adequately address the force.

(vi) Average Billet Temperature on Zinc Content: Correlation: -0.34 (Moderate Negative)

The moderate negative correlation between Average Billet Temperature and Zinc (Zn) content indicates that higher zinc content will decrease billet temperature. This might be due to the variation in thermal characteristics between zinc and aluminum, such that alloys containing more zinc will be of lower thermal conductivity or heat-holding capacity.

This will imply that if zinc content needs to be higher in the alloy, the preheating of the billet can need to be modified. Zinc-rich alloys could require proper tuning in the heat parameters so that thermal mismatch does not occur during hot extrusion.

4.5. 3D Scatter Plot Analysis: Influence of Alloying Elements and Process Parameters on Peak Stem Force

To analyze the influence of process parameters and alloying elements on peak stem force during aluminum extrusion, 3D scatter plots were produced. The plot 4.34 illustrates the interaction between billet temperature, dead cycle time (DCT), and two most influential alloying elements magnesium (Mg) and zinc (Zn) versus peak stem force. Markings represent only the highest 10% of peak stem forces to indicate major operating conditions.

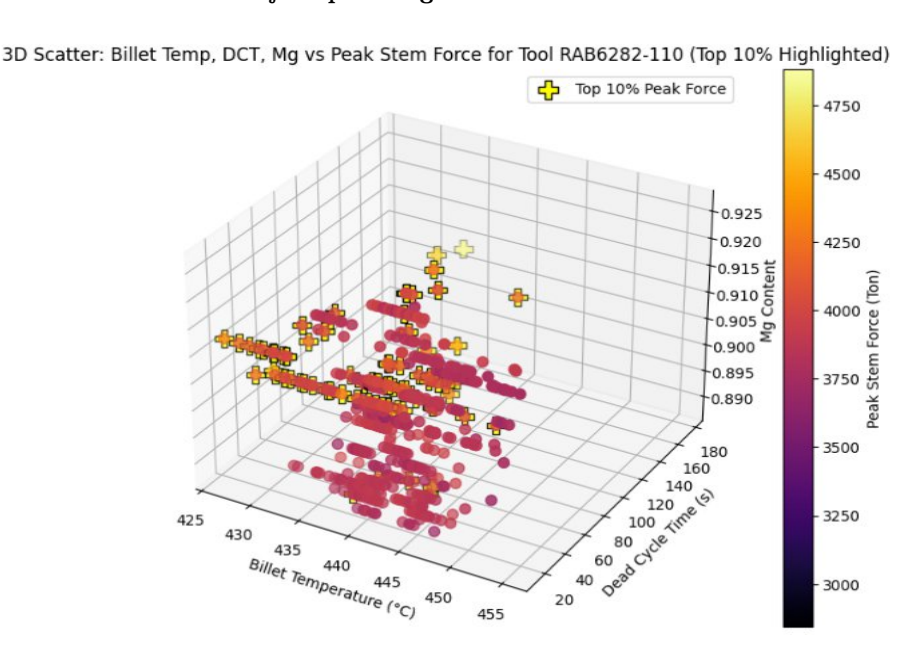


Figure 4.34: 3D scatter plot- billet temperature, DCT, Mg versus peak stem force

This plot billet temperature on the x-axis, dead cycle time on the y-axis, and Mg content on the z-axis with color representing peak stem force size. The yellow-stamped markers represent the 10% largest peak stem force values.

Key Observations:

- Highest peak stem forces are found at higher Mg content values in the range 0.91% to 0.925%.
- •These high-force conditions also exist with intermediate billet temperatures (425–440 $^{\circ}$ C) and dead cycle times of 40–100 seconds.
- •Lower Mg content data points also plot out lower peak stem forces, showing a positive correlation between Mg content and extrusion force.
- •Magnesium has been found to have a stable and strong influence on the maximum stem force. This could be because Mg contributes towards a substantial factor of the solid-solution strengthening which improves its resistance to deformation during extrusion.

•Higher Mg levels imply a higher force for forming, that may have an impact on tool wear, energy use, and dimensional control and therefore tight control over Mg content is required in optimization of the process.

Billet Temperature:

- •The Billet Temperature shows the opposite trend with the Peak Stem Force. The higher the billet temperature, the lower the Peak Stem Force, which would be consistent with the established principle that hot material flows better, requiring lower forces to deform. The lower temperature range (nearer 425°C to 440°C) is associated with greater peak forces.
- •Top 10% of Peak Forces lie mostly within the lower temperature range, indicating that material properties (i.e., Mg content) play a significant role in determining the force required even at high temperatures.

Dead Cycle Time (DCT):

- Dead Cycle Time (DCT) has a large contribution towards the peak stem force. As DCT increases, Peak Stem Force also does the same. This is because of material hardening or greater resistance when the ram is stationary for extended time intervals. From the plot it is observed that with elevated DCT values, there are greater peak forces, especially when magnesium content is also elevated.
- •Peak 10% of Forces group within regions where both higher Mg content and longer DCT overlap. This indicates that excessive idling time in the extrusion process increases higher force demands, indicating the necessity to lower DCT for improved extrusion efficiency.

The plot 4.35 below illustrates identical process conditions but replaces Mg content with Zn content on the z-axis.

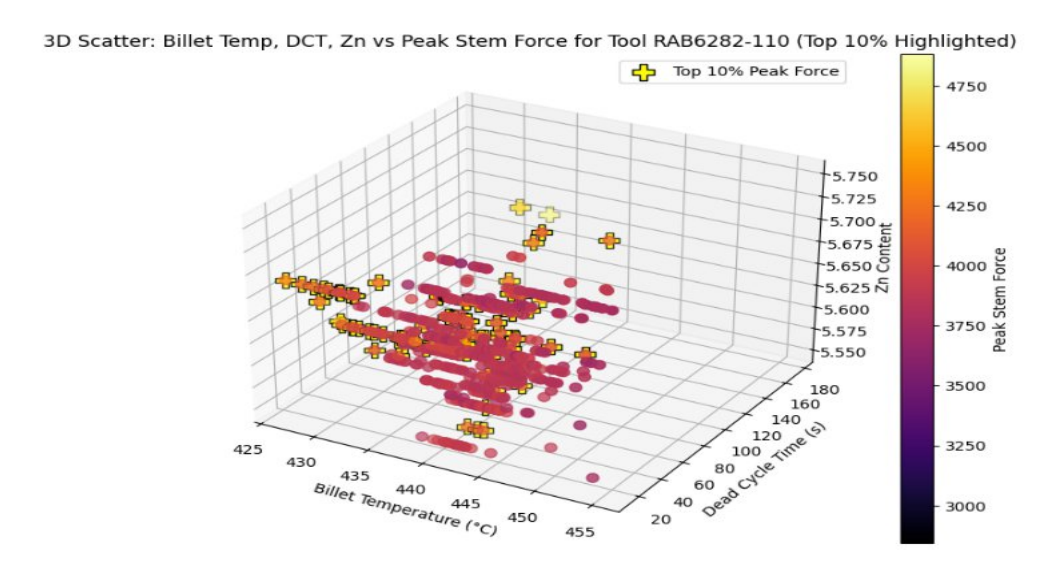


Figure 4.35: 3D scatter plots - billet temperature, DCT, zinc (Zn) versus peak stem force

Major Observations:

- •The 10% peak stem force values appear more scattered over a larger range of Zn content (approximately from 5.6% to 5.7%).
- •While with Mg, there is one narrow Zn content band which is strongly associated with the maximum peak forces, here there is no such Zn content band. This means Zn content is not highly or directly related to peak stem force under conditions investigated. Fluctuation of peak force appears to be influenced more significantly by billet temperature and DCT, but not Zn alone.
- Zn content has a less clear or secondary effect on peak stem force than Mg. While Zn's expression in the strength of 7000 series alloys (e.g., in precipitation hardening combined with Mg) makes sense, its effect on forming force at extrusion does not have to be as direct.
- •Managing Zn content is nevertheless important to mechanical properties post-extrusion, but it has less influence on peak forming loads.

Billet Temperature:

• Similar to the previuos plot, Billet Temperature has a negative correlation with Peak Stem Force. Higher billet temperatures enhance the ductility of the material, reducing flow resistance and therefore the less force required. In the plot, however, Top 10% of Peak Forces are located in lower temperatures (around 430°C), and this suggests that the two elements of higher coercivity with higher zinc content and lower temperature optimize the force required.

Dead Cycle Time (DCT):

- •DCT is yet another important parameter in establishing the Peak Stem Force. Again, similar to the first plot, increased values of DCT are related to increased Peak Stem Forces, particularly when zinc concentrations are also high. This again confirms the earlier observation that increased idle times in the extrusion cycle lead to higher resistance and greater forces involved.
- The Top 10% of Maximum Forces occur in areas with higher zinc content and higher DCT, highlighting the requirement for accurate regulation of cycle times and chemical content to avoid high force during extrusion process.

Summary of Key Insights

The 3D scatter plot analysis offers the following key insights into the determinants of Peak Stem Force in 7XXX series aluminum alloy extrusion:

- Magnesium and Zinc Content: Both Magnesium (Mg) and Zinc (Zn) content have a positive correlation with Peak Stem Force. More alloying elements strengthen the material and make it less deforming, which requires more force during extrusion. This suggests that strict control over alloy composition must be controlled for the proper management of the peak stem force.
- Billet Temperature: Billet Temperature shows a steady negative relationship with Peak Stem Force, as material resistance is lowered and force required for extrusion decreases with increasing temperatures. Lower temperatures (around 430°C), however, are seen to be associated with high peak forces, especially when the alloy has higher Mg or Zn content.
- Dead Cycle Time (DCT): Both charts show a direct correlation between DCT and Peak Stem Force, i.e., the higher the downtime during the extrusion cycle, the higher the resistance encountered when the ram resumes, and the higher the peak stem force necessary. Minimization of Dead Cycle Time is a crucial move towards the optimization of extrusion process and the avoidance of excessive force generation.
- Process Optimization: It is seen that the regulation of Billet Temperature and Dead Cycle Time plays a crucial role in sustaining the required Peak Stem Force. It must attempt to maintain ideal billet temperatures and have fewer idle times for extrusion so as to minimize peak stem force.
- Alloy Design: Regulation of the Mg and Zn content within the alloy is also emphasized in the analysis as being crucial. While these elements increase the strength of the alloy, they also increase the required peak stem force. There must be a trade-off between achieving the desired material properties and maintaining the extrusion forces within limits.

Briefly, by optimizing billet temperature, cycle time, and alloy composition (especially magnesium and zinc levels), manufacturers can maximize the efficiency of the extrusion process and reduce tool and machinery wear.

4.6. Feature importance analysis

To better understand the relative impact of individual process parameters and chemical composition elements on peak stem force in aluminum extrusion of 7XXX series alloys, feature importance analysis using two tree-based ensemble machine learning algorithms, Gradient Boosting and Random Forest, was conducted. These two models were chosen due to their capability to establish non-linear influences and interactions between features, as common in advanced manufacturing processes. The model (in Figure 4.36) was constructed with the dominant input features: dead cycle time (DCT), billet average temperature, ram speed average, magnesium (Mg) content, and zinc (Zn) content. The aim was to predict peak stem force and identify the relevance of each parameter.

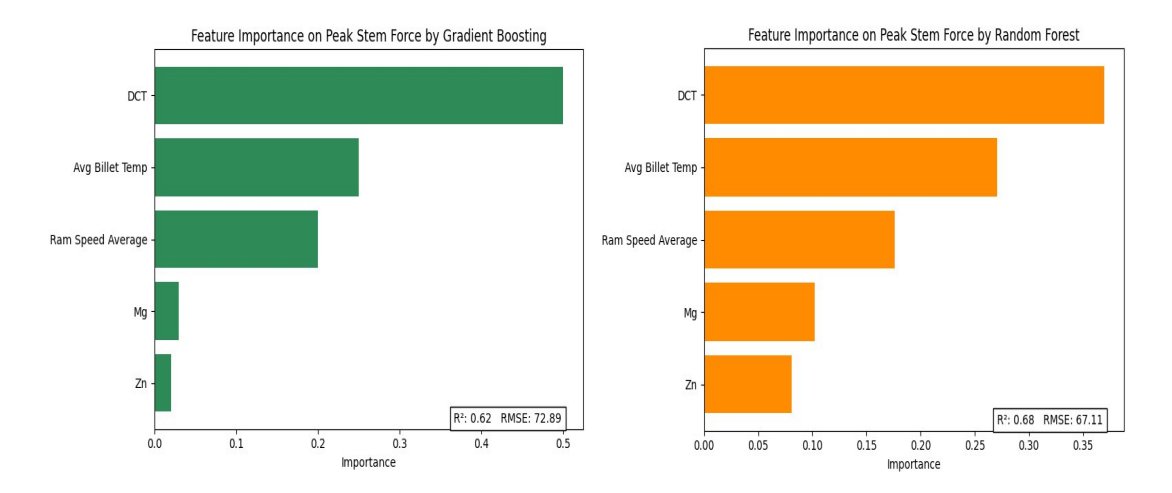


Figure 4.36: Machine learning Model wise feature importance analysis

Gradient Boosting Model Results

Figure 4.36 illustrates the importance features of importance scores obtained by the Gradient Boosting regression model. Among all variables considered, Dead Cycle Time (DCT) was observed to be the most important parameter, which carried a weightage of nearly 50% in the decision-making process of the model. This reflects that regulation of the container temperature with some degree of accuracy is vital to minimize or manage the peak stem force in extrusion.

The Ram Speed Average and Average Billet Temperature were the second most critical parameters, showing the significance of thermal and dynamic conditions of the process. On the other hand, alloying additives Magnesium (Mg) and Zinc (Zn) expressed relatively low significance for this model, which would mean that during the composition range investigated, process conditions prevail over compositional variations in their influence on peak stem force.

The R² measure of 0.62 and Root Mean Square Error (RMSE) measure of 72.89 for the Gradient Boosting model indicate a moderate degree of accuracy in detecting the underlying relationships between the input variables and target variable.

Random Forest Model Results

Random Forest regression model gave an alternative perspective on feature importance as depicted in Figure 4.36. As well as consistent with the outcome of Gradient Boosting, DCT was followed by Average Billet Temperature and Ram Speed Average. Notably, this model put a larger weight on the chemical composition variables Mg and Zn, which reflects the ability of Random Forest to capture complex feature interactions as well as potential nonlinear effects that may not be so salient in Gradient Boosting.

The Random Forest model further showed superior predictive precision compared to Gradient Boosting at $0.68~\rm R^2$ and at a lower RMSE of 67.11. This reflects a stronger generalization ability, particularly in handling heterogeneous data that includes process and material-related attributes.

Comparative Insights

Both ensemble models have consistently pointed towards the dominant influence of thermal process parameters, especially DCT and billet temperature, in controlling the peak stem force during extrusion. Though mechanical parameters such as ram speed play an influential role as well, chemical composition appears to play a secondary role within the investigated range of composition.

The slight differences between the models for feature weighting represent the merit of using multiple modeling methods to guarantee correct interpretation. Furthermore, the fairly low rank of chemical content may mean that, for the alloys and process window investigated, extrusion force is more sensitive to immediate process conditions than to small changes in the alloy.

These results correspond with the metallurgical knowledge that thermal gradients and friction conditions during extrusion have a key influence on material flow and deformation resistance. Therefore, regulation of DCT and billet heating parameters can be efficient levers for the optimization of extrusion force and tool wear.

4.7. SHAP-Based Model Interpretation

To enhance the interpretability of the machine learning model used to make predictions of peak stem force in the aluminum extrusion process, SHAP (SHapley Additive exPlanations) analysis was performed. The technique allows for greater appreciation of the way each feature is contributing to the model's response for any prediction. Unlike feature importance scores that describe only relative impact, SHAP values both describe the magnitude and direction (positive or negative) of each feature's impact on the model output.

SHAP Summary Plot: In-Depth Analysis

Figure 4.37 illustrates the SHAP summary plot of the regression model. One dot per individual observation, colored by actual feature value (blue low, red high). The x-axis coordinate (SHAP value) indicates the impact of the feature on the predicted peak stem force, with positive values shifting predictions up and negative values shifting them down.

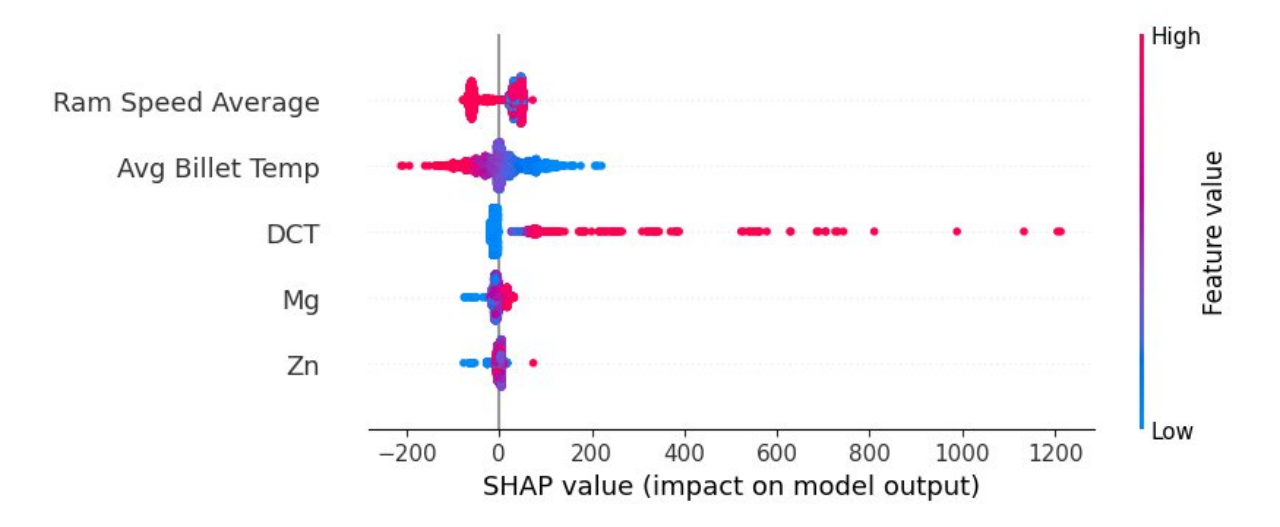


Figure 4.37 : SHAP summary plot of the regression model.

Dead Cycle Time (DCT)

- Takes greatest positive impact on peak stem force. Higher values of DCT (red, e.g., >200 seconds) are most significantly associated with positive SHAP values, in certain cases adding +800 to +1200 units to peak stem force predictions.
- •Simpler dead cycles (blue, <50 seconds) will decrease predicted stem force (SHAP values near 0 or negative).
- Longer dead cycles most likely result in heat loss from the tooling or billet and lead to higher deformation resistance in the subsequent extrusion cycle. The billet is colder and the flow stress is increased, so more force is needed.

Average Billet Temperature

- Average billet temperatures around 440–460°C (red) tend to have a negative impact on peak force predictions (SHAP values between -50 and -200), i.e., material softening at higher temperatures.
- •Lower billet temperatures (blue, below 425°C) map to SHAP values over zero, often shifting the model estimate by +100 to +300. This agrees with metallurgical principles tougher to deform at lower temperature billets. This captures the temperature-dependent flow stress behavior of 7XXX series aluminum alloys.

Ram Speed Average

- •The ram speed effect is more complex. Higher speeds (red, $>\sim$ 6 mm/s) have very variable SHAP values (-100 to +150), suggesting nonlinear interactions.
- •Lower speeds (blue, <4 mm/s) mostly contribute positively to force, typically in the +50 to +200 range. This may be due to less dynamic heating and greater friction with slower extrusion.

Magnesium (Mg)

- •Mg content shows a mild influence. Elevated Mg content (>0.8 wt%) shows minor positive SHAP contributions ($\sim+50$), which suggests a weak strengthening effect on the alloy matrix.
- •Minimum Mg content results in zero or negative SHAP values, confirming that composition effects are secondary to process conditions.
- •The model predicts a weak strengthening effect of Mg on the basis of solid solution and precipitation hardening.

Zinc (Zn)

- •Zn content clusters around zero SHAP values. However, reducing Zn (below ~ 4 wt%, blue) sometimes has a negative effect (SHAP ~ -50), while rising values (>5.5 wt%, red) tend to exert a weak positive force effect (+up to 50).
- •The contribution of Zn is relatively moderate but not entirely insignificant with respect to stem force.

Summary and Practical Implications

This SHAP analysis confirms that process conditions, in this case DCT and billet temperature, are the leading factors of peak stem force. Quantitatively, DCT alone will increase predicted force by greater than +1000 units in certain cases. This defines a key area for process optimization: by reducing dead cycle lengths, reduced stem force can directly be achieved, improving equipment efficiency and product quality. By comparison, chemical composition factors like Mg and Zn have

secondary, smaller impacts of no greater than ± 50 –100 units. Such results not only validate the order of significance derived from feature importance plots but also provide transparent, interpretable data that can be helpful for real-time control of the process. For example, extrusion operators would endeavor to maintain billet temperatures at the upper range (450–470°C) and avoid holding too-high values of DCT to reduce peak stem force and tooling stress.

SHAP Dependence Plot Analysis: Billet Temperature and DCT

To establish the impact of single process parameters on the simulated peak stem force during 7XXX-series aluminum alloy extrusion, SHAP dependence plots were examined. The following sections describe in detail the effect of Dead Cycle Time and Average Billet Temperature, along with their interaction with others.

SHAP Dependence of DCT (Dead Cycle Time)

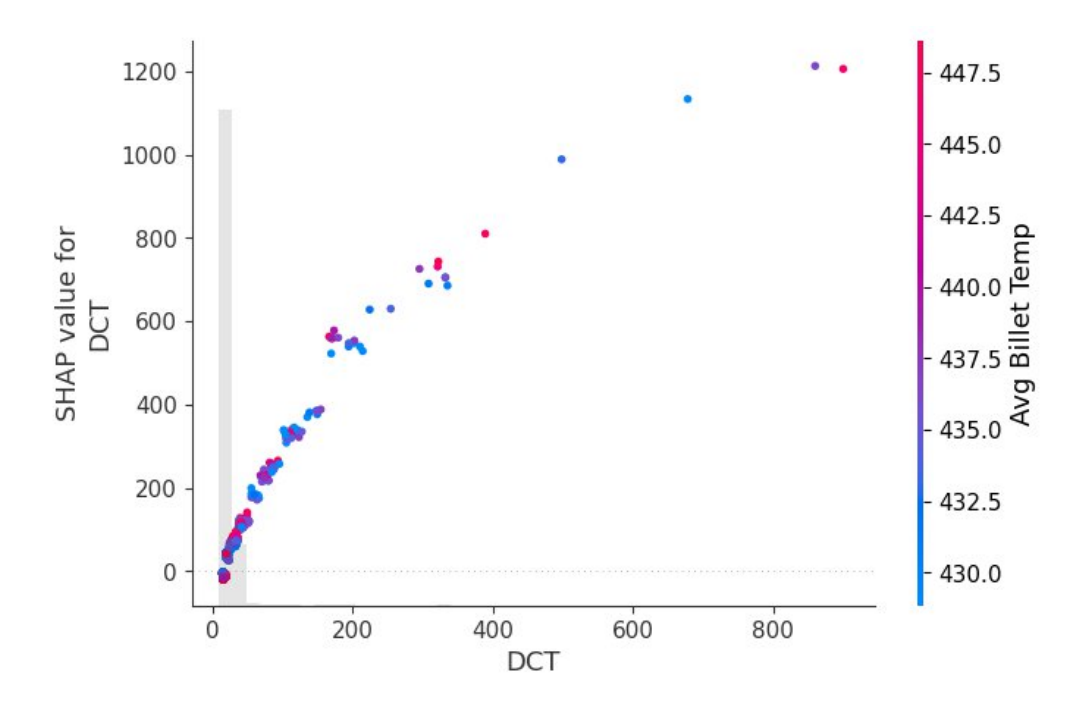


Figure 4.38 : SHAP value for DCT values, color-coded by Average Billet Temperature.

This plot 4.38 illustrates the influence of Dead Cycle Time (DCT) or the idle time between the extrusion cycles on the model's predicted maximum stem force. The x-axis is DCT from 0 to 850 seconds, and the y-axis represents SHAP values between 0 and considerably more than 1200.

Interpretation:

•DCT < 100 seconds: SHAP values remain low (below 200), indicating very minor influence on maximum force as a function of short idleness. In this interval, the billet remains warm and maintains some degree of ductility.

- •DCT 100–400 seconds: SHAP values increase rapidly to 700–800, indicating that even short idleness results in quite significant cooling of the billet, resulting in material flow stress and resistance build-up.
- DCT > 400 seconds: SHAP values reach levels of 1200, illustrating that high dead times cause extreme billet cooling. This leads to significantly higher peak stem force since the billet is not very ductile and harder to deform.

Interaction with Avg Billet Temperature:

Color represents Average Billet Temperature (range: 430° C to 447.5° C).

- Lower billet temperatures (blue colors) with higher DCT accompany higher SHAP values, once more confirming that cooling of the billet (and not the die) during DCT is the primary cause for force rise.
- Higher billet temperature (magenta points) at the same DCT even can reduce rise in force, again suggesting thermal control at the idle stage.

Long DCT billet cooling is the primary source of additional stem force, consistent with physical intuition and the SHAP trend.

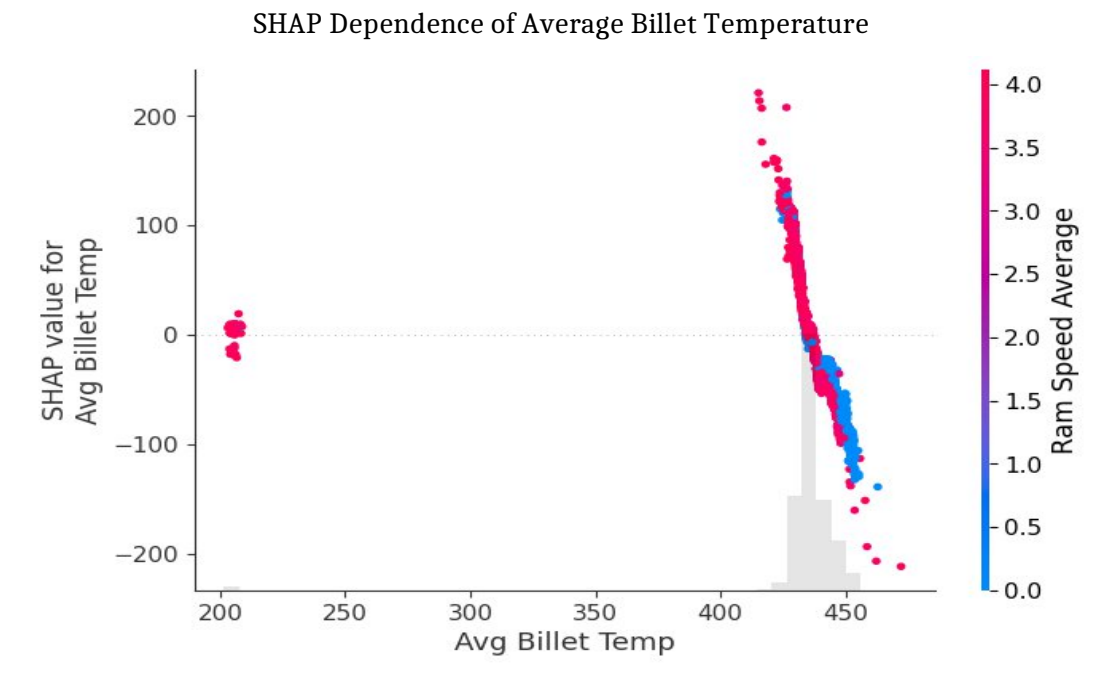


Figure 4.39: SHAP value for Average Billet Temperature, color-coded by Ram Speed Average.

This plot 4.39 shows how Average Billet Temperature, from $\sim 200^{\circ}\text{C}$ to 455°C, influences the predicted maximum stem force. SHAP values vary from +200 to -200, meaning whether temperature increases or decreases the required force.

- 200°C 400°C: SHAP values remain close to zero (~0 to +50), indicating little or slightly rising contribution towards stem force. It suggests poor softening at lower temperature ranges.
- 430°C 455°C: SHAP values plummet to -200, indicating that elevated billet temperatures reduce the peak stem force considerably through thermal softening of the billet.

This is an instantaneous function of physical behavior: a warmer billet can be more easily pushed through the die, reducing mechanical resistance and extrusion load.

Interaction with Ram Speed:

Color maps Ram Speed Average (0 to 4.0 mm/s range):

- Low ram speeds (blue) at high temperatures have more negative SHAP values, indicating maximum softening effect.
- Higher ram speeds (red) reduce thermal advantage partially, possibly due to strain rate hardening or absence of heat transfer time.

Billet temperature is a strong inverse predictor of maximum stem force, and ram speed has additional moderates its effect. Production at high billet temperatures and low ram speeds has significant reducing effects on stem force.

SHAP Dependence Analysis of Magnesium (Mg) Content

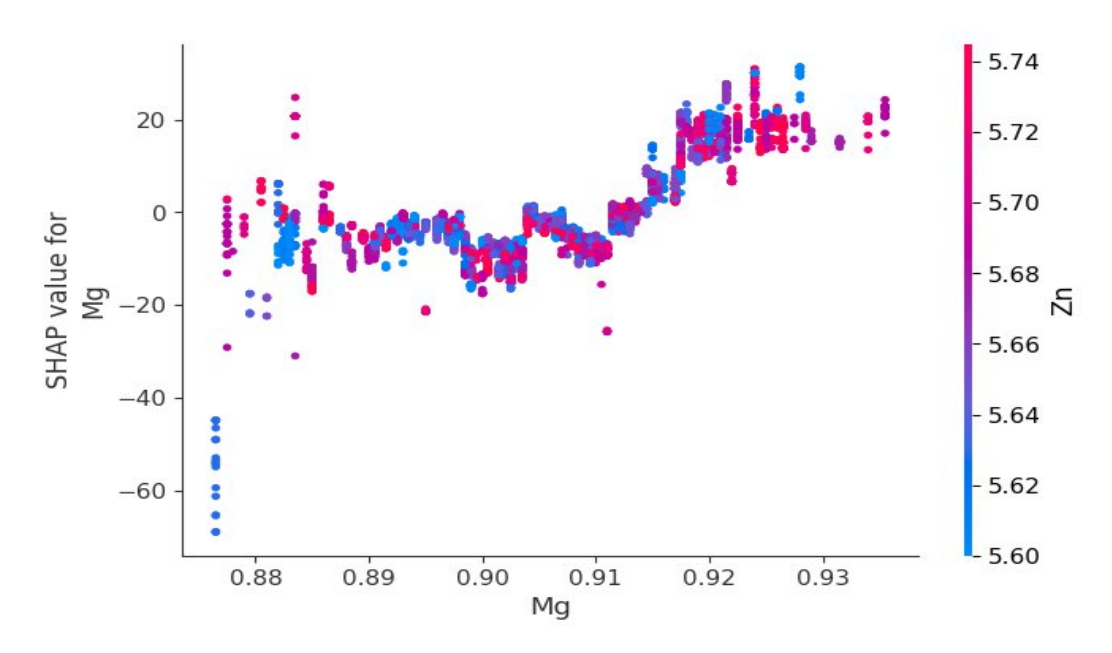


Figure 4.40: SHAP values for Mg content, color-coded by Zn content.

In Figure 4.40, the SHAP dependence plot provides a description of the influence of content of Magnesium (Mg) on peak stem force predicted. The x-axis is actual Mg percentages ranging from 0.875 to 0.935 wt%, and the y-axis is relative SHAP values ranging from -60 to +30 and representing the contribution of Mg to the model prediction.

Most significant observations from the plot are:

- \cdot For Mg < 0.88 wt%, SHAP values are strongly negative (as high as -60), which indicates a great negative contribution of low Mg content to peak stem force. This means that the material is compromised by not having sufficient Mg content, minimizing the resistance of material to deformation.
- For the mid-range of 0.885 to 0.915 wt%, SHAP values remain clumped around 0 to -10, which is an indication of weakly negative or no impact. It is likely a stable region wherein Mg has no significant impact on force.
- There is also a strong rising trend between Mg > 0.915 wt%, where SHAP values rise sharply to +25, meaning that higher levels of Mg have a positive effect on stem force. This may be reflective of solid-solution strengthening or the formation of Mg-Zn intermetallic phase.

Color-coded based on Zn content (5.60 to 5.74 wt%), the pattern of interaction suggests that

- With increasing Zn content (>5.72 wt%, pink dots), the beneficial effect of Mg on SHAP increasingly dominates at large values of Mg.
- This suggests a synergistic strengthening between Zn and Mg, in agreement with well-established precipitation hardening mechanisms (e.g., MgZn₂ precipitation in 7XXX series alloys).

SHAP Dependence Analysis of Zinc (Zn) Content

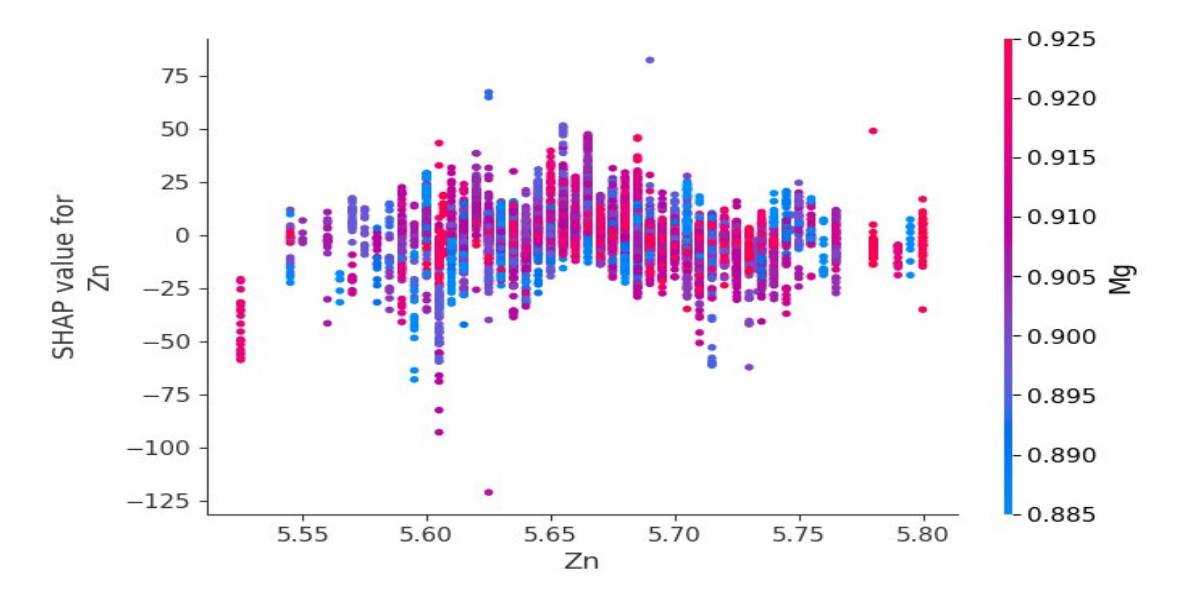


Figure 4.41 : SHAP values for Zn content, color-coded by Mg content.

Figure 4.41 depicts SHAP dependence of Zinc (Zn) content, 5.54-5.80 wt%, and SHAP values -125 to +75. The figure shows a non-monotonic and complex effect of Zn on the predicted peak stem force.

Key observations:

- •For Zn < 5.60 wt%, SHAP values have large negative spikes (up to -100), i.e., low Zn contents significantly reduce stem force, likely due to too little strengthening.
- For the range 5.60 to 5.70 wt%, SHAP values go from -25 to +25, indicating a close to zero to slightly positive contribution in this middle zone, possibly a threshold zone for precipitation hardening.
- \cdot For Zn > 5.75 wt%, SHAP values rise towards +50, pointing towards an unmistakable positive effect on the model prediction.

The coloration by Mg composition (0.885 to 0.925 wt%) illustrates interaction behavior

- More positive Mg content (red points, >0.915 wt%) is related to more positive SHAP values for Zn, particularly in the regime Zn > 5.72 wt%.
- Lower Mg content (blue points) is related to more negative SHAP values, even at elevated Zn.

This creates a significant interdependence of Mg and Zn in a contribution to stem force. The effectiveness of Zn to harden the alloy is maximized by sufficient Mg, again suggesting $MgZn_2$ phase contributions that dominate in precipitation-hardened 7xxx series alloys.

Influence of Chemical Composition on Extrusion Force

SHAP dependency plots for Mg and Zn both validate metallurgical behavior expected of 7XXX series aluminum alloys:

- Both Mg and Zn are essential contributors of solid solution and precipitation interaction for alloy strength.
- Both elements need to be present in quantities required to exert a beneficial impact on maximum stem force.
- Interaction effects between Mg and Zn are non-linear and cooperative, and their joint tuning is important to ensure maximum stem force and alloy performance.

Chapter 5 Discussion

5.1. Wall Thickness Variation

Wall thickness analysis from multiple profiles revealed distinct patterns of process stability and

dimensional consistency. In profile RAB5954, front measurements deviated minimally,

demonstrating stable extrusion behavior near the die entry area. The rear positions most notably

Pos 15 and Pos 17 exhibited greater deviations, perhaps resulting from localized perturbation in

flow or cooling imbalance. In general, the profile had high process control and adjusted only by

fine amounts to remain uniform.

In RAB6146, the rear was less variable, whereas front positions, and particularly Pos 28, were

more variable. This suggests that material flow and early cooling variations near die entry are

more likely to influence the front region over the back in certain designs.

Profile RAB6782 had the highest deviations. Rear positions (Pos 14 and Pos 11) had significant

deviation from the nominal values, and front Pos 03 had a deviation beyond the upper

specification limit (USL). These deviations were largely accounted for by compounded effects of

non-uniform cooling, die wear, and material flow disturbance.

Across all profiles, there was a uniform trend: front locations are resistant to movement away

from nominal size due to proximity to the die entry, whereas rear locations are more sensitive to

cooling rates, alloy flow, and tool wear. Cpk analysis indicated that most positions were below

the target value of >1.33, indicating marginal capability of the process. Percentile analysis

substantiated that front measurements tended to be close to median nominal values, while rear

measurements had wider spread.

The main causes of influence are:

Tool Wear: Alters paths of material flow, which have greater impact on rear zones.

Cooling Variation: Differential rates can generate differential contraction along length.

Material Properties: Alloy composition and hardness gradients can affect stability.

Process Conditions: Temperature gradient of the billet, extrusion pressure, and ram speed induce

localized deviations. These findings stress the importance of targeted rear-position process

optimization and proactive die maintenance.

57

5.2. Dimensional Accuracy - Straightness and Twist

Dimensional stability was checked according to DIN EN 755-9:2016-10 specifications: 1.35 mm straightness for 900 mm and 0.6 mm twist for every 300 mm. All the measured deviations were within specification, but there was a clear positional pattern. Whereas the feeler gauge method gave the basis for twist and straightness measurement, secondary verification by the CMM provided the reliability in measurements. CMM's better resolution detected little local errors not consistently registered manually but did not alter overall dimensional trends. This demonstrates that whereas feeler gauges can be sufficient for routine testing in factory application, CMM gives better accuracy for detailed examination.

Front sections consistently exhibited the smallest deviations from straightness (mean ~ 0.12 mm, $\sim 9\%$ of the tolerance) and twist (mean ~ 0.07 mm, $\sim 12\%$ of the tolerance). Middle sections were comparable to front values, and rear sections exhibited the largest deviations of up to 17% of the straightness limit and 19% of the twist limit.

The progressive rearward drift is characteristic of extrusion metallurgy: thermal gradients build up along the billet, cooling rates become progressively less uniform, and material flow stability lowers towards the stroke end. Die wear may contribute to this rear-end bias as well. Although these deviations were within normal tolerance limits, they offer scope for increased billet temperature uniformity and regulation of cycle time to yield uniform quality along the full billet length.

5.3. Process Parameter and Chemical Composition Effects on Peak Stem Force

From the analysis, it is clear that the process parameters directly impact peak stem force most directly during 7xxx-series aluminum alloy extrusion, whereas the chemical composition directly impacts to a lesser but measurable degree. Among all the parameters taken into account, Dead Cycle Time (DCT) and average billet temperature were the most critical.

Dead Cycle Time imposed the most dominant influence. Long idling times allowed the tooling and the surface of the billet to cool significantly before restarting extrusion, and augmented flow resistance in the entrance die with a highly excessive increase in force required. SHAP analysis once more confirmed that very long idling times (>400 s) can increase predicted forces by over 1,000 units compared to brief idling times (<50 s). Such heavy loads would lead to higher energy consumption, tool wear and tear, and greater likelihood of product dimensional deviation.

Mean temperature of the billet exhibited a clear moderating effect on extrusion load. Higher temperatures reduced flow stress, with billets ranging from 440–455 °C developing forces of a

maximum of 200 units less than for those below 420 °C. Uniform thermal profile through the length of the billet is therefore critical to control load and ensure consistent product quality. Very high temperatures would, however, have to be carefully watched so that no negative effects are imparted to the end microstructure.

Chemical compositionally, both magnesium (Mg) and zinc (Zn) influenced peak stem force, though in one less significant than the principal process parameters. Correlation coefficients showed a very slightly stronger simple linear correlation for Zn, but rankings of feature importance from the Random Forest and Gradient Boosting models suggested Mg had the larger overall influence. This discrepancy is a reflection that extrusion behavior is the product of non-linear interactions amongst elements, which are retained in the machine learning models but not in plain correlations.

Mg content above approximately 0.915 wt% continuously increased peak stem force by approximately 25–50 units, while Zn above approximately 5.75 wt% had a less pronounced but still positive effect. The effect of Mg was greatest where the content of Zn was also high, indicating that the two metals act together to enhance the strength of the alloy and thus the extrusion pressure. Billets with low contents of Mg and Zn, however, tended to extrude with lower force, especially when accompanied by good thermal and cycle time conditions.

Besides the effects induced by processing, the role of alloy chemistry can be explained in terms of solid-solution and precipitation hardening mechanisms. Mg contributes substantially through solid-solution hardening in 7xxx-series alloys, and Zn combined with Mg enables the existence of η' (MgZn₂) precipitates to contribute further to plastic flow resistance. Higher concentrations of Mg increase the base flow stress, and Zn–Mg interaction determines the intensity of precipitation strengthening. These processes align with those found by machine learning, whereby Zn and Mg had measurable but secondary effects relative to billet temperature and dead cycle time. Thus, while process parameters remain the dominant variables, chemical composition determines the inherent hardness of the billet and supplements its influence under less ideal thermal or cycle conditions.

Interaction analysis indicated that stronger compositions would be more vulnerable to the effects of prolonged idle times, and DCT would overstate the load penalty under these conditions. Alternatively, maintaining higher billet temperatures would compensate somewhat for higher force at higher Mg/Zn content, allowing a practical solution to hot working stronger alloys without undue press load.

In practice, they confirm the worth of giving precedence to process control over composition alteration in order to address peak stem force in manufacturing. The most effective approaches are:

Reducing DCT to below 100 s wherever operationally practicable.

Maintaining billet temperatures at more than 440 °C within safe limits.

Adjusting billet temperature and ram velocity during extruding high-Mg/Zn billets to maximize strength vs. press load. While alloy chemistry cannot be altered frequently in production, knowledge of its effect enables better scheduling and process parameter tuning. The combined use of process monitoring and data-driven modeling is a sound basis for maintaining both product quality and efficiency.

5.4. Machine Learning Insights

Application of machine learning (ML) models in this research study provided a complementary view to standard statistical and metallurgical analysis, which established the ability to identify complex, non-linear relationships between extrusion variables and peak stem force. Though correlation analysis in Section 5.3 also validated dead cycle time (DCT) and billet temperature as the dominant drivers, the ML framework correctly estimated the size, interaction behaviors, and conditional effects of the variables.

The best predictive Random Forest model ($R^2 = 0.68$, RMSE = 67.11) ranked DCT as the most influential variable, followed closely by the billet temperature. Gradient Boosting ranked the same, contributing to the robustness of these findings. However, the SHAP (SHapley Additive exPlanations) analysis yielded findings not directly evident from linear correlations. Specifically, it identified that DCT (Dead cycle time) does not have a consistent effect on peak stem force ,its effect is augmented at low billet temperatures ($<425\,^{\circ}$ C),but diminished at high billet temperatures ($>445\,^{\circ}$ C). Such conditional dependence is a significant consideration for real-world press operation, where billet temperature control may be less than optimum.

Another major SHAP dependence plot finding was the interaction between zinc and magnesium levels. While both individually had low correlations with maximum stem force, the ML models revealed that there was a synergistic effect: magnesium levels > \sim 0.915 wt% had a greater force-increasing effect when the zinc content was > \sim 5.72 wt%. This is consistent with precipitation strengthening behavior typical in 7xxx alloys, but the non-linear modeling revealed that such an effect occurs only in some ranges of composition — information less apparent in simple scatter plot analysis.

ML analysis also found subtle non-linear impacts for ram speed. Though correlation indicated a very minor correlation, the models indicated that very low ram speeds (< 4 mm/s) could slightly increase extrusion load, particularly with long DCTs. This indicates that operators attempting to offset heavy loads by reducing velocity can actually increase force under certain conditions.

Operationally, the ML output indicates the capability to forecast load levels and parameter setpoint regulation. Integration into a press control system would enable predictive high-load forecasting in real time, as well as pre-adjustment of billet preheat or cycle timing ahead of deviations. This predictive capability extends beyond the ability of conventional process monitoring, which reacts after deviations have occurred.

In general, the machine learning approach validated the prevailing process parameter influences reported in Section 5.3 while uncovering non-linear interactions, condition-dependent behavior, and composition-sensitive regimes not otherwise attainable. All this makes the case ever stronger for applying data-driven predictive control systems to aluminum extrusion processes to enable better process stability as well as reduced mechanical loading of equipment.

5.5. Industrial Practical Consequences for Extrusion Plants

Wall thickness, dimensional deviation, process parameters, and chemical composition analysis using the data provided here provide straight recommendations to improve the 7xxx-series aluminum alloy extrusion process. Primary consequences of practical outcomes for industry are discussed below:

1. Dead Cycle Time (DCT) and Billet Temperature control

The studies consistently revealed that longer DCT and lower billet temperatures improve maximum stem force and have an indirect influence on dimensional stability. Maintaining billet temperatures above $440-460\,^{\circ}\text{C}$ and minimizing idle times (< $100\,\text{s}$) reduces extrusion load, limits die wear, and helps achieve more uniform wall thickness and dimensional accuracy over the profile length. Billet temperature real-time control and scheduling of production orders to minimize idle times can realize significant operating benefits.

2. Alloy Composition Considerations

Mg and Zn content influence peak stem force, but only secondarily to process parameters. Small changes in Mg content, particularly where provided with Zn >5.72 wt%, can optimize precipitation strengthening, but process control is the predominant influence. Therefore, even though chemical composition should be within target specifications, reproducibility of operation is more important for day-to-day production stability.

3. Dimensional Quality and Product Consistency

Profiles consistently adhered to tolerance values DIN EN 755-9:2016-10, but positional tendencies reflected higher deviations in rear parts. Cooling pattern control and distribution of uniform die temperature will reduce straightness and twist deviations. Die condition and lubrication procedure care will additionally increase dimensional repeatability.

4. Energy and Tooling Savings

Minimizing peak stem force through process optimization directly reduces energy consumption and mechanical stress on the press. Lower forces result in less die wear, longer tool life, and lower scrap percentages, which is economically preferable for large-volume production.

5. Recommendations for Operational Implementation

Incorporate predictive monitoring systems to monitor DCT, billet temperature, and extrusion load in real-time.

Schedule maintenance and die replacement in advance according to wall thickness trends and dimensional deviation.

Consider process parameter guidelines for some batches of alloys to offset Mg–Zn interactions, such that the extrusion loads are within desired ranges.

Reduce rear-section deviations by optimizing cooling and billet handling operations.

These process-focused observations point out that consistent process control rather than minor adjustments in the chemical composition of the alloys is the best leverage to improve the quality of the extrusion, reduce energy consumption, and extend tool life. Implementing these practices can potentially yield measurable operational and economic benefits in 7xxx-series aluminum extrusion plants.

5.6. Limitations & Sources of Error

The current work provides valuable insights into aluminum alloy extrusion, but there are limitations to be mentioned. The data set has a finite number of billets, extrusion runs, and profile shapes and therefore might not have included extreme process conditions. The dimensional readings and peak force stem data, being accurate, rely on instrument resolution and very small variability of common industrial measurements. In addition, unmeasured variables such as die wear, uniformity of lubrication, and environment may have influenced force needs and dimensional shifts. Finally, the machine learning algorithms, although being very successful in identifying the significant process parameters, are constrained by the observable data range and

cannot always extrapolate behavior at conditions untested. In recognition of these limitations, realistic interpretation of results and avenues of future research are guaranteed and informed.

5.7. Recommendations and Future Directions

The findings of this study provide valuable insights into the effects of process parameters and alloy composition on dimensional accuracy and peak stem force in 7xxx-series aluminum extrusion. From the findings, the following future directions and recommendations are proposed for enhancing process control, product quality, and future research:

Measurement System Verification: Although complete-wall thickness, straightness, and twist were measured, routine verification of equipment and procedures is recommended to assure continued accuracy and reproducibility. This adds a further level of confidence that any observed variation is due to the extrusion process and not due to measurement artifacts.

Die Design and Maintenance Optimization: Rear billet sections were more deviated, suggesting that wear, replacement cycles, and die geometry could affect dimensional consistency. Targeted research evaluating die performance and potential design optimization would reduce such variations, particularly for complex profiles.

Enhanced Thermal Control: Minimization of cooling of billets while idle and optimization of preheating practices will also minimize temperature gradients along the billet. Enhanced thermal control is expected to enhance dimensional stability, minimize top stem force, and enhance the overall process efficiency in general.

Real-Time Process Monitoring: Installation of advanced monitoring systems for billet temperature, extrusion speed, and pressure can provide pre-emptive identification of abnormalities, which will allow adaptive adjustments to ensure uniform extrusion load and profile accuracy.

Alloy Composition Effects: While Mg and Zn content had a secondary effect on peak stem force, it may be beneficial to track their interactions under product applications that involve extreme thermal or mechanical stresses. Optimization of composition within the given ranges may provide incremental force control and product consistency gains.

Batch-to-Batch Analysis: Repeated comparison of batches of production can identify underlying trends from differences in materials, operator methods, or environmental conditions to allow for continuous improvement of quality.

Process Optimization for Energy and Tooling Efficiency: Minimizing dead cycle times, running at higher billet temperatures, and optimizing the ram speed can reduce extrusion forces, die wear, and scrap rates, which directly lead to energy savings and cost-effectiveness.

Chapter 6 Conclusion

Dimensional quality and extrusion behavior of aluminum profiles were investigated thoroughly in this study, taking wall thickness, straightness, twist, process parameters, and chemical composition into account. All profiled samples were within the tolerance limits set by DIN EN 755-9:2016-10, and only small deviations were noticed towards the rear parts of the billets. Positional shifts are due to thermal gradients, changes in material flow, die-effects etc., which highlights that the dimensional quality must be consistent and process stability is necessary.

Process analysis concluded that Dead Cycle Time (DCT) and billet temperature most significantly impact peak stem force. Increased idling times and reduced billet temperatures greatly increase forces, but ram speed affects peak force to a lesser extent. Although Mg and Zn levels do contribute towards peak force through precipitation-hardening reactions, their effect takes a backseat to thermal and processing conditions. These findings were supported by machine learning models of Random Forest and Gradient Boosting, with SHAP analysis providing quantitative data on the direction and size of the effect of each factor.

The engineering consequences are straightforward: maintaining billet temperatures over critical levels and minimizing DCT can considerably lower stem forces, improve energy efficiency, reduce tool wear, and promote wall thickness, straightness, and twist consistency. The synergy of advanced experimental measurement with predictive machine learning provides an appealing, data-driven route to extrusion process improvement in industry.

While adequately supported conclusions, the scope is restricted by the process windows, compositions, and bulk measurements investigated and may not include localized anomalies or rare operating events. Future prospects are to expand the dataset across a broader operating space, die design and replacement evaluation, and incorporation of real-time monitoring systems to allow proactive control.

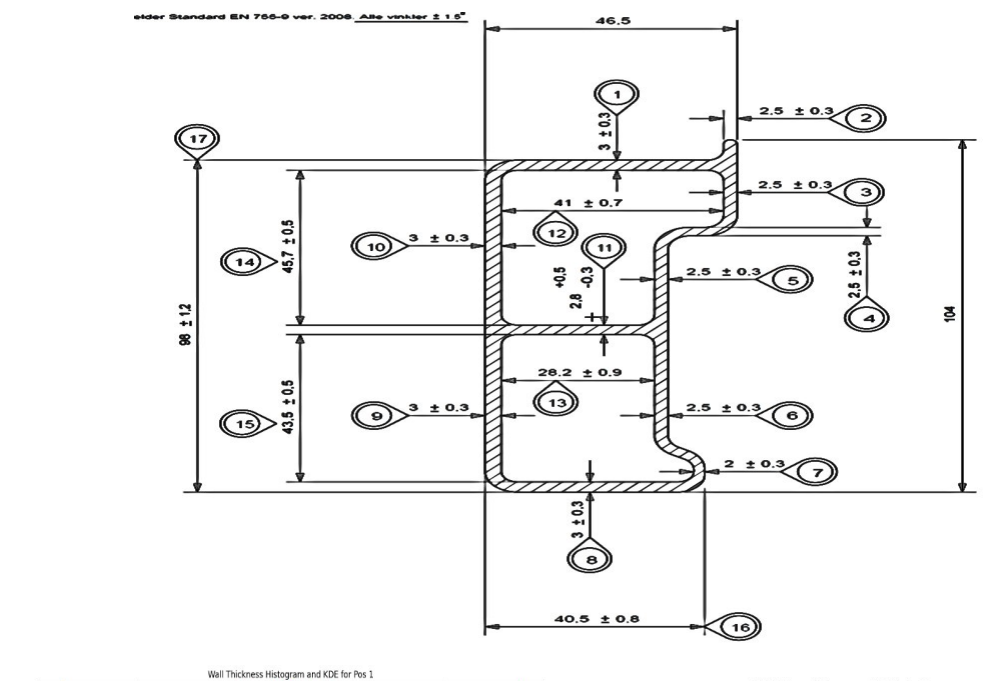
Overall, this research is in line with confirming that control of process parameters —precise thermal control and reduced idle time is the primary reason for extrusion performance in aluminum alloys. Secondary chemical composition effects have a synergistic role in strengthening. Chemical composition influences, though contributing factors, have a synergistic effect toward strengthening. This study combines empirical observation with state-of-the-art predictive modeling to be able to provide a practical platform for consistent quality attainment, wastage of material reduction, and operational efficiency enhancement in aluminum extrusion.

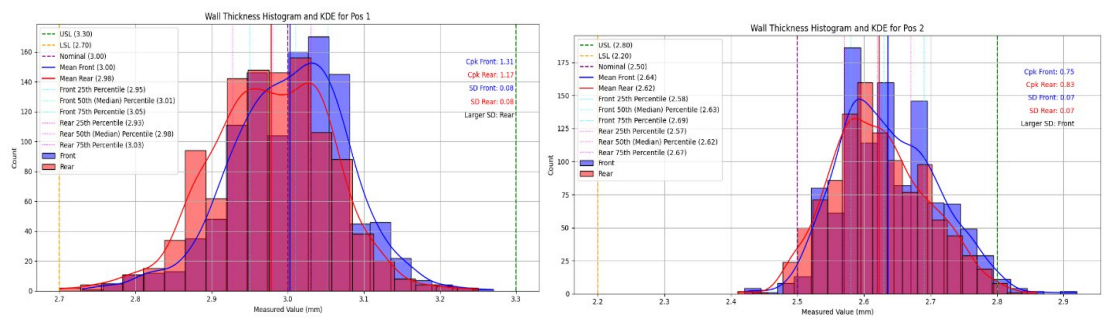
Appendix

Histogram

Figure A1: The Histogram for profile RAB5954

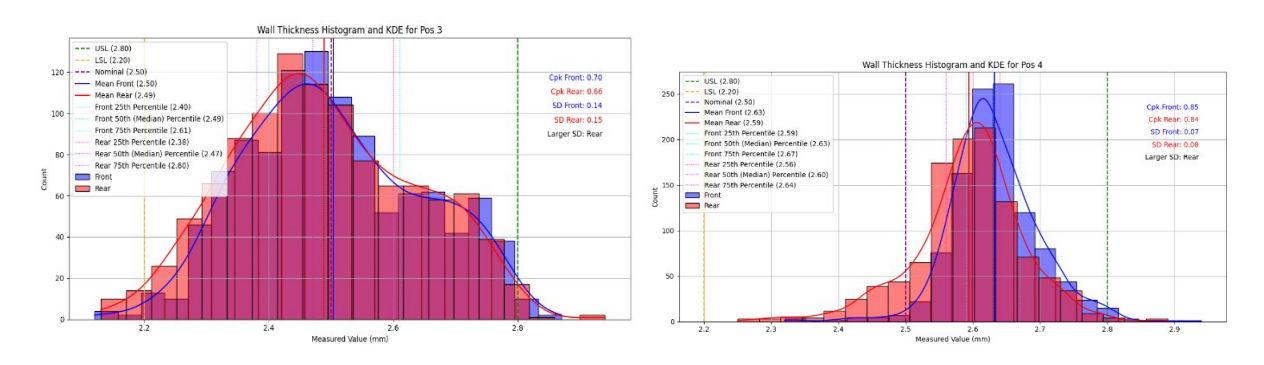
All Positions show uniform distribution near the nominal value.





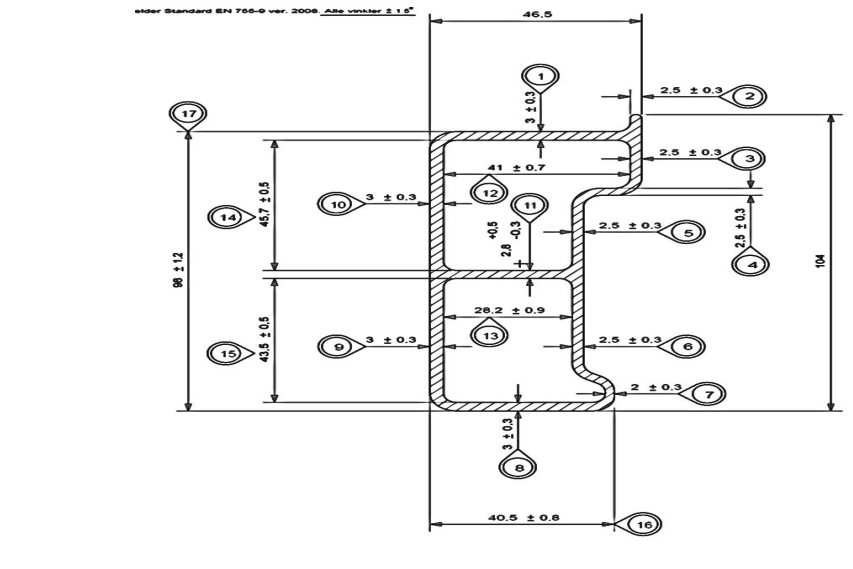
Profile RAB5954, Pos 1

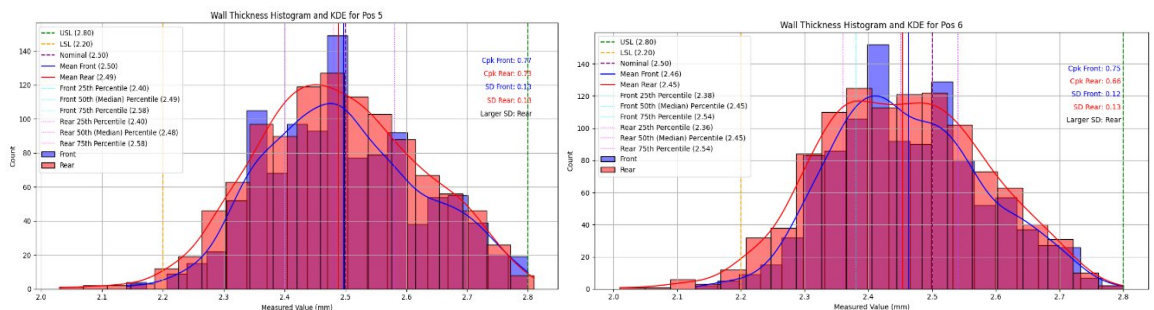
Profile RAB5954, Pos 2



Profile RAB5954, Pos 3

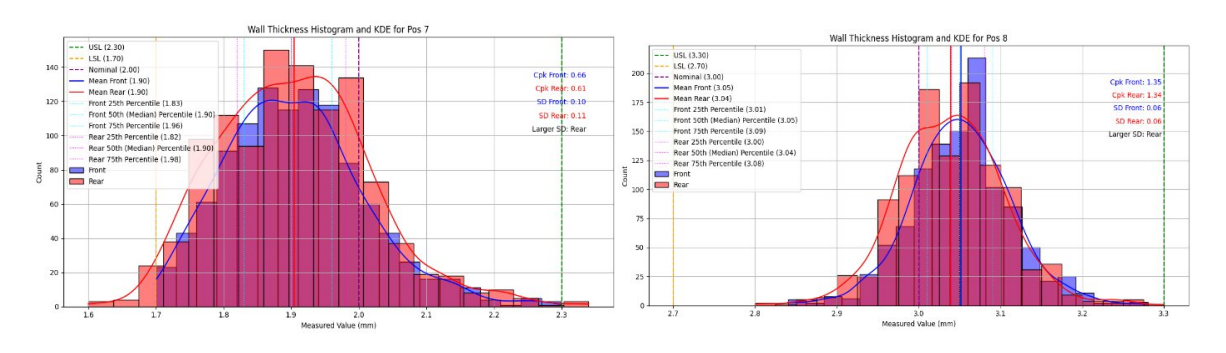
Profile RAB5954, Pos 4





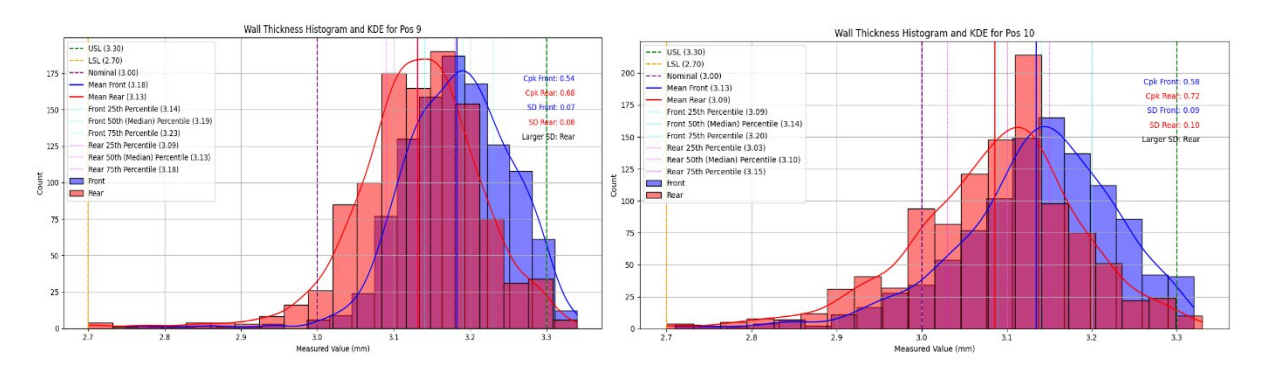
Profile RAB5954, Pos 5

Profile RAB5954, Pos 6



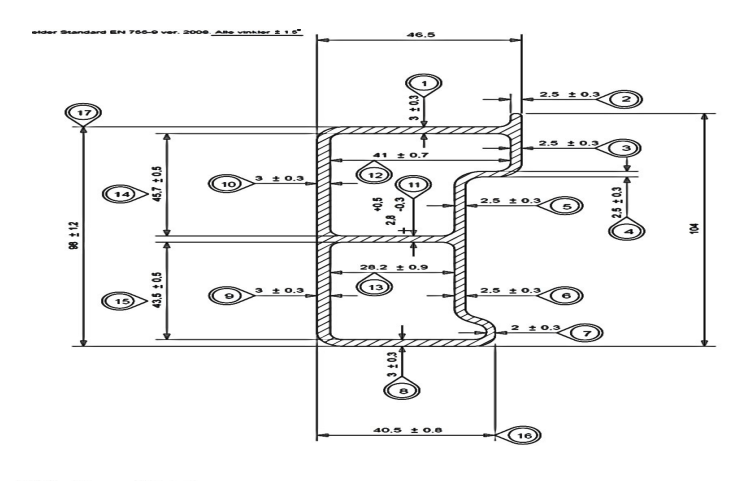
Profile RAB5954, Pos 7

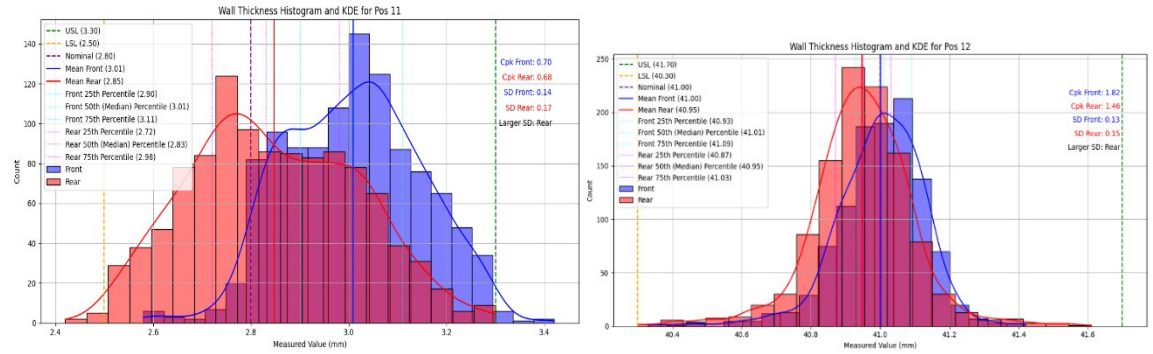
Profile RAB5954, Pos 8



Profile RAB5954, Pos 9

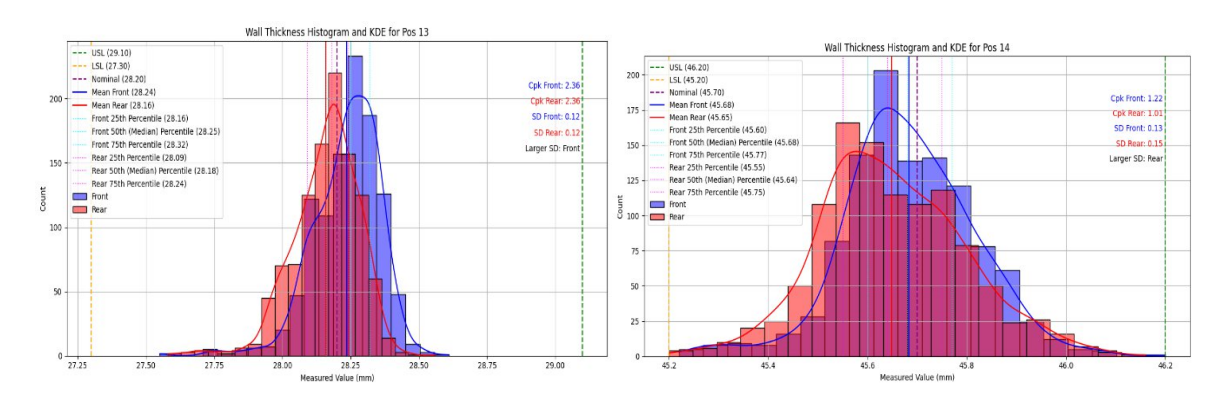
Profile RAB5954, Pos 10





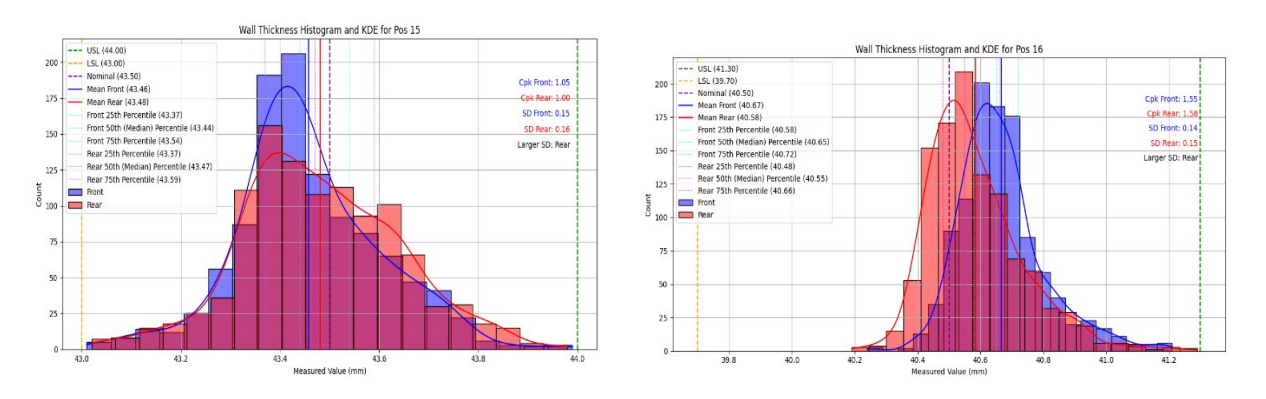
Profile RAB5954, Pos 11

Profile RAB5954, Pos 22



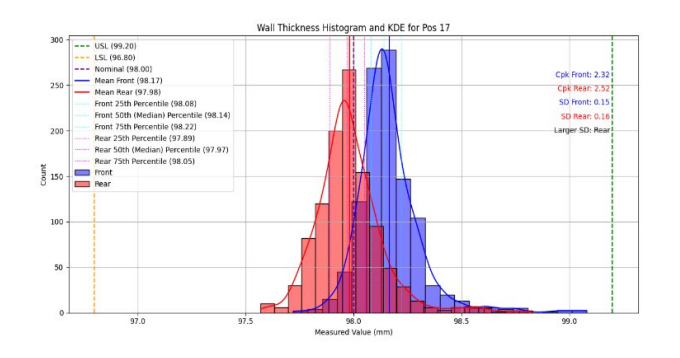
Profile RAB5954, Pos 13

Profile RAB5954, Pos 14



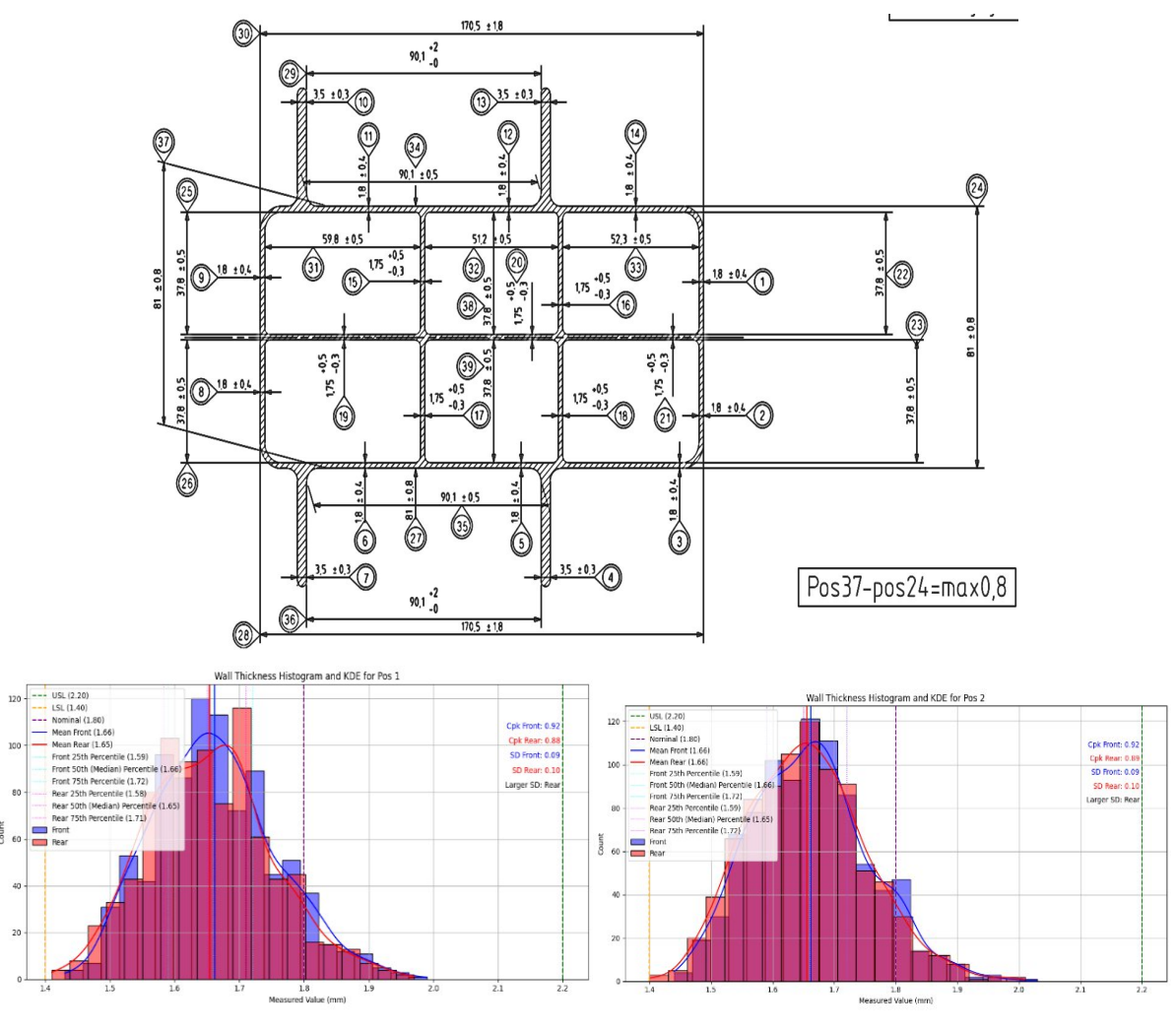
Profile RAB5954, Pos 15

Profile RAB5954, Pos 16



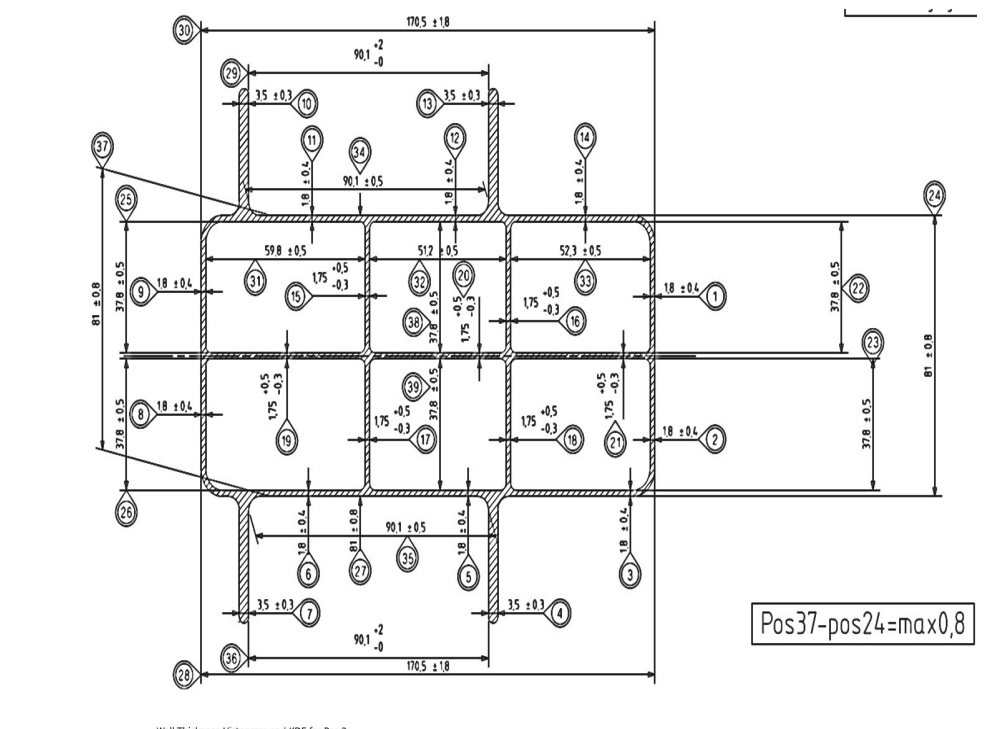
Profile RAB5954, Pos 17

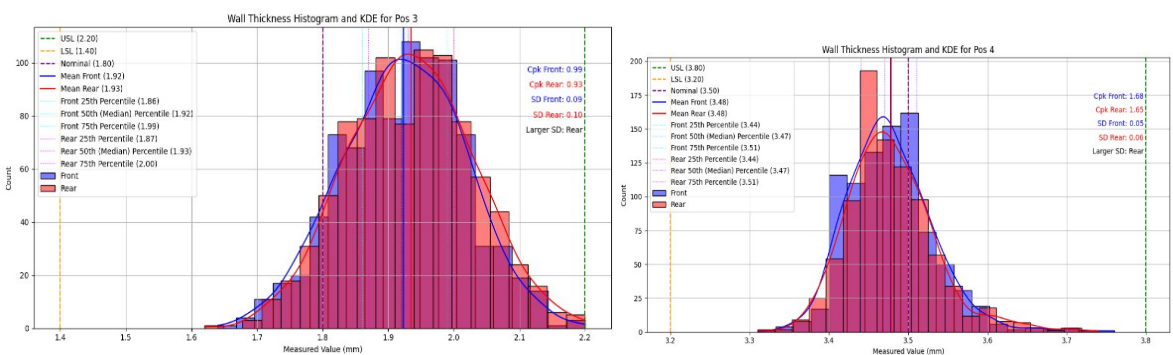
Figure A2: The Histogram for Profile RAB6146



Profile RAB6146, Pos 1

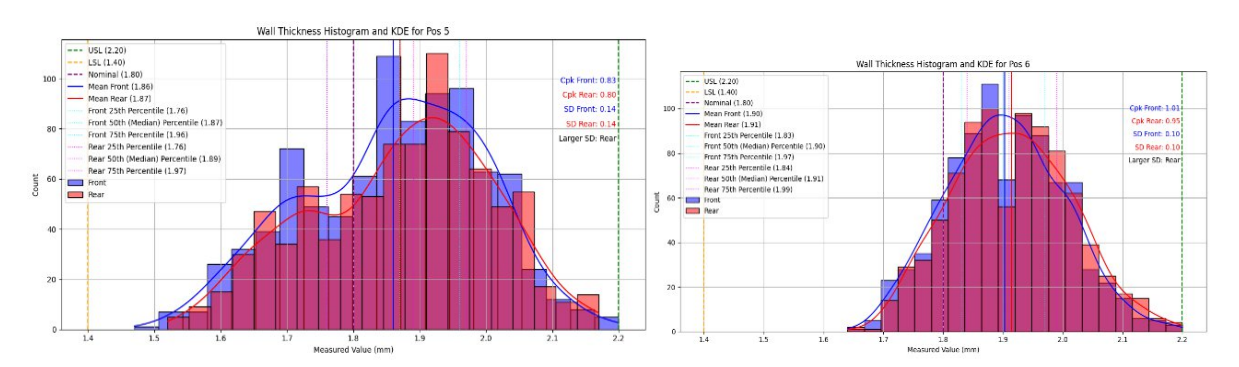
Profile RAB6146, Pos 2





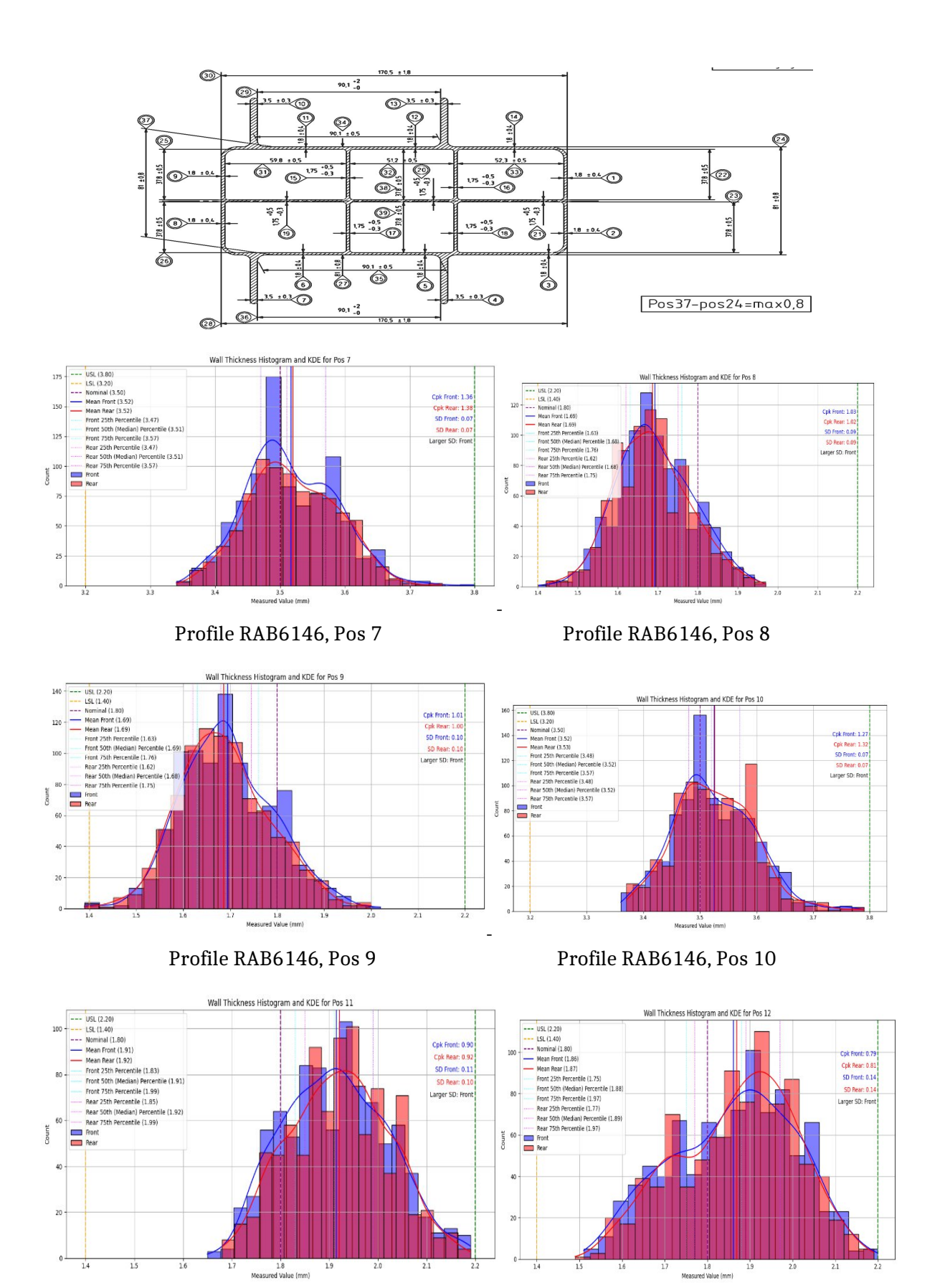
Profile RAB6146, Pos 3

Profile RAB6146, Pos 4



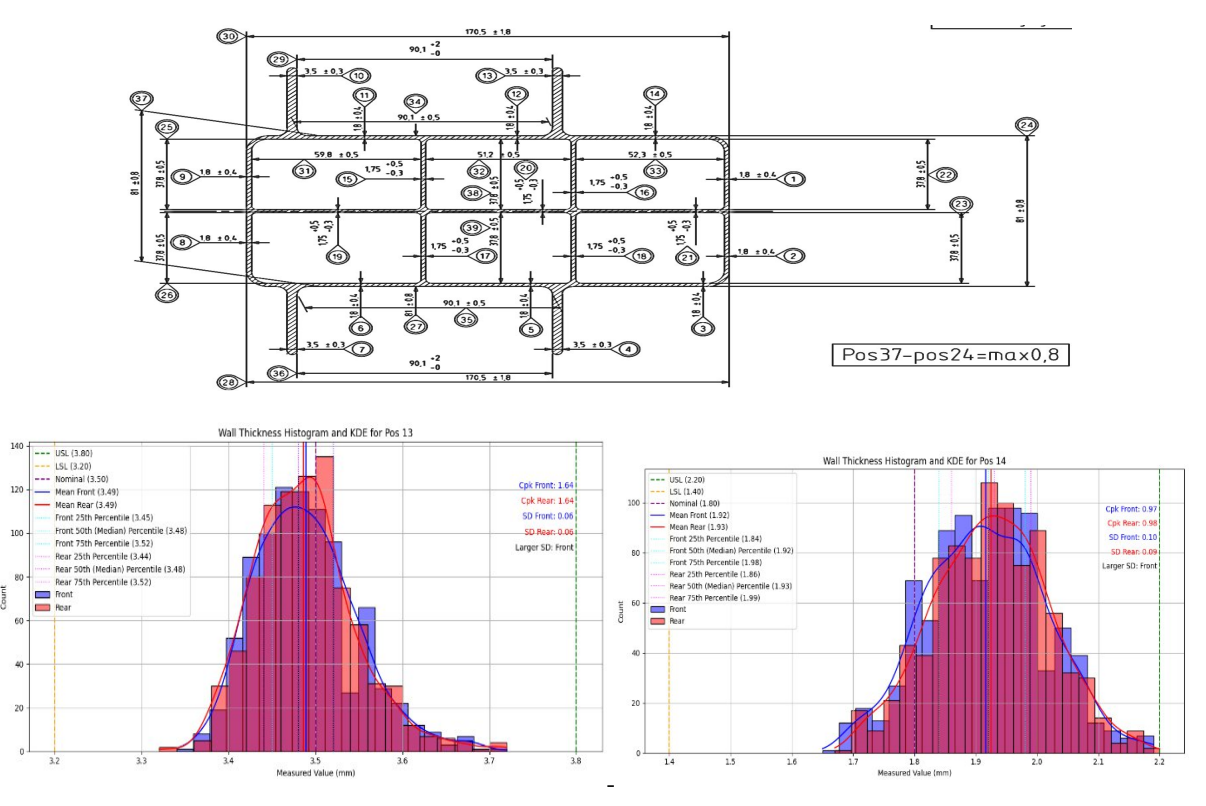
Profile RAB6146, Pos 5

Profile RAB6146, Pos 6



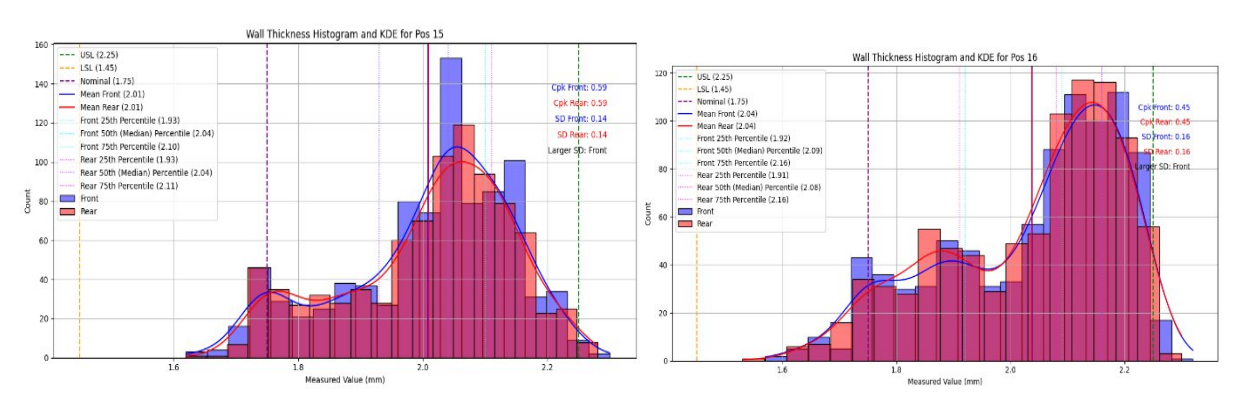
Profile RAB6146, Pos 11

Profile RAB6146, Pos 12



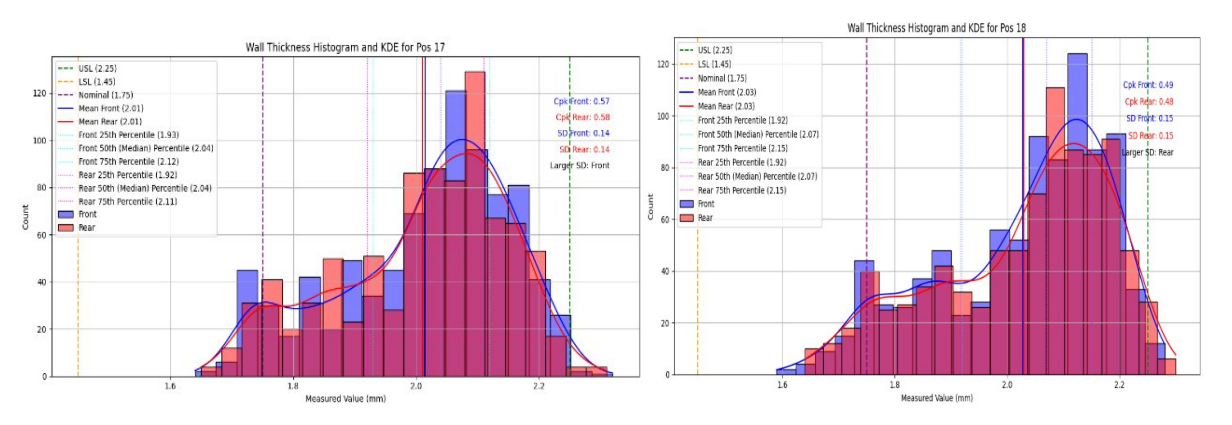
Profile RAB6146, Pos 13

Profile RAB6146, Pos 14



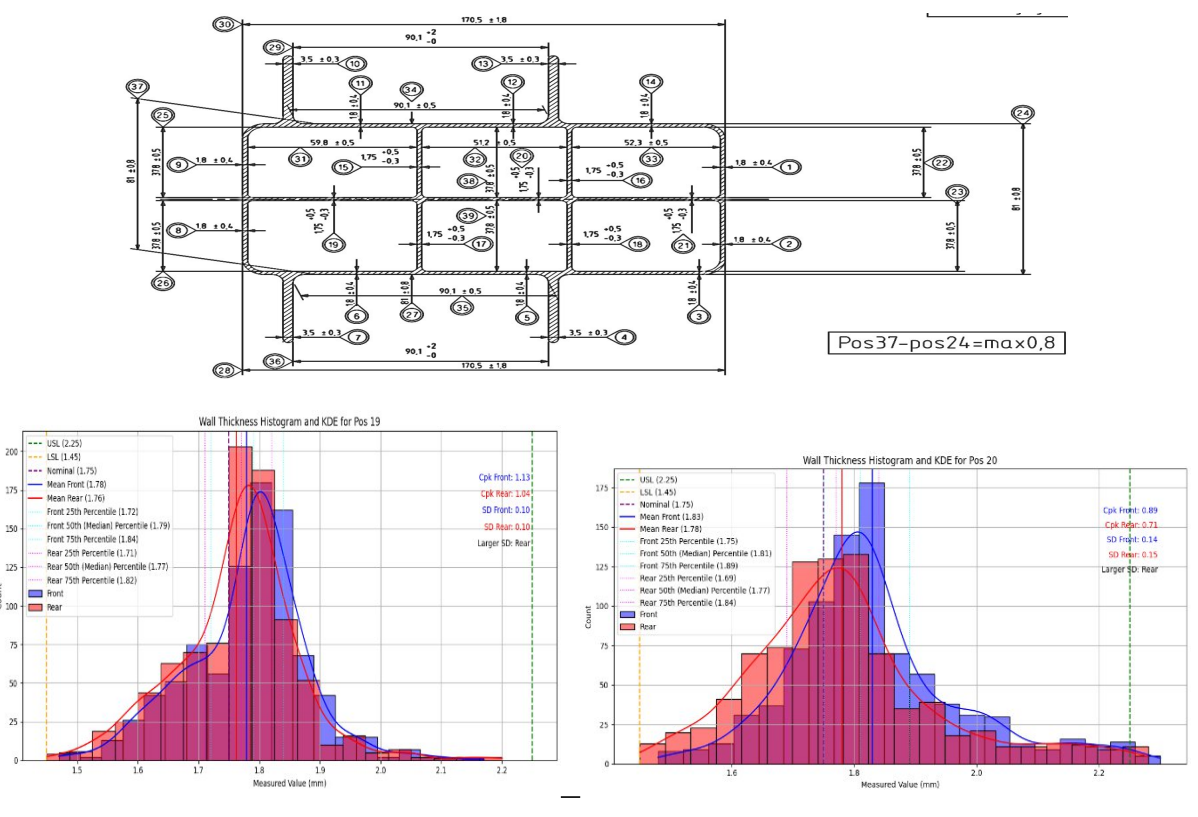
Profile RAB6146, Pos 15

Profile RAB6146, Pos 16



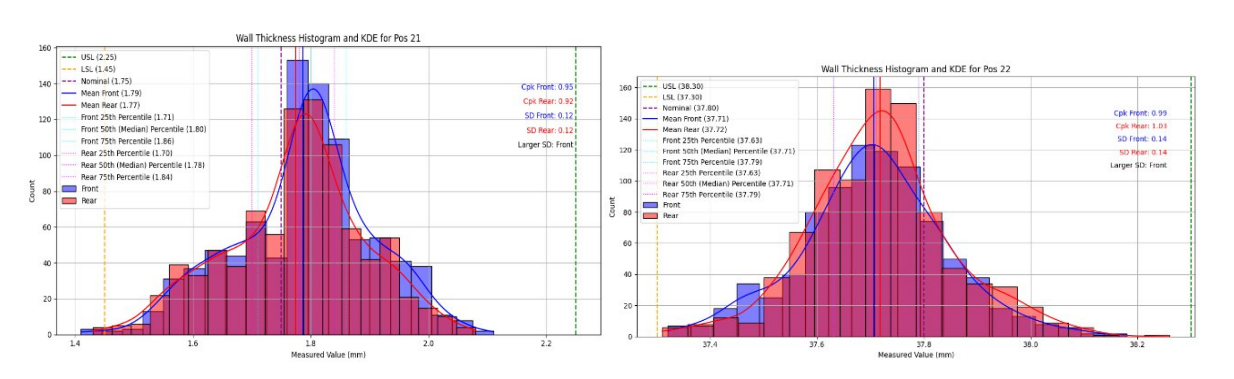
Profile RAB6146, Pos 17

Profile RAB6146, Pos 18



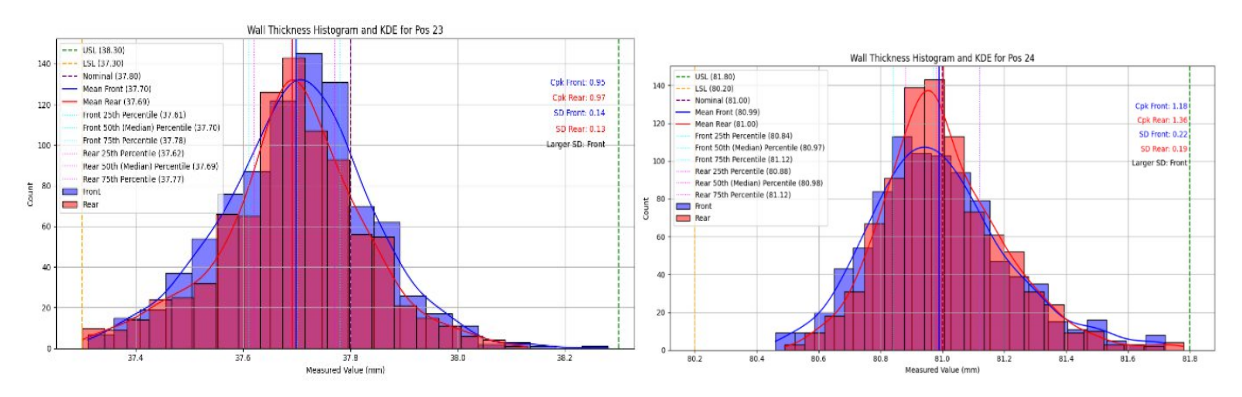
Profile RAB6146, Pos 19

Profile RAB6146, Pos 20



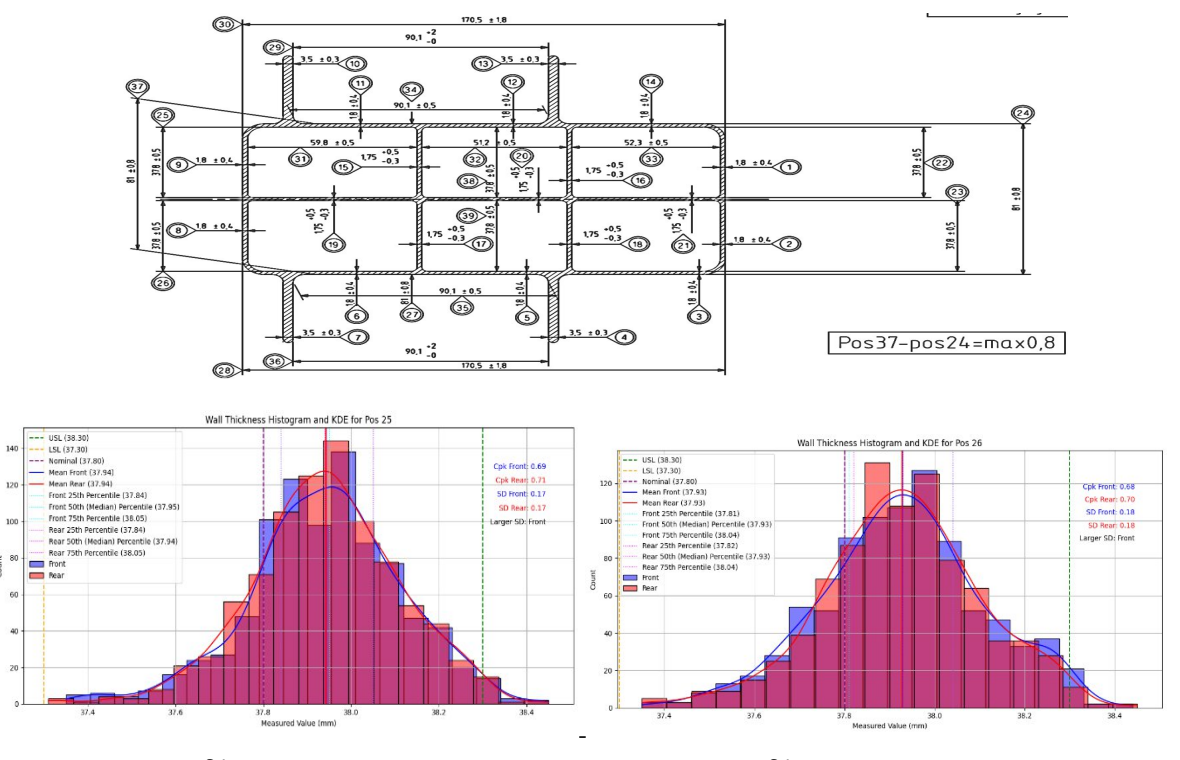
Profile RAB6146, Pos 21

Profile RAB6146, Pos 22



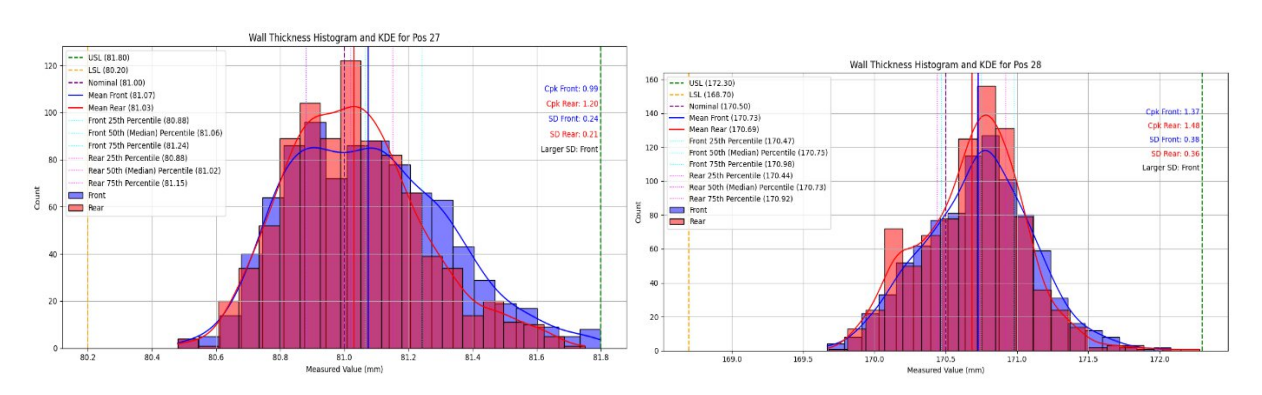
Profile RAB6146, Pos 23

Profile RAB6146, Pos 24



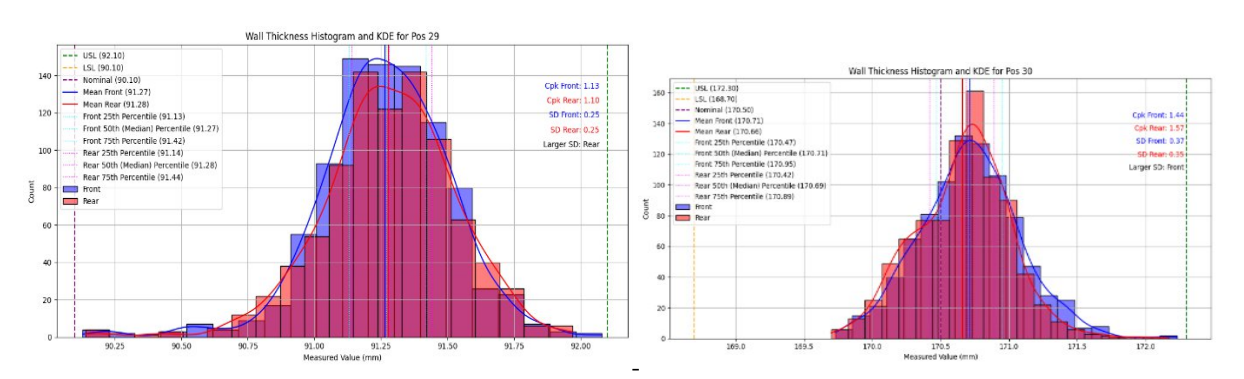
Profile RAB6146, Pos 25

Profile RAB6146, Pos 26



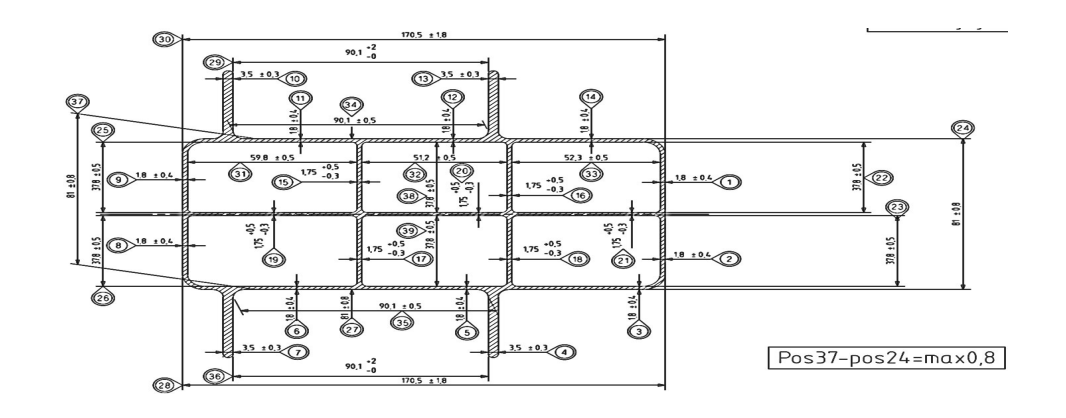
Profile RAB6146, Pos 27

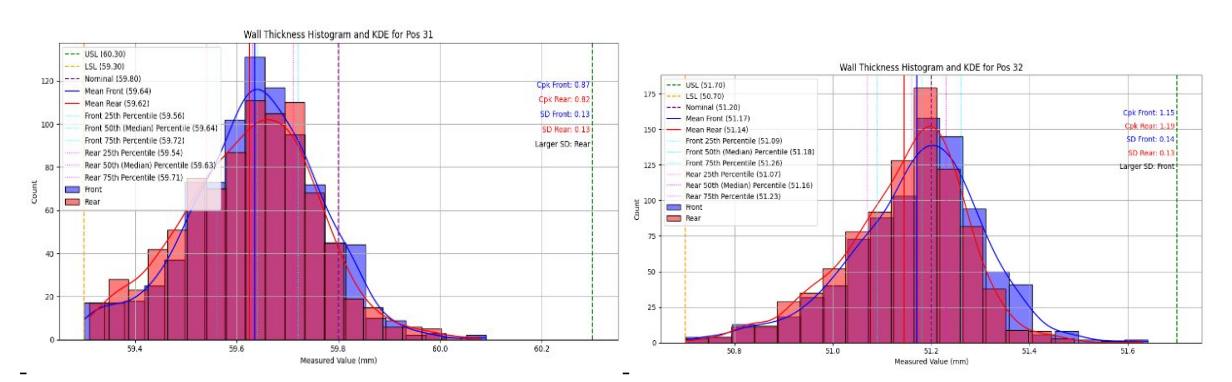
Profile RAB6146, Pos 28



Profile RAB6146, Pos 29

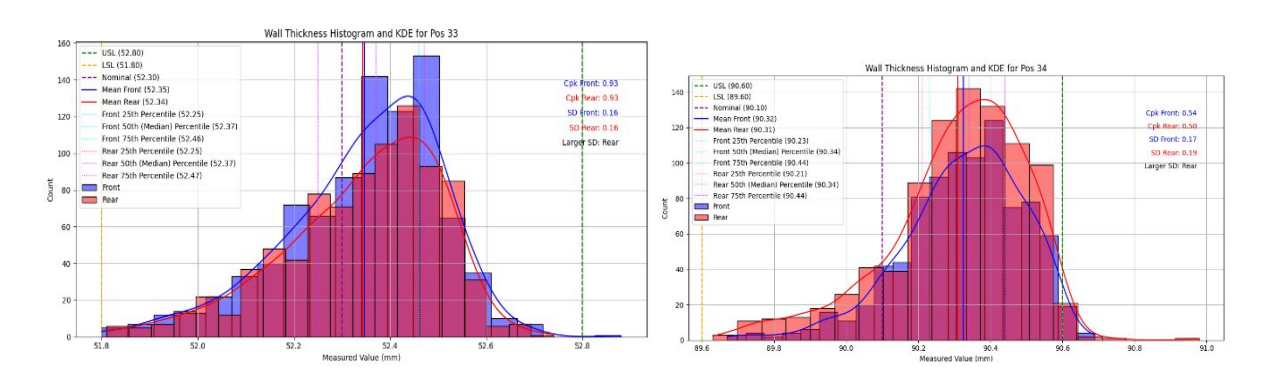
Profile RAB6146, Pos 30





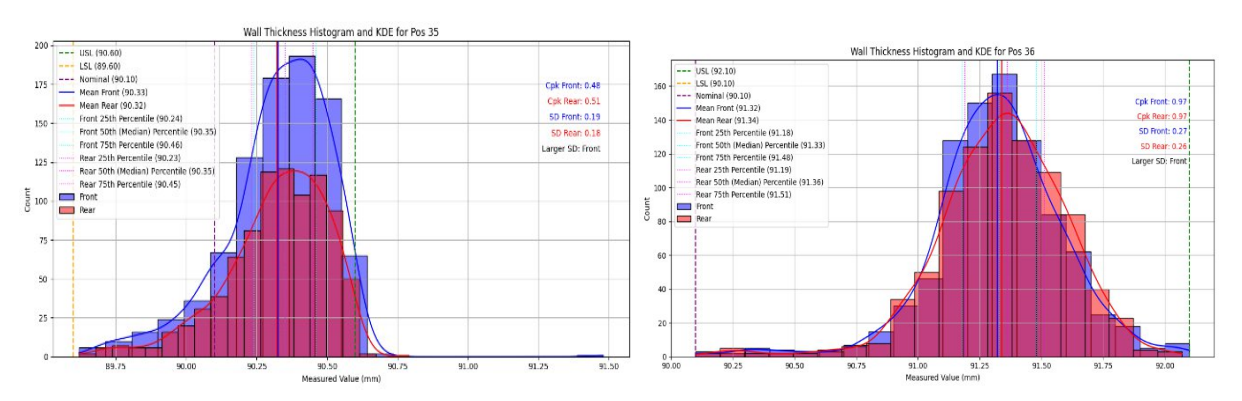
Profile RAB6146, Pos 31

Profile RAB6146, Pos 32



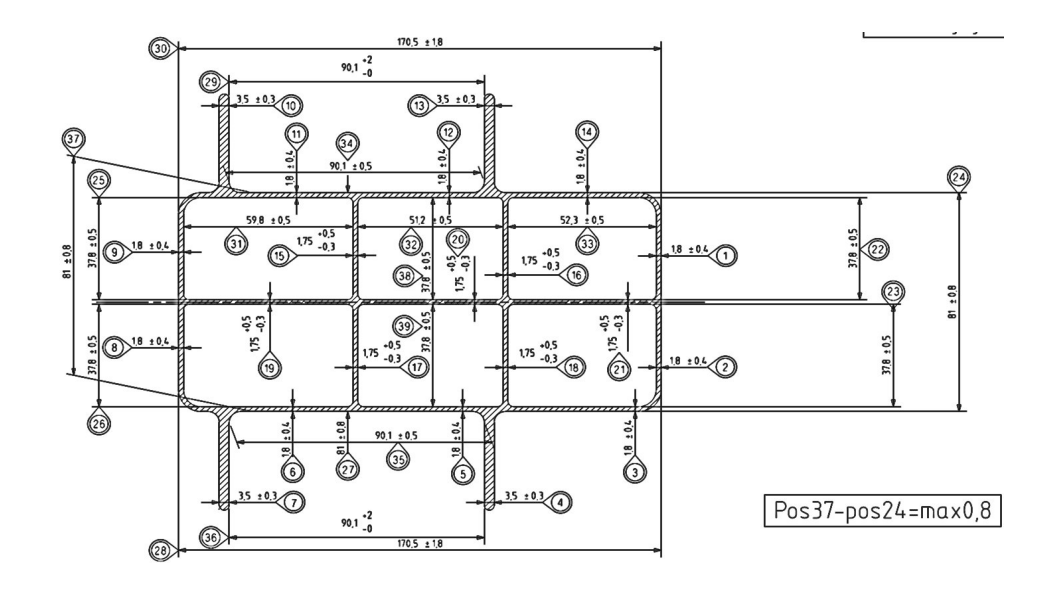
Profile RAB6146, Pos 33

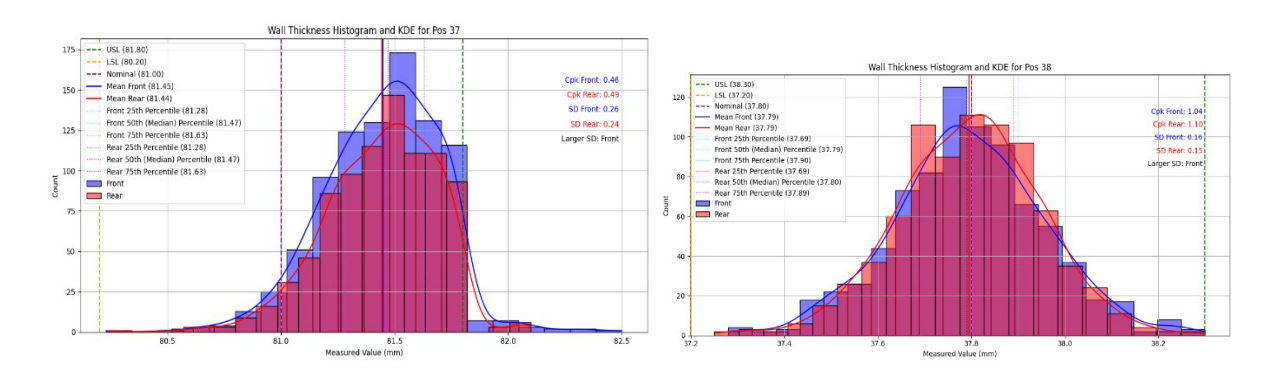
Profile RAB6146, Pos 34



Profile RAB6146, Pos 35

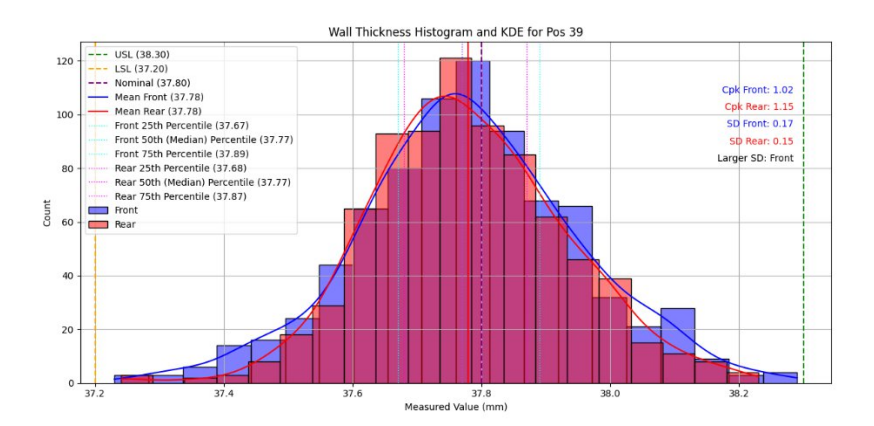
Profile RAB6146, Pos 36





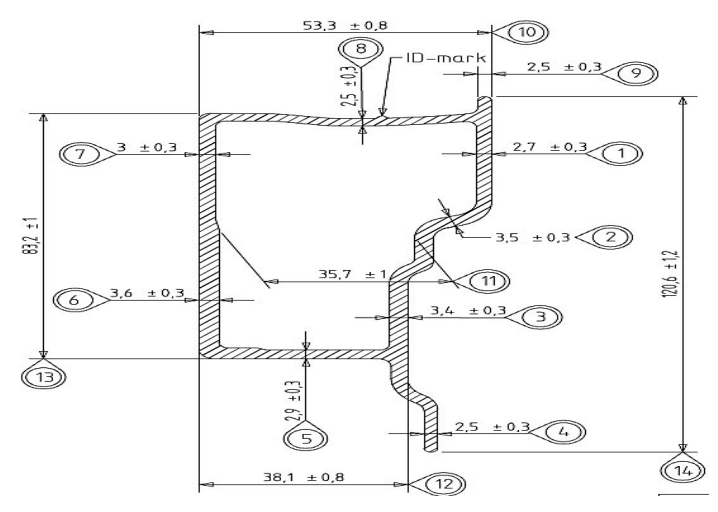
Profile RAB6146, Pos 37

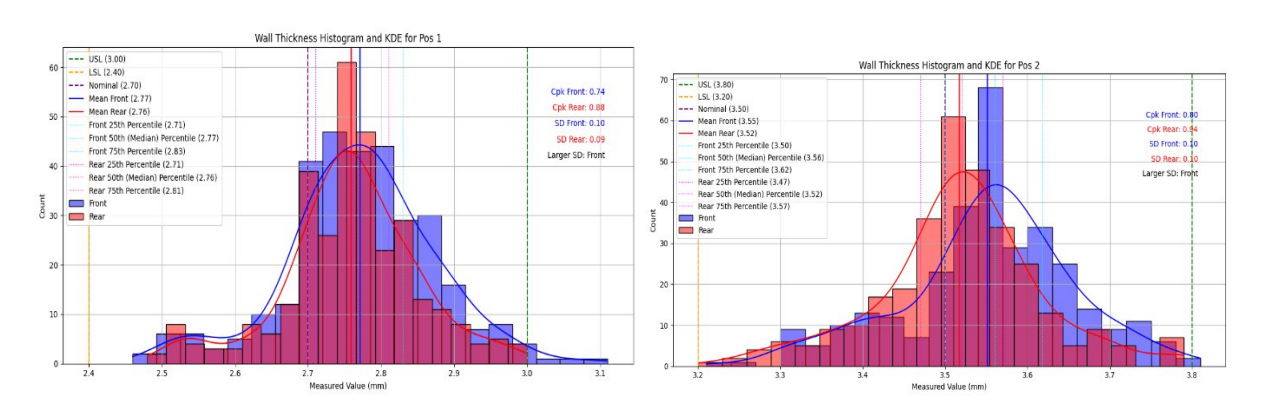
Profile RAB6146, Pos 38



Profile RAB6146, Pos 39

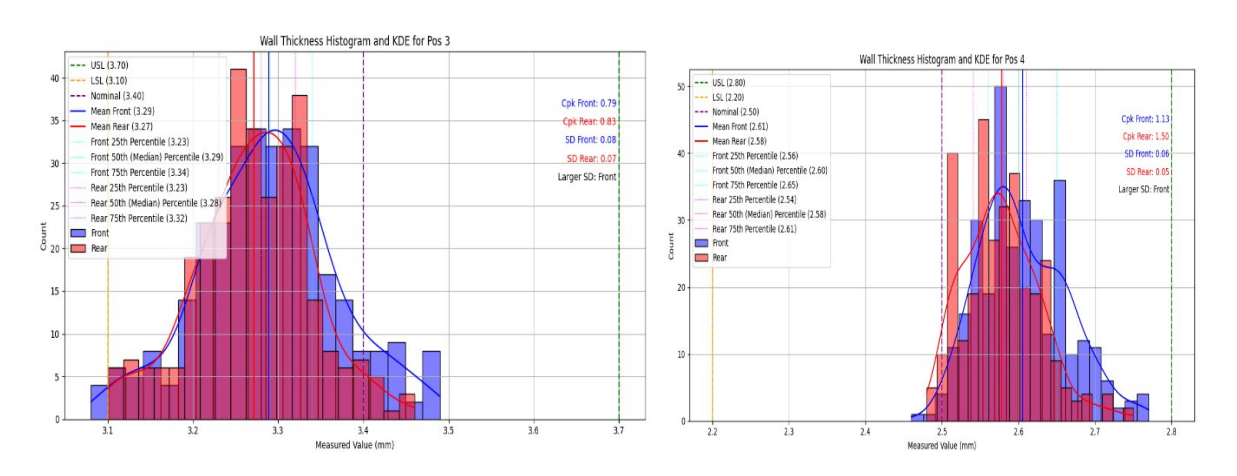
Figure A3: The Histogram for Profile RAB6782





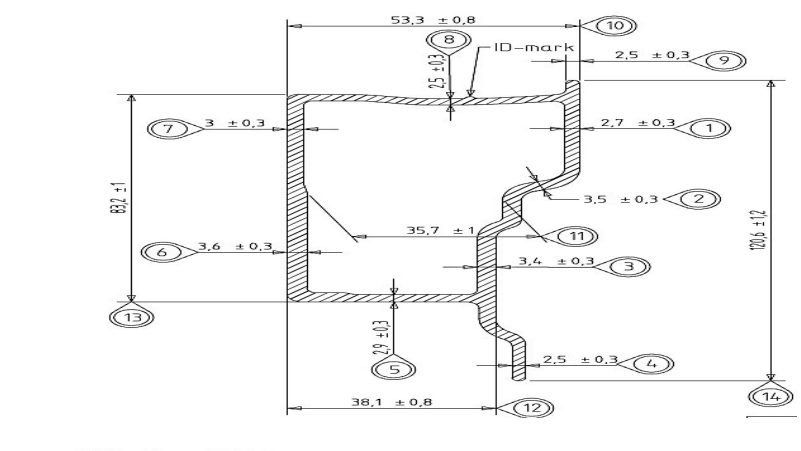
Profile RAB6782, Pos 1

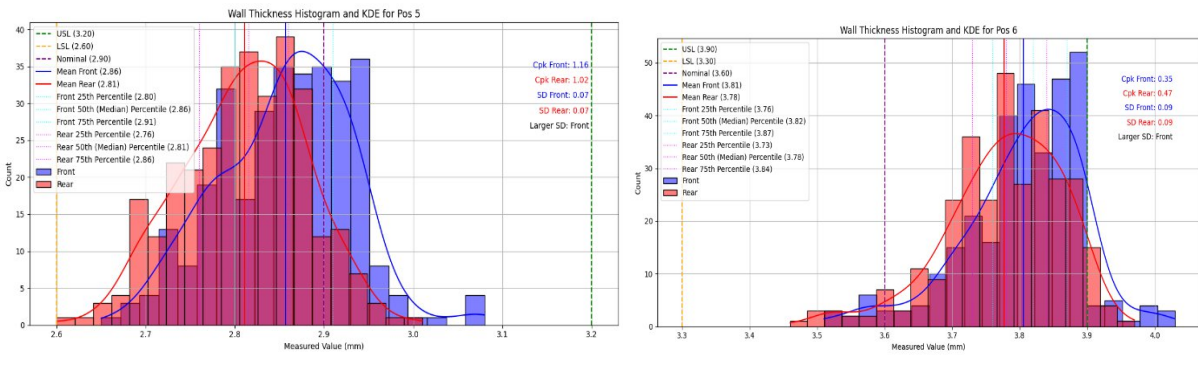
Profile RAB6782, Pos 2



Profile RAB6782, Pos 3

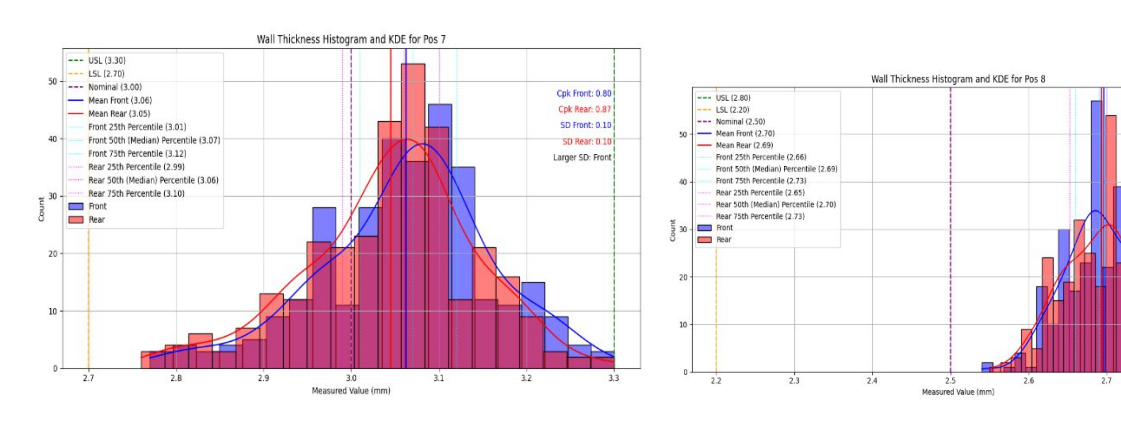
Profile RAB6782, Pos 4





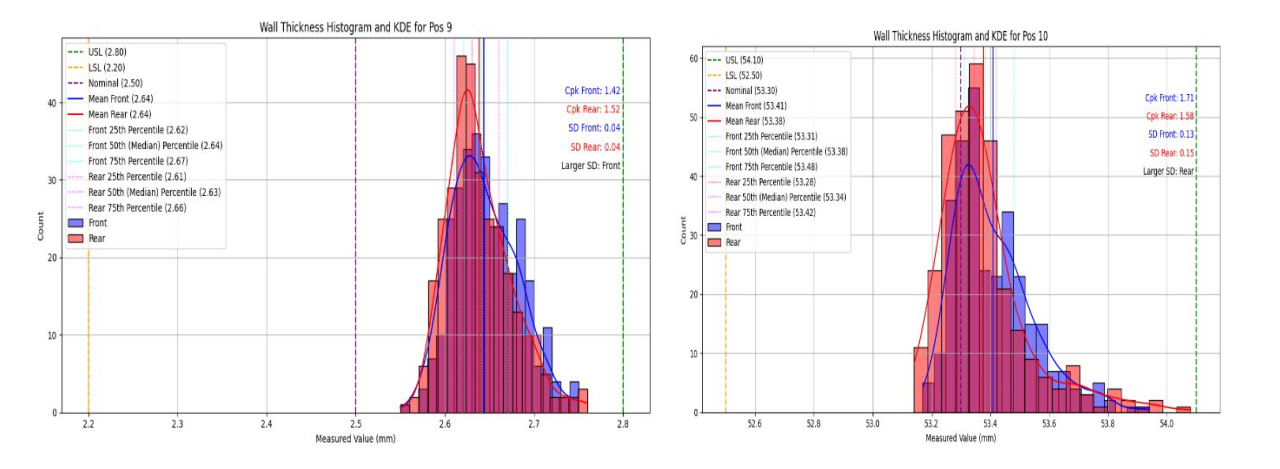
Profile RAB6782, Pos 5

Profile RAB6782, Pos 6



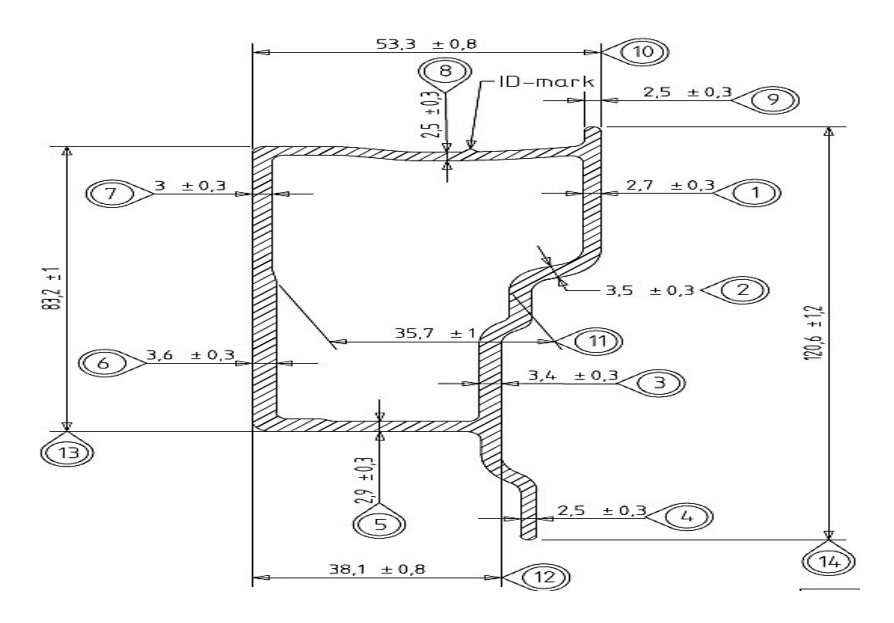
Profile RAB6782, Pos 7

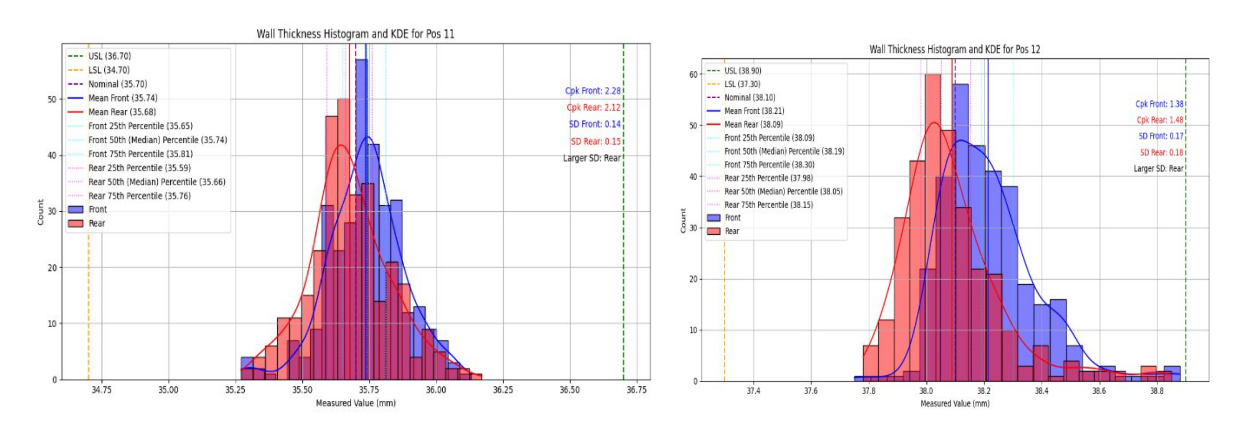
Profile RAB6782, Pos 8



Profile RAB6782, Pos 9

Profile RAB6782, Pos 10





Profile RAB6782, Pos 11

Profile RAB6782, Pos 13

83.00 83.25 Measured Value (mm)

Profile RAB6782, Pos 14

Profile RAB6782, Pos 12

Table

Table: Profile RAB5954

Position	Cpk Front	Cpk Rear	Percentiles Front	Percentiles Rear
Pos 12	1.818594	1.456925	{'25th': 40.93, '50th': 41.01, '75th': 41.09}	{'25th': 40.87, '50th': 40.95, '75th': 41.03}
Pos 13	2.361708	2.364527	{'25th': 28.16, '50th': 28.25, '75th': 28.32}	{'25th': 28.09, '50th': 28.18, '75th': 28.24}
Pos 14	1.224743	1.013686	{'25th': 45.6, '50th': 45.68, '75th': 45.77}	{'25th': 45.55, '50th': 45.64, '75th': 45.75}
Pos 15	1.049151	1.001211	{'25th': 43.37, '50th': 43.44, '75th': 43.54}	{'25th': 43.37, '50th': 43.47, '75th': 43.59}
Pos 6	0.748639	0.656495	{'25th': 2.38, '50th': 2.45, '75th': 2.54}	{'25th': 2.36, '50th': 2.45, '75th': 2.54}
Pos 5	0.773541	0.725306	{'25th': 2.4, '50th': 2.49, '75th': 2.58}	{'25th': 2.4, '50th': 2.48, '75th': 2.58}
Pos 17	2.317065	2.519372	{'25th': 98.08, '50th': 98.14, '75th': 98.22}	{'25th': 97.89, '50th': 97.97, '75th': 98.05}
Pos 7	0.659747	0.605869	{'25th': 1.83, '50th': 1.9, '75th': 1.96}	{'25th': 1.82, '50th': 1.9, '75th': 1.98}
Pos 3	0.697486	0.65551	{'25th': 2.4, '50th': 2.49, '75th': 2.61}	{'25th': 2.38, '50th': 2.47, '75th': 2.6}
Pos 11	0.702972	0.675686	{'25th': 2.9, '50th': 3.01, '75th': 3.11}	{'25th': 2.72, '50th': 2.83, '75th': 2.98}
Pos 16	1.545341	1.579959	{'25th': 40.58, '50th': 40.65, '75th': 40.72}	{'25th': 40.48, '50th': 40.55, '75th': 40.66}
Pos 1	1.306513	1.17485	{'25th': 2.95, '50th': 3.01, '75th': 3.052499999999998}	{'25th': 2.9275, '50th': 2.98, '75th': 3.03}
Pos 4	0.84653	0.838504	{'25th': 2.59, '50th': 2.63, '75th': 2.67}	{'25th': 2.56, '50th': 2.6, '75th': 2.64}
Pos 8	1.347065	1.339162	{'25th': 3.01, '50th': 3.05, '75th': 3.09}	{'25th': 3.0, '50th': 3.04, '75th': 3.08}
Pos 9	0.537093	0.678131	{'25th': 3.14, '50th': 3.19, '75th': 3.23}	{'25th': 3.09, '50th': 3.13, '75th': 3.18}
Pos 10	0.583558	0.716402	{'25th': 3.09, '50th': 3.14, '75th': 3.2}	{'25th': 3.03, '50th': 3.1, '75th': 3.15}
Pos 2	0.748046	0.825815	{'25th': 2.58, '50th': 2.63, '75th': 2.69}	{'25th': 2.57, '50th': 2.62, '75th': 2.67}

Table: Profile RAB6146

Position	Cpk Front	Cpk Rear	Percentiles Front	Percentiles Rear
Pos 28	1.367806	1.483482	{'25th': 170.47, '50th': 170.75, '75th': 170.98}	{'25th': 170.44, '50th': 170.73, '75th': 170.92}
Pos 30	1.440101	1.571262	{'25th': 170.47, '50th': 170.71, '75th': 170.95}	{'25th': 170.42, '50th': 170.69, '75th': 170.89}
Pos 37	0.457977	0.490374	{'25th': 81.28, '50th': 81.47, '75th': 81.63}	{'25th': 81.28, '50th': 81.47, '75th': 81.63}
Pos 39	1.015295	1.150608	{'25th': 37.67, '50th': 37.77, '75th': 37.89}	{'25th': 37.68, '50th': 37.77, '75th': 37.87}
Pos 38	1.038433	1.103191	{'25th': 37.69, '50th': 37.79, '75th': 37.9}	{'25th': 37.69, '50th': 37.8, '75th': 37.89}
Pos 24	1.182241	1.362659	{'25th': 80.84, '50th': 80.97, '75th': 81.12}	{'25th': 80.88, '50th': 80.98, '75th': 81.12}
Pos 27	0.990095	1.201647	{'25th': 80.88, '50th': 81.065, '75th': 81.24249999999999}	{'25th': 80.88, '50th': 81.02, '75th': 81.15}
Pos 31	0.874036	0.819428	{'25th': 59.56, '50th': 59.64, '75th': 59.72}	{'25th': 59.54, '50th': 59.63, '75th': 59.71}
Pos 33	0.931635	0.93405	{'25th': 52.25, '50th': 52.37, '75th': 52.46}	{'25th': 52.25, '50th': 52.37, '75th': 52.47}
Pos 32	1.15423	1.18535	{'25th': 51.09, '50th': 51.18, '75th': 51.26}	{'25th': 51.07, '50th': 51.16, '75th': 51.23}
Pos 23	0.952111	0.973238	{'25th': 37.61, '50th': 37.7, '75th': 37.78}	{'25th': 37.62, '50th': 37.69, '75th': 37.77}
Pos 22	0.98661	1.027983	{'25th': 37.63, '50th': 37.71, '75th': 37.79}	{'25th': 37.63, '50th': 37.71, '75th': 37.79}
Pos 25	0.685205	0.712326	{'25th': 37.84, '50th': 37.95, '75th': 38.05}	{'25th': 37.84, '50th': 37.94, '75th': 38.05}
Pos 35	0.480303	0.507513	{'25th': 90.24, '50th': 90.35, '75th': 90.46}	{'25th': 90.23, '50th': 90.35, '75th': 90.45}
Pos 34	0.543711	0.503963	{'25th': 90.23, '50th': 90.34, '75th': 90.44}	{'25th': 90.21, '50th': 90.34, '75th': 90.44}
Pos 26	0.680249	0.701614	{'25th': 37.81, '50th': 37.93, '75th': 38.04}	{'25th': 37.82, '50th': 37.93, '75th': 38.04}
Pos 9	1.011468	0.998466	{'25th': 1.63, '50th': 1.69, '75th': 1.76}	{'25th': 1.62, '50th': 1.68, '75th': 1.745}
Pos 2	0.921477	0.892012	{'25th': 1.59, '50th': 1.66, '75th': 1.72}	{'25th': 1.59, '50th': 1.65, '75th': 1.72}
Pos 8	1.031889	1.019865	{'25th': 1.63, '50th': 1.68, '75th': 1.76}	{'25th': 1.62, '50th': 1.68, '75th': 1.75}

Pos 1	0.922395	0.880599	{'25th': 1.59, '50th': 1.66, '75th': 1.72}	{'25th': 1.5825, '50th': 1.65, '75th': 1.71}
Pos 21	0.954805	0.924	{'25th': 1.71, '50th': 1.8, '75th': 1.86}	{'25th': 1.7, '50th': 1.78, '75th': 1.84}
Pos 5	0.826302	0.799918	{'25th': 1.76, '50th': 1.87, '75th': 1.96}	{'25th': 1.76, '50th': 1.89, '75th': 1.97}
Pos 12	0.789756	0.805216	{'25th': 1.75, '50th': 1.88, '75th': 1.97}	{'25th': 1.77, '50th': 1.89, '75th': 1.97}
Pos 19	1.132871	1.040277	{'25th': 1.72, '50th': 1.79, '75th': 1.84}	{'25th': 1.71, '50th': 1.77, '75th': 1.82}
Pos 20	0.891104	0.713736	{'25th': 1.75, '50th': 1.81, '75th': 1.89}	{'25th': 1.69, '50th': 1.77, '75th': 1.84}
Pos 16	0.445735	0.453111	{'25th': 1.92, '50th': 2.09, '75th': 2.16}	{'25th': 1.91, '50th': 2.08, '75th': 2.16}
Pos 4	1.681145	1.645093	{'25th': 3.44, '50th': 3.47, '75th': 3.51}	{'25th': 3.44, '50th': 3.47, '75th': 3.51}
Pos 13	1.638379	1.639952	{'25th': 3.45, '50th': 3.48, '75th': 3.52}	{'25th': 3.44, '50th': 3.48, '75th': 3.52}
Pos 3	0.989335	0.930728	{'25th': 1.86, '50th': 1.92, '75th': 1.99}	{'25th': 1.87, '50th': 1.93, '75th': 2.0}
Pos 7	1.36143	1.379067	{'25th': 3.47, '50th': 3.51, '75th': 3.57}	{'25th': 3.47, '50th': 3.51, '75th': 3.57}
Pos 6	1.01355	0.948146	{'25th': 1.83, '50th': 1.9, '75th': 1.97}	{'25th': 1.84, '50th': 1.91, '75th': 1.99}
Pos 18	0.492446	0.481836	{'25th': 1.92, '50th': 2.07, '75th': 2.15}	{'25th': 1.9175, '50th': 2.07, '75th': 2.15}
Pos 11	0.896375	0.915919	{'25th': 1.83, '50th': 1.91, '75th': 1.99}	{'25th': 1.85, '50th': 1.92, '75th': 1.99}
Pos 14	0.966306	0.976685	{'25th': 1.84, '50th': 1.92, '75th': 1.98}	{'25th': 1.86, '50th': 1.93, '75th': 1.99}
Pos 10	1.267582	1.315502	{'25th': 3.48, '50th': 3.52, '75th': 3.57}	{'25th': 3.48, '50th': 3.52, '75th': 3.57}
Pos 15	0.59364	0.592419	{'25th': 1.93, '50th': 2.04, '75th': 2.1}	{'25th': 1.93, '50th': 2.04, '75th': 2.11}
Pos 17	0.565364	0.577283	{'25th': 1.93, '50th': 2.04, '75th': 2.12}	{'25th': 1.92, '50th': 2.04, '75th': 2.11}
Pos 36	0.969256	0.966573	{'25th': 91.18, '50th': 91.33, '75th': 91.48}	{'25th': 91.19, '50th': 91.36, '75th': 91.51}
Pos 29	1.12897	1.09727	{'25th': 91.13, '50th': 91.27, '75th': 91.42}	{'25th': 91.14, '50th': 91.28, '75th': 91.44}

Table :Profile RAB6782

Position	Cpk Front	Cpk Rear	Percentiles Front	Percentiles Rear
Pos 1	0.744656	0.878307	{'25th': 2.71, '50th': 2.77, '75th': 2.83}	{'25th': 2.71, '50th': 2.76, '75th': 2.81}
Pos 2	0.797068	0.944079	{'25th': 3.5, '50th': 3.56, '75th': 3.6175}	{'25th': 3.47, '50th': 3.52, '75th': 3.57}
Pos 4	1.131291	1.498277	{'25th': 2.56, '50th': 2.6, '75th': 2.65}	{'25th': 2.54, '50th': 2.58, '75th': 2.61}
Pos 6	0.354353	0.467128	{'25th': 3.76, '50th': 3.82, '75th': 3.87}	{'25th': 3.73, '50th': 3.78, '75th': 3.84}
Pos 7	0.79717	0.87487	{'25th': 3.01, '50th': 3.07, '75th': 3.12}	{'25th': 2.99, '50th': 3.06, '75th': 3.1}
Pos 14	0.933864	1.102118	{'25th': 120.6825, '50th': 120.92, '75th': 121.0975}	{'25th': 120.35, '50th': 120.58, '75th': 120.82}
Pos 9	1.415448	1.523371	{'25th': 2.62, '50th': 2.64, '75th': 2.67}	{'25th': 2.61, '50th': 2.63, '75th': 2.66}
Pos 5	1.161342	1.023708	{'25th': 2.8, '50th': 2.86, '75th': 2.91}	{'25th': 2.76, '50th': 2.815, '75th': 2.86}
Pos 3	0.788472	0.834237	{'25th': 3.23, '50th': 3.29, '75th': 3.34}	{'25th': 3.23, '50th': 3.28, '75th': 3.32}
Pos 10	1.709751	1.579149	{'25th': 53.31, '50th': 53.38, '75th': 53.48}	{'25th': 53.28, '50th': 53.345, '75th': 53.42}
Pos 8	0.669229	0.697236	{'25th': 2.66, '50th': 2.69, '75th': 2.73}	{'25th': 2.6525, '50th': 2.7, '75th': 2.73}
Pos 11	2.27614	2.119998	{'25th': 35.65, '50th': 35.74, '75th': 35.81}	{'25th': 35.59, '50th': 35.66, '75th': 35.76}
Pos 13	1.790853	1.897605	{'25th': 83.25, '50th': 83.34, '75th': 83.43}	{'25th': 83.06, '50th': 83.17, '75th': 83.29}
Pos 12	1.375149	1.480274	{'25th': 38.09, '50th': 38.19, '75th': 38.3}	{'25th': 37.98, '50th': 38.05, '75th': 38.15249999999996}

Bibliography

- [1] S. Majumdar, A. Sinha, A. Das, P. Datta, and D. Nag, "An Insight View of evolution of advanced aluminum alloy for aerospace and automotive industry: current status and future prospects," *Journal of The Institution of Engineers (India): Series D*, pp. 1–18, 2024.
- [2] I. Polmear, Light alloys: from traditional alloys to nanocrystals. Elsevier, 2005.
- [3] N. Parson, J. Fourmann, and J.-F. Beland, "Aluminum extrusions for automotive crash applications," SAE Technical Paper, 2017.
- [4] Aluminum Association's Transportation Group (ATG), "Driving Innovation with Automotive Aluminum," 2022. Accessed: Sep. 07, 2025. [Online]. Available: https://drivealuminum.org/wp-content/uploads/2022/05/ATG-SEMA-Presentation-DAR-Final-Nov-15.pdf
- [5] Deutsches Institut für Normung (DIN), "Aluminium and aluminium alloys Extruded rod/bar, tube and profiles Part 9: Profiles, tolerances on dimensions and form," Berlin, Oct. 2016.
- [6] N. Carvalho, A. Correia, and F. De Almeida, "The evaluation of defects in the aluminium extrusion process through quality tools," *WSEAS Trans Environ Dev*, vol. 14, no. 1, pp. 1–5, 2018.
- [7] W. Z. Misiolek and R. M. Kelly, "Extrusion of aluminum alloys," in *Metalworking: Bulk Forming*, ASM International, 2005, pp. 522–527.
- [8] T. Trzepieciński and S. M. Najm, "Current trends in metallic materials for body panels and structural members used in the automotive industry," *Materials*, vol. 17, no. 3, p. 590, 2024.
- [9] D. O. Odoh, "Effect of Alloy Composition on the Hot Deformation Behavior, Extrudability and Mechanical Properties of AA6XXX Aluminum Alloys," Doctoral dissertation, University of Waterloo, 2017. Accessed: Aug. 30, 2025. [Online]. Available: http://hdl.handle.net/10012/12116
- [10] European Aluminium Association, "Aluminium in Cars: Unlocking the Lightweight Potential," Aug. 2020. Accessed: Aug. 24, 2025. [Online]. Available: https://www.european-aluminium.eu/wp-content/uploads/2020/10/Aluminium-in-Cars-Unlocking-the-Lightweight-Potential.pdf
- [11] T. Sheppard, Extrusion of aluminium alloys. Springer Science & Business Media, 2013.
- [12] J. Haraldsson and M. T. Johansson, "Review of measures for improved energy efficiency in production-related processes in the aluminium industry–From electrolysis to recycling," *Renewable and Sustainable Energy Reviews*, vol. 93, pp. 525–548, 2018.
- [13] Atieuno, "The ultimate guide to aluminium extrusion process." Accessed: Aug. 30, 2025. [Online].

- Available: https://www.atieuno.com/2023/07/17/aluminium-extrusion-process-guide/
- [14] M. Bauser, G. Sauer, K. Siegert, and A. F. Castle, Extrusion. ASM international, 2006.
- [15] A. Chahare and K. H. Inamdar, "A review on process parameters affecting aluminium extrusion process," *Int. J. Innov. Res. Sci. Eng*, vol. 2, no. 12, pp. 193–198, 2016.
- [16] N. Parson, J. Fourmann, and J.-F. Beland, "Aluminum extrusions for automotive crash applications," SAE Technical Paper, 2017.
- [17] S. Das, "Life cycle energy and environmental assessment of aluminum-intensive vehicle design," SAE International Journal of Materials and Manufacturing, vol. 7, no. 3, pp. 588–595, 2014.
- [18] I. Polmear, D. StJohn, J.-F. Nie, and M. Qian, *Light alloys: metallurgy of the light metals*. Butterworth-Heinemann, 2017.
- [19] N. Carvalho, A. Correia, and F. De Almeida, "The evaluation of defects in the aluminium extrusion process through quality tools," *WSEAS Trans Environ Dev*, vol. 14, no. 1, pp. 1–5, 2018.
- [20] D. Leśniak *et al.*, "FEM numerical and experimental study on dimensional accuracy of tubes extruded from 6082 and 7021 aluminium alloys," *Materials*, vol. 16, no. 2, p. 556, 2023.
- [21] T.-T. Truong, Q.-C. Hsu, and V.-C. Tong, "Effects of solid die types in complex and large-scale aluminum profile extrusion," *Applied sciences*, vol. 10, no. 1, p. 263, 2019.
- [22] S. Shamsudin, Z. W. Zhong, S. N. A. Rahim, and M. A. Lajis, "The influence of temperature and preheating time in extrudate quality of solid-state recycled aluminum," *The International Journal of Advanced Manufacturing Technology*, vol. 90, no. 9, pp. 2631–2643, 2017.
- [23] S. Subramanian, "Leveraging IoT data streams for AI-based quality control in smart manufacturing systems in process industry," *Journal of AI-Assisted Scientific Discovery*, vol. 3, no. 3, p. 37, 2023.
- [24] G. Manohar, K. A. Francy, and C. S. Rao, "A framework for prediction of extrusion responses using machine learning algorithm," *International Journal on Interactive Design and Manufacturing* (*IJIDeM*), pp. 1–14, 2024.
- [25] P. T. Moe, A. Willa-Hansen, and S. Støren, "Optical Measurement Technology For Aluminium Extrusions," in *AIP Conference Proceedings*, American Institute of Physics, 2007, pp. 596–601.
- [26] R. B. Bergmann, M. Kalms, and C. Falldorf, "Optical in-process measurement: Concepts for precise, fast and robust optical metrology for complex measurement situations," *Applied Sciences*, vol. 11, no. 22, p. 10533, 2021.
- [27] Y. Shen, J. Ren, N. Huang, Y. Zhang, X. Zhang, and L. Zhu, "Surface form inspection with contact coordinate measurement: a review," *International Journal of Extreme Manufacturing*, vol. 5, no. 2,

- p. 022006, 2023.
- [28] C. A. Raknes, T. Welo, and F. Paulsen, "Dimensional accuracy of aluminium extrusions in mechanical calibration," in *AIP Conference Proceedings*, AIP Publishing LLC, 2018, p. 160024.
- [29] P. K. Saha, Aluminum extrusion technology. Asm International, 2000.
- [30] IQS Directory, "Process, Properties, and Benefits of Extruded Aluminum." Accessed: Aug. 30, 2025. [Online]. Available: https://www.iqsdirectory.com/articles/aluminum-extrusion/extruded-aluminum.html
- [31] M. M. Marín, A. M. Camacho, and J. A. Pérez, "Influence of the temperature on AA6061 aluminum alloy in a hot extrusion process," *Procedia Manuf*, vol. 13, pp. 327–334, 2017.
- [32] C. Mondal, A. K. Mukhopadhyay, T. Raghu, and V. K. Varma, "Tensile properties of peak aged 7055 aluminum alloy extrusions," *Materials Science and Engineering: A*, vol. 454, pp. 673–678, 2007.
- [33] S. N. A. Rahim, M. A. Lajis, and S. Ariffin, "Effect of extrusion speed and temperature on hot extrusion process of 6061 aluminum alloy chip," *ARPN J. Eng. Appl. Sci*, vol. 11, no. 4, pp. 2272–2277, 2016.
- [34] O. M. Ikumapayi, S. T. Oyinbo, O. P. Bodunde, S. A. Afolalu, I. P. Okokpujie, and E. T. Akinlabi, "The effects of lubricants on temperature distribution of 6063 aluminium alloy during backward cup extrusion process," *Journal of Materials Research and Technology*, vol. 8, no. 1, pp. 1175–1187, 2019.
- [35] V. Jayaseelan and K. Kalaichelvan, "Lubrication effect on friction factor of AA6063 in forward extrusion process," *Procedia Eng*, vol. 97, pp. 166–171, 2014.
- [36] C. Zhang, G. Zhao, Z. Chen, H. Chen, and F. Kou, "Effect of extrusion stem speed on extrusion process for a hollow aluminum profile," *Materials Science and Engineering: B*, vol. 177, no. 19, pp. 1691–1697, 2012.
- [37] X. Duan, X. Velay, and T. Sheppard, "Application of finite element method in the hot extrusion of aluminium alloys," *Materials Science and Engineering: A*, vol. 369, no. 1–2, pp. 66–75, 2004.
- [38] W. Wei, C. Yuan, R. Wu, and W. Jiao, "Prediction of breakthrough extruding force in large-scale extrusion process using artificial neural networks," *Sci Prog*, vol. 104, no. 1, p. 0036850421992609, 2021.
- [39] M. Staley and M. Tiryakioglu, "Physical metallurgy and the effect of alloying additions in aluminum alloys," *Handbook of Aluminum Volume 1. ç Physical Metallurgy and Processes. CRC Press, New York*, pp. 81–211, 2003.
- [40] T. Ye et al., "Deformation behavior of an extruded 7075 aluminum alloy at elevated temperatures,"

Materials, vol. 17, no. 5, p. 1210, 2024.

[41] Y. Birol, "The effect of homogenization practice on the microstructure of AA6063 billets," *J Mater Process Technol*, vol. 148, no. 2, pp. 250–258, 2004.